UNIVERSITY OF SOUTHAMPTON

FACULTY OF ENGINEERING, SCIENCE & MATHEMATICS

School of Engineering Sciences

An Investigation of the Effects of Curvatures on Natural Vibration Characteristics of Curved Beams and Plates

Bo Hu

Thesis for the degree of Doctor of Philosophy

June, 2009

UNIVERSITY OF SOUTHAMPTON

ABSTRACT

FACULTY OF ENGINEERING, SCIENCE & MATHEMATICS

SCHOOL OF ENGINEERING SCIENCES

Doctor of Philosophy

AN INVESTIGATION OF THE EFFECTS OF CURVATURES ON NATURAL VIBRATION CHARACTERISTICS OF CURVED BEAMS AND PLATES

by Bo Hu

Curved structures are mostly investigated through the numerical method. In the numerical model, the curved beam or plate is easily simulated by assembled elements. Although the approximate solution can be obtained, numerical results are inadequate to demonstrate the effect of the curvature on the whole system. In order to reveal such effect and implicative mechanism of the curvature, an analytical way needs to be proved applicable to the curved structure. The present thesis thus develops the perturbation method to analyze the natural behaviour of curved beam structures.

The governing equations for curved beams with the variable and arbitrary curvature are derived. The complex parameter introduced by the curvature is modified by the perturbation method. Simplified equations physically reveal the feature of the mode transition, impacts in terms of boundary conditions, etc. due to the change of curvatures. Based on the asymptotic solutions, the singly curved plate is analyzed by using the Rayleigh- Ritz method. The analysis is further developed to the laminated composite

curved beam. Examples present extra characteristics brought by the composite materials. In order to support the analytical solutions, finite element models of the curved beam with different type of varying curvatures are established. Numerical results illustrate more phenomena in transition of mode shape following the change of curvatures and the wave propagation behaviour of curved beams.

KEY WORDS

Varying curvature, curved beams, Laminated, Composite, S-shape strip,

Free vibration, wave propagation, mode sequence, FEM

Acknowledgement

It is hard to describe my five years' life in UK by some words. It is a kind of simple but with a bit complex. I remembered before my PhD study, in the discussion of my future with Professor Shenoi, I said some topic was complex. Ajit said the life is complex. No one of my father's generation has ever said that to me before, so I often remember it when I meet difficulties.

During these years, if using a word for all, I would say, thankfulness. I would say thanks to Professor Shenoi, 'you give me the chance and not once'. I would say thanks to Professor Xing, 'I am very lucky. You care me not only at the study but also the ordinary life'. The most important, I would say thank you to both Professors, 'thank you for your support and understanding all the time. I would also feel great thankful to meet my wife in Southampton. Of course, for my parents and sister, not only say thanks, I am also going to say sorry, 'I know how much you worried about me'.

I am happy there are many friends and colleagues who shared the life with me in Southampton. Weibo and Jingzhe are alumni of my university in both Shanghai and Southampton. I believe we are the forever friends.

Last but not least, I gratefully acknowledge the DSTL for providing financial support enabling me to study in the University of Southampton to engage this research, especially thanks to Dr J Smith for his deep discussion, guidance and supervision during the research project period.

List of Contents

Chapter 1 Introduction

1.1 Research Background 1

1.1.1 Overview of curved structure 1

1.1.2 Characteristics of curved structures 4

1.2 Literature Review 7

1.2.1 Thin-wall curved beam and shell theories 8

1.2.2 Static and dynamic behaviours 9

1.2.3 Variable parameters 11

1.2.4 Approaches 15

1.3 The Present Work 21

1.4 Layout of the Thesis 22

Chapter 2 Theoretical Formulation

2.1 Brief Outline of the Theory of Surfaces 24

2.1.1 The first quadratic form of the surface 25

2.1.2 The second quadratic form 26

2.1.3 Curvature of a curve 26

2.2 Deformation of the Surface 28

2.2.1 Displacement field 28

2.2.2 Strain-displacement equation 29

2.2.3 Constitutive equations 30

2.3 Equilibrium Equations 31

2.4 Dimensionless Governing Equations 36

2.5 Boundary Conditions 38

2.6 Summary....40

Chapter 3 Perturbation Analysis

3.1 Transformation of Governing Equations....41
3.2 Zero Order Approximations....44
3.3 First Order Approximation Equations....48
3.4 Second Order Approximation Equations....51
3.5 Summary....53

Chapter 4 Finite Element Models

4.1 General Procedure....54
4.2 FEA Solutions of Natural Vibration....56
4.3 The Choice of Element....57
4.4 FE model of Curved Beam....60
4.4.1 The circular curved beam....60
4.4.2 The S-shape strip....61
4.4.3 Other curvatures....62
4.5 Boundary Conditions Treatment....64

Chapter 5 Curved Beam with Varying Curvatures

5.1 Curved Beam with Constant Curvature....66
5.1.1 Hinged boundary conditions....67
5.1.2 Clamped boundary conditions....74
5.1.3 Simply supported boundary conditions....79
5.2 S-shape Strip....80
5.2.1 Hinged boundary conditions....81
5.2.2 Clamped boundary conditions....83
5.3 Summary....85
5.3.1 Discussion on different order perturbations....85
5.3.2 Discussion on natural frequencies change for large curvatures....85
5.3.3 Summary....86

Chapter 6 Curved Beam with Arbitrary Curvatures
6.1 Treatment of Arbitrary Curvature 87
6.2 Natural Vibration of a Parabolic Arc 89

Chapter 7 Effects of Curvature on the Curved Plate
7.1 Application of Perturbation Solution 90
7.2 Propagation Behaviour of the Curved Plate 93
7.2.1 Circular curved plate 93
7.2.2 S-shape strip 97

Chapter 8 Effects of Curvature on Composite Curved Beams
8.1 Effect on Natural Frequency 102
8.2 Result Comparisons 106

Chapter 9 Conclusions and Future Works
9.1 Achievements 108
9.1.1 Mode sequence changes 108
9.1.2 Boundary conditions 109
9.1.3 Wave propagation behaviour 109
9.1.4 Effects from characteristics of composite materials 110
9.2 Conclusions 111
9.3 Future works 112

List of Figures

Figure 1.1 arch: Ex Estrados; In intrados; K keystone; S springer; v voussoirs (Wikipedia)…… 2
Figure 1. 2 structure of the thesis……...23
Figure 2. 1 sketch of the curved surface……24
Figure 2. 2 definition of curvature..…..……27
Figure 2.3 the deformation of the curved body from the initial configuration to the current configuration……...……29
Figure 2.4 notation and positive directions of force resultants in shell coordinates……..32
Figure 2.5 notation and positive directions of moment resultants in shell coordinates….32
Figure 2.6 sketch of forces on a beam element……..34
Figure 4.1 convergence study of SHELL93 element…….59
Figure 4.2 geometry of curved beam with a constant curvature…….……...61
Figure 4.3 finite element model for the strip with varying curvature…….…….……..62
Figure 5.1 Non-dimensional eigenvalue of a circular curved beam with hinged boundary conditions……..…….…….68
Figure 5.2 Natural frequency of a circular curved beam with hinged boundary conditions……..…….…….69
Figure 5.3 Result comparisons of non-dimensional eigenvalue of circular beam with hinged boundary conditions……...……70
Figure 5.4 Variation in mode sequence due to the rising in curvatures……72
Figure 5.5 Non-dimensional eigenvalue of a circular beam with clamped boundary conditions……75
Figure 5.6 Mode shape for circular curved beam with increasing curvatures……...76
Figure 5.7 Symmetric mode shape transitions for a clamped curved

beam……..…….……76
Figure 5.8 extension varies with the curvature……..77
Figure 5.9 Simply support boundary condition……79
Figure 5.10 Non-dimensional eigenvalue of an s-shape strip with hinged end conditions……82
Figure 5.11 Mode shape transition of S-shape with hinged ends…...……..83
Figure 5.12 Non-dimensional eigenvalue of an s-shape strip with clamped end condition…….…….84
Figure 5.13 Non-dimensional eigenvalue comparisons of a thin curved beam…….……86
Figure 5.14 Non-dimensional eigenvalue comparisons of a thin curved beam…….86
Figure 6.1 sketch of a parabola curved beam……88
Figure 7.1 Normal displacement for first three symmetric waveguide modes of an elastic strip……94
Figure 7.2 Dispersion curves for second symmetric lateral vibration mode of circular curved strip. Four curves represent four strips with different curvatures (subtended angles)……...94
Figure 7.3 Natural frequency of circular curved beam with two ends clamped……..95
Figure 7.4 Natural frequency of circular curved beam with full clamped boundaries…96
Figure 7.5 Curved plate with full clamped boundaries with second and third symmetric wave mode…….……96
Figure 7.6 natural frequency of curved plate with full free boundary condition.....97
Figure 7.7 Variation in mode sequence due to the rising of curvature parameter.....98
Figure 7.8 the first three symmetric waveguide modes of an elastic strip of varying curvature……100
Figure 7.9 Natural frequencies against curvatures for clamped boundary conditions at both ends (also for all kind boundary conditions at both ends……..…101
Figure 7.10 Natural frequencies against curvatures for full clamped boundary conditions ……..101
Figure 8.1 Clamped beam with constant curvatures……103
Figure 8.2 S-shape strip with clamped end conditions……....104
Figure 8.3 Natural frequency increasing ratio of circular curved beam.....105

Figure 8.4 First anti-symmetric mode of clamped S-shape strip.....106
Figure 8.5 First symmetric mode of hinged circular beam.....107

List of Tables

Table 1.1 Examples of curved structures……...5
Table 3.1 Differences between different order perturbations…….53
Table 4.1 Selected elements in ANSYS…….57
Table 4.2 natural frequency of selected elements…….….58
Table 4.3 Curvature function of various curves…….63
Table 6.1 Natural frequency of parabolic arch (Hz)……89
Table 7.1 Natural frequency of circular curved beam with hinged edges…….……..91
Table 7.2 Natural frequency of curved plate with hinged edges……..92
Table 8.1 Material properties of curved laminated beam…….102

Nomenclature

a	the width of the beam
b	curvature amplitude
f	frequency
h	thickness of beam
I	second moment of inertia
k	curvature
$\bar{k}$ $\hat{k}$	non-dimensional curvature, scaled non-dimensional curvature
l	the length of the curved beam
r	radius of curvature
s $\bar{s}$	the length of curved edge, non-dimensional expression
t	time parameter
u	tangential displacement function
$\bar{u}, \hat{u}$	non-dimensional and scaled tangential displacement
w	transverse displacement function
$\bar{w}$	non-dimensional transverse displacement
z	normal to the mid-surface
A	cross-section area per unit width
D	flexural rigidity
E	Young's modulus of elasticity
G_{12}	shear modulus
M	residual moment
N	residual force
Q	shear force

A	extensional stiffness matrix
B	coupling stiffness matrix
D	flexural stiffness matrix
M	general expression for bending moment matrix
N	general expression for axial force matrix
γ	shear angle
ε, ϵ	strain
η	stiffness ratio
θ	subtended angle
κ	change in curvature
λ	eigenvalue or square of non-dimensional frequency based on the tension vibration frequency
μ	Poisson's ratio
ρ	density
ϕ	rotation angle of cross section normal to mid surface
ω	angular frequency
Λ	eigenvalue or square of non-dimensional frequency based on the bending vibration frequency

Chapter 1 Introduction

1.1 Research Background

1.1.1 Overview of curved structure

Curved structures classified by their geometry are usually named as arches and shells which are the most common construction elements in the nature and the technology. An arch has the capacity of spanning a space while maintaining its shape and supporting significant loads. It was first developed in the Indus Valley civilization circa 2500 BC and subsequently in Mesopotamia, Egypt, Assyria and Etruria. Arches were used for underground structures such as drains and vaults till ancient Romans were the first to use them widely as an important technique in cathedral buildings. China has built the world first open- spandrel stone segmental arch bridge since 605 AD. The arch is significant because when subjected to vertical loads, its two ends develop reactions inwardly within horizontal direction. The Roman doorway, for example, shown in Figure 1.1, its construction depends on a series of wedge-shaped blocks set side by side in a semi-circular curve or along two intersecting arcs (as in a pointed arch). The central block is called the keystone, and the two points where the arch rests on its supports are known as the spring points. The arch can carry a much greater load than a flat beam of the same size and material, because downward pressure forces the blocks together instead of apart. In order to keep the system in a state of equilibrium, the resulting outward thrust must be resisted by the arch's supports. In order to minimize the horizontal thrust, the highly rigid building materials such as lightweight monolithic (one-piece) arches of steel, concrete, or laminated wood are thereby largely used.

Shell construction began in the 1920s and emerged as a major long-span concrete structure after World War II. In the building construction, a thin, curved plate element is

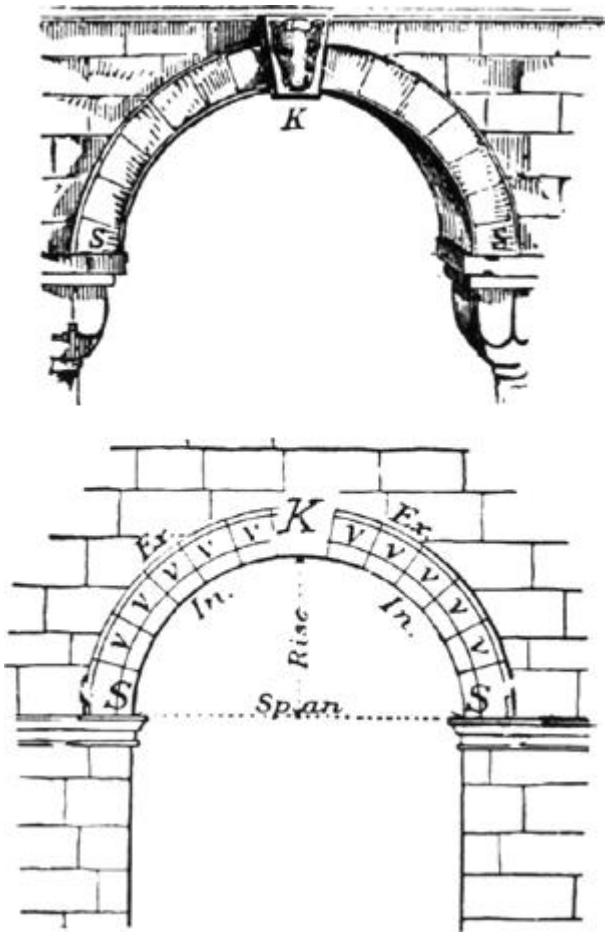

Figure 1.1 arch: Ex Estrados; In intrados; K keystone; S springer; v voussoirs (Wikipedia)

shaped to transmit applied forces by compressive, tensile, and shear stresses which describes its resistance to deformation in terms of separable stretching and bending effects; these curved elements are then assembled to large structures in the plane of the surface and spreads forces throughout the whole structure, which means every part of the structure supports only a small part of the load, giving it its strength.

In the present day, applications of the curved structure are tremendously expanded. Independent of the specific scale, curved structures make an important contribution to the development of several branches of engineering. In the architecture aspect, thin shells are used for roofing purposes which could increase the internal space with the minimal amount of materials. They are commonly seen as the roof of the warehouse. Architects also largely adopted curve structures in buildings for their fashionable design and other special functions. The most recent example is the new Beijing Olympic Stadium, the

whole structure of which is constructed by steel curved beams. In bridge engineering, arch bridges are developed to span long distance over rivers, valleys or channels without supports from columns. In offshore engineering, pressure vessels and associated pipe work are manufactured by shell elements. Pipes are normally bent into the curved state when laying down and staying underwater, which could be treated as curved beams in mathematic models. In structural engineering, optimal design needs the use of curved structures. In mechanical engineering, machine blades with curvature are important functional parts. In naval architecture, the idea of utilizing a curved structural concept with great potential for the construction is applied, for example, to an inland waterway vessel. The basic concept is taking advantage of the inherent strength capacity of a plate after the bending resistance limit is exceeded. This can be done by giving the shell plating a specific curvature and that transforms bending stresses into membrane stresses which will give a general drop in stress level. More recently, the introduction of fiberglass and similar lightweight composite materials has impacted the construction of exterior skin of vehicles ranging from boats, racing cars, fighter and stealth aircraft, and so on, which utilize the hydrodynamic, aerodynamic and some functional aspects of thin curved structures.

This large amount of engineering applications is mainly due to the following advantages of the curved structure;

(i) Significant span capacity can be achieved;

(ii) In addition to the slenderness, curved beam or shell structures own high compression-resistance characteristics allowing advantageous dynamic and stability capacities;

(iii) Variable curvature configuration expands the structure design flexibility and fashionable look;

(iv) To apply walls as thin as possible is a natural optimization strategy to reduce dead load and minimize construction material;

(v) Significant benefits of using composite materials are expected to result in a 30-40% weight savings and a 10-30% cost reduction compared to conventional metallic structure.

1.1.2 Characteristics of curved structures

In general, engineering problems are mathematical models of physical situations. Thin-walled curved structures attracted lots of researchers' interests. Various mathematics models were developed generally based on spatial form geometries such as curved beams, curved plates and shells. These models are analyzed to reveal their features, which make them recognizable as useful objects in engineering. The curved beam is usually modelled in one dimension, by neglecting the lateral motion. The complexity of the curved beam primarily comes from the curvature which is not only involved in the geometrical parameter, but also has impact on the resultant stress, stiffness and displacement functions. The curvature along with the arc-length direction can be either constant or variable. It is still straightforward to analyze constant curved structures; by contrast, the variation in curvature brings mathematical difficulties and even nonlinearity considerations into equations of motion. Sorted by curvature, curved beams appear in different shapes like circular, parabolic, elliptic, s-shaped and so on. The curved beam can be also classified by the type of cross section, such as symmetrical, unsymmetrical, continuously varying or hybrid. For the two-dimensional configuration, the terminology of "curved plate", also called "shell panel" is referring to a shell having small changes in slope of the un-deformed middle surface. The analysis of the curved plate is usually based on thin shell theory which is applied when the thickness is relatively small compared to its other dimensions and in which deformations are not large compared to thickness. The curved plate has curvatures in two dimensions, which could be variable or constant in either direction. Table 1.1 lists some examples of the most common geometric forms of curved structures in engineering applications.

The challenge of the curved beam and the curved plate studies can be shown in many aspects. Unlike the straight beam, the curvature of the curved beam introduces geometric coupling between the axial and transverse motions and even with the rotations. The inherent coupling is the source for the element's efficiency, which requires two coupled displacement functions for the in-plane vibration behaviour, and three coupled displacement functions for the out-plane vibration problem. These functions coupled in the differential equations are required to be known functions rather than unknown

Table 1.1 Examples of curved structures

Different types of arch bridges

Different types of roofs

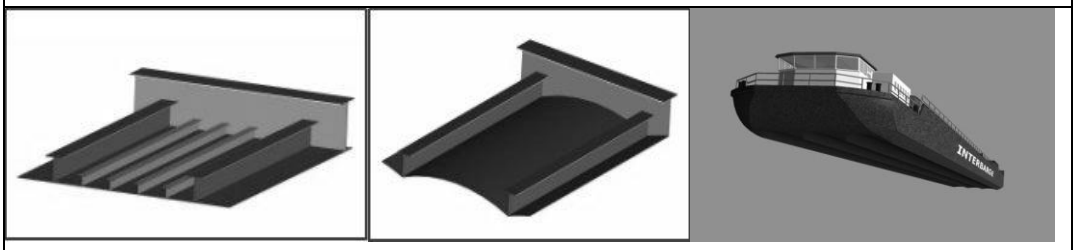

The INTERBARGE project from FEM Engineering AS company brings curved elements into several key areas of vessel design which is vital for an efficient and economical way of transporting cargo on the inland rivers/waterways of Europe.

Shells in composite materials

in the curved beam. These displacement expressions also have to fulfil specific boundary conditions. Plenty of efforts have been made to find the trial functions that increase the efficiency and accuracy of solutions. However, it is difficult to build up a structural

system to control variable coefficients existing in the curvature, cross section, material property, load case and boundary conditions. These coefficients in the equations of motion might be constant, linear or even nonlinear. It is not difficult to find a mathematic way to decouple equations with constant coefficients. The closed form solution can be then obtained by solving the differential equations by providing the boundary conditions. However, for those curved beams which have variable parameters, it is not straightforward to get the decoupled differential equations. Vast research work is focused on creating more accurate mathematical models and revealing the characteristics of curved structures. In the mean time, researchers have to overcome errors generated in the solution procedure such as membrane and shear locking phenomena. On the other hand, in the real world, many methods were invented to simplify the manufacture procedure of the curved structure, reduce storage space and minimize the cost in the construction.

The research works on curved beam and shell panel structures are comprehensively reviewed in the present thesis, in the following categories:

(i) Thin-walled curved structure theories;
(ii) Static and dynamic behaviours;
(iii) Variable parameters;
(iv) Composite materials;
(v) Analytical and numerical approaches.

1.2 Literature Review

Studies on the curved beam could be traced back to the early twenty century. Taken as the milestone in the history, Den Hartog (1928) obtained the lowest natural frequency of circular arcs using the Rayleigh-Ritz method. Forsberg (1964) studied the influence of boundary conditions on the modal characteristics of thin-walled cylindrical shells. Deb Nath (1969) designed experiments to verify the analytical results of the circular curved plate. Fleisher (1974) developed planar curved structure elements for the curved beam and different types of curved plates; his studies firstly showed that the variation in curvatures leads to a significant change in natural vibration characteristics.

During the last two decades the most progress has been achieved in terms of both theoretical development and engineering availability. Large amount of research work was published to demonstrate achievements on curved structure studies, among which there are several important review papers. Laura and Maurizi (1987) gave a brief discussion of recent work dealing with the dynamic behaviour of arches. Recommendations are given with respect to straightforward calculations of fundamental frequencies of arch-type structures. Several complicating factors are accounted for. Chidamparam and Leissa (1993) attempted to organize and summarize the extensive published literature on in-plane, out-plane and coupled vibrations of curved bars, beams, rings and arches. Particular attention was given to the effects of initial static loading, nonlinear vibrations and the application of finite element techniques. Auciello and De Rosa (1994) examined a number of approaches from the Ritz and Galerkin methods to the finite element techniques on the free vibration of different kinds of stepped arches and arches with linearly varying cross-section. Most recently, Zhao *et al*. (2006) reviewed advances of research on curved beams. Based on a discussion of equilibrium equations, strain-displacement relations and governing equations of curved beams, a summary of basic static theories and dynamic theories, and modelling methods for curved beams, and in-plane vibrations and out-plane vibrations are given in the paper.

Despite the merely academic motive behind some of the publications, potential engineering applicability does exist in many areas. The present thesis attempts to review

the most recent achievements on the vibration behaviour of curved beam and curved plate structures.

1.2.1 Thin-wall curved beam and shell theories

The majority of existing beam theories are invariably based on the Euler-Bernoulli hypothesis of plane cross sections remaining plane during deformation, which also applies to the thin curved beam. Thin walled theories typically include the postulates expressed in Love's first approximation (Love, 1944). These postulates may be written as follows:

- the thickness of a beam is small compared to a characteristic dimension. Here a beam is considered as thin if the ratio of its thickness to the radius of the curvatures of its surface is less than or approximately equal to one-tenth.
- the deflections of the beam are small. This permits the use of the equations of the un-deformed beam to describe its subsequent deformation and with the use of Hooke's law, results in a linear elastic theory.
- the transverse normal stress is negligible. This is a result of postulate 1.
- normal to the reference surface of the beam remain normal and the beam thickness remains unchanged.

The Timoshenko theory relaxes the normality assumption of the Euler-Bernoulli beam theory and gives a better approximation to the true behaviour of the beam by taking into account a constant state of transverse shear strain with respect to the thickness coordinate. However, it is known that the shear stress distribution across the cross section is non-uniform. Timoshenko theory that does not account for a non-uniform variation of the through thickness shear stress uses a shear correction factor depending on the cross section in order to compensate for the errors introduced. The higher order theories (Lo *et al*., 1978) eliminate dependence on the shear correction factor, which normally assume cubic in-plane displacements in the through thickness direction and transverse inextensibility.

Wang (1995) presented the deflection and stress resultants of single-span

Timoshenko straight beams with general loading and boundary conditions, in terms of the corresponding Euler-Bernoulli beam solutions. The deflection relationships show clearly the effect of shear deformation, which allow engineers to readily obtain the bending solutions of Timoshenko beams from the Euler-Bernoulli solutions without more complicated flexural-shear deformation analysis. Reddy and Wang (1997) developed the relationship between the bending solutions of the Euler-Bernoulli beam theory and the refined higher order beam theory. In (2001) they further developed exact relationship between the bending solutions of the Levinson beam and plate theories and the Euler-Bernoulli beam and Kirchhoff plate theories. However, all these relationships are limited to the bending solutions. For the curved beam, the coupling effects from the extensional vibration cannot be neglected.

The vibration problem of the open-form thin shell panel or the curved plate is usually based on thin shell theories which typically include the hypothesis expressed in Love's (1944) first approximation. Equations of motion of thin elastic shells are derived by Krauss (1967) and Leissa (1973). Vinson (1989) summarized formulations and classical solutions of the thin walled structures. Liew *et al*. (1997) comprehensively reviewed vibration of shallow shells. Price *et al*. (1998) analyzed the vibration of cylindrical pipes and open shells based on different thin shell theories including Donnell's theory, Love's theory and an improved theory.

1.2.2 Static and dynamic behaviours

The dynamic problems of a curved structure generally involve the in-plane vibration which primarily consists of bending-extensional modes, the out-plane vibration which is essentially bending-twisting dynamics, and coupled motions consisting of extension, flexure, shear and twist. Yu *et al*. (1995) presented exact and accurate analytical solutions for the free vibration of circular cylindrical shell panels with arbitrary combinations of simple boundary conditions. An effective computer program using the transfer matrix method is presented by Yildirim (1997) for both in-plane and out-of-plane free vibration analysis of elastic uniform arcs having double-symmetrical cross-sections. Goh (1998) formulated governing equations using thin shell theory and applied to a pressurized arch

shell component. A numerical investigation based on the Rayleigh-Ritz method is utilized to determine the behaviour of arch-shell under various types of loading including a snow load, a wind load and a horizontal side load distributed along the arc length. Tarnopolsky and De Hoog (1999) obtained asymptotic approximations for vibrational modes of helices. Walsh and White (2000) described the vibrational power transmission due to flexural, extensional and shears types of travelling wave in a curved beam which has a constant radius of curvature. They also studied the effect of curvature in three different frequency regions whose limits depend upon the type of wave considered. Eisenberger and Efraim (2001) presented the exact dynamic stiffness matrix of a circular shear deformable beam by considering them as the end forces of the beam when it is deformed with unit displacement at its ends. The stiffness matrix is frequency dependent, and the natural frequencies are those that cause the matrix to become singular. Therefore, the natural frequencies are obtained by equating the stiffness matrix to zero. Lee and Hsiao (2002) developed the semi-exact solutions for the free in-plane vibrations of curved non-uniform beams with constant radius. The two coupled governing differential equations are reduced to complete sixth-order ordinary differential equations with variable coefficients in the longitudinal displacement. Numerical analysis shows that the taper ratio, the centre angle and the arc length have significant influence on the natural frequencies. Kang *et al*. (2003) provided a systematic approach for the free vibration problem of multi-span planar circular curved beams with general boundary conditions and supports. The system considered multiple point discontinuities. Dispersion equations are solved by combining the wave reflection, transmission and the field transfer matrices. Huang *et al*. (2003) developed an analytical solution to the proposed governing equations to analyze the free vibration and stability of a circular arch under initial stresses due to the static preloading. Differing from traditional ways, this paper considered not only the most important factor, static stress resultant, also all initial stress resultants. Kim *et al.* (2002) used energy method to solve the in-plane and out-plane free vibration problem of the curved beam with non-symmetric thin-walled cross-section. Two thin-walled curved beam elements corresponding to extensional and inextensional conditions are developed using third and fifth order Hermitian polynomials. The influences of the thickness-curvature effect are investigated. Wu and Chiang (2004) investigated the dynamic

response of an arch with a moving load using the curved beam element with implicit shape functions. Gridin *et al*. (2005) presented convincing evidence for the existence of trapped modes localized in the regions of maximal curvature, and offered predictions of when and why such trapping occurs. To this end, two methods were developed, one is asymptotic, which assumes smallness of dimensionless curvature, and the other is numerical.

Besides the in-plane vibration, Lee and Chao (2000) derived the uncoupled and reduced sixth order ordinary differential equations with variable coefficients in the out-of-plane flexural displacement and the tensional displacement, respectively. The exact solutions of curved non-uniform beams are obtained by providing the material and geometric properties in arbitrary polynomial forms. Tufekci and Dogruer (2006) presented an exact solution of the equations for out-of-plane deformations of arches with arbitrary axes and cross sections by using the initial value method by which the displacement, slope, twist angle and stress resultants can be calculated analytically along the arch axis. The equation takes into account the shear deformation effect. An advantage of the method is that the high degree of static indeterminacy adds no extra difficulty to the solution.

1.2.3 Variable parameters

Properties of the curved structure might usually not be constant. These properties represent the state of the geometry and the material, which are expressed as the parameters in the mathematical equations. While the application of curved structures with constant parameters is well catered for, the solution for those with variable parameters is not yet completely understood. In addition to the geometry and material as the main category, it is possible to subdivide the variation in the geometric parameters as varying curvature and variable cross section.

- Geometric parameters

The analytical solution of a non-circular curved beam must be formulated by the series solution method. The series solution method is reliable, but needs lots of terms and

is restricted by the convergence ratio. Researchers usually expand the curvature as Fourier or Taylor series with respect to the arc-length in order to represent varying curvature. Non-circular elastic curved beams were firstly studied by Romanelli and Laura (1972) by using Rayleigh's principle. Wang and Moore (1973) determined the lowest natural extensional frequency of a clamped elliptic arch with constant section, which indicated the effect of arc angle on the natural frequencies of the arc. Wang (1975) studied the fundamental frequency of clamped parabolic arcs. Based on the same numerical method, Lee and Wilson (1989) obtained frequencies and modes for parabolic, sinusoidal and elliptic arches. Experimental validations of the lowest four natural modes were included. Guierrez *et al*. (1989) obtained the lowest frequency coefficients of symmetrical and unsymmetrical arch-type structures, using polynomial coordinate functions and the Ritz method. Scott and Woodhouse (1992) studied the musical saw behaviour by examining the underlying physics of the confinement process. The paper analyzed the trapped modes of the curved strip in S-shaped configuration. The analysis revealed the essential nature of the internal reflection process, in terms of the change with curvature of the dispersion characteristics of the strip. Charpie and Burroughs (1993) gave a comprehensive review on the free in-plane vibration of beams with variable curvature and depth. They also provided an analytical model with a quadratic polynomial trial function considering shear deformation, rotatory inertia and centreline extensibility and the equations of motion were solved by an extension of the classic Galerkin method. Tarnopolskaya and Hoog (1996) demonstrated the coupling between the membrane and flexural modes of curved beams using asymptotic analysis. The curvature function is used to define the shape of curved beams. Experiments with piezo-electric foils confirm the validity of the asymptotic approximation for high mode-number extensional vibrations. Tseng *et al*. (1997) developed an approach which introduces the concept of dynamic stiffness matrix into a series solution for in-plane vibrations of arches with variable curvature. The variable coefficients were expressed in their Taylor expansion series about a point on the arch. The first six modes for parabolic and elliptic arches with various boundary conditions are calculated. Huang *et al*. (1998) developed an exact solution for in-plane vibration of arches with variable curvature as well as cross section using the Frobenius method combined with the dynamic stiffness method. Examples for a series of

parabolic arches show the effects of rise to span length, slenderness ratio and variation of cross section. Oh *et al*. (1999) investigated the in-plane vibrations of non-circular arches such as parabolic, elliptic and sinusoidal including the effects of rotatory inertia, shear and axial deformations. The governing equations are solved numerically and the lowest four natural frequencies are obtained. A buckling formulation for anisotropic variable curvature panels is presented by Jaunky *et al*. (1999). The segment approach was used where displacements fields within each shell segment are represented by Bezier polynomials. Ambur (2001) applied the same method to the optimal design of grid-stiffened panels with variable curvature. Many researcher such as Leung and Zhou (1995) and Kim *et al*. (2003) adopt dynamic stiffness matrix methods to solve vibrations of non-uniform curved beams. The proposed approach basically introduces the concept of dynamic stiffness matrix into a series solution in terms of polynomials which are derived as explicit expressions of displacement functions for governing equations. The arch under consideration is decomposed into several spans with different radii of curvature and in each sub-domain. For the system with many variables, numerical scheme on the quadratic eigenproblem in calculating the exact dynamic stiffness matrix is more efficient and successful.

In addition to the papers introduced above which studied the variable cross section, Suzuki and Takahashi (1977), Irie *et al*. (1980) and Sakiyama (1985) also made contributions in the earlier stage. Laura and Irassar (1988) studied the arches with linear varying thickness. Most recently, Wu and Chiang (2003) constructed a hybrid beam by using an arch segment connected with a straight beam segment at each of its two ends.

- Material parameter

Geist (1998) applied the asymptotic formulae to the variable mass density and show how the natural frequencies of the Timoshenko beam depend on the material and geometric parameters which appear in the differential equations. In Awrejcewicz (1999)’s paper, the doubly curved shells considered were constituted by isotropic material which shows in-plane non-homogeneity in the sense that Young’s modulus is taken as a function of the in-plane shell coordinate. Forster and Weidl (2006) proved the existence of trapped

modes in elastic strips perturbed by local changes of Young's modulus. The asymptotic formula is derived to describe the behaviour of the trapped modes in the limit case of small differences of Young's modulus.

Research work on the static and the dynamic behaviour of curved structures is mostly limited to the isotropic material. Only a few papers were devoted to composite materials. Composite materials show the benefits of high strength-weight ratio and corrosion-resistance through careful design. Researchers have developed various theories for analyzing the laminated composite structures. Based on the singular layer equivalent assumption, the classical laminate theory (CLT) (Love, 1888) and the first-order shear deformation theory (FSDT) (Reissner, 1945; Mindlin, 1951) are developed. Accounting for transverse shear deformations, the higher-order shear deformation theory (HSDT) (Reddy, 1984) is developed. Nosier and Reddy (1992) processed the vibration and stability analysis of cross-ply laminated circular cylindrical shells. Lam and Loy (1995) studied the influence of boundary conditions on laminated thin cylindrical shells. Noor and Burton (1996) classified a number of references on vibration of sandwich panels and shells. Bardell *et al*. (1997) analyzed vibrations of thin laminated cylindrically curved panels using finite element method. Yahnioglu and Selim (2000) investigated some bending problems for a composite strip with a periodically curved structure. Results show that the effect of the geometrical nonlinearity on the foregoing stress distribution decays with changes in material properties. Tseng *et al*. (2000) based on the Timoshenko curved beam theory, studied the free vibration of composite laminated beams of variable curvature. The dynamic stiffness method is used to overcome the difficulty of convergence ratios for the whole beam by the subdividing of sub-domains. For elliptic arches, the effects of stacking sequence, short and long axes ratios, material orthotropic ratio, and opening angles on the natural frequencies are also studies. Bozhevolnaya and Frostig (2001) modelled the curved sandwich beams with a transversely flexible core. Wang (2001) studied the flexural behaviour of the composite curved beam with variable curvature and demonstrated the delamination phenomena. Fares *et al*. (2003) based on the higher-order shell theory, derived formulations to design the orthotropic laminated spherical and cylindrical shells. The discrepancy between different theories is

investigated by numerical examples. Towfighi and Kundu (2003) studied elastic wave propagation problem in anisotropic curved plates. Bozhevolnaya and Sun (2004) studied free vibrations of singly curved sandwich beams by applying the Galerkin method. The model takes into consideration both radial and circumferential displacements of the beam core with the assumption of linear distribution across the thickness. The faces of the sandwich are treated as thin beams. It is shown that there are four types of eigen-modes and a coupling coefficient is introduced to study the dynamic coupling of motions in these types of eigen-modes.

1.2.4 Approaches

Mathematical models are differential equations with a set of corresponding boundary and initial conditions. The differential equations are derived by applying the fundamental laws and principles of nature to a system or a control volume. These governing equations represent balance of mass, force, or energy. When possible, the exact solution of these equations renders detailed behaviour of a system under a given set of conditions. The analytical solutions are composed of two parts: a homogenous part and a particular part. In any given engineering problem, there are two sets of parameters that influence the way in which a system behaves. First, there are those parameters that provide information regarding the natural behaviour of a given system. These parameters include properties such as modulus of elasticity, thermal conductivity, and viscosity. On the other hand, there are parameters that produce disturbances in a system. Examples of these parameters include external forces, moments, temperature difference across a medium, and pressure difference in fluid flow. The system characteristics dictate the natural behaviour of a system, and they always appear in the homogenous part of the solution of a governing differential equation. In contrast, the parameters that cause the disturbances appear in the particular solution. It is important to understand the role of these parameters in finite element modelling in terms of their respective appearances in stiffness or conductance matrices and load or forcing matrices. The system characteristics will always show up in the stiffness matrix, conductance matrix, or resistance matrix, whereas the disturbance parameters will always appear in the load matrix.

The closed form solution for either the curved beam or the shell panel is obtained from the determination of the displacement expressions in the equations of motions. These expressions of the displacement need to be satisfied with the boundary conditions. The curvature brings the coupling effect into the governing equations, so even for one dimensional curved beam, it is difficult to obtain the exact solution for either every kind of curvature or every boundary condition. In order to obtain the analytical solutions, the task is to find the homogenous and particular part of the displacement expressions. However, the disturbances caused by curvature exist in the particular solution. It could be more complex if nonlinearity is introduced into vibration modes. Other than straightforward solution of the differential equations, many other approaches are used to obtain the approximate solutions, from analytical methods such as Rayleigh-Ritz method, Galerkin method and asymptotic methods etc. to the numerical method such as the finite strip method and the finite element method etc.

- Energy method

Carmichael (1959) demonstrated the Rayleigh-Ritz method through an analysis which was made of the vibration of a rectangular plate whose edges are elastically restrained against rotation. Plate deflections are represented by a set of functions which define the normal modes of vibration of a beam whose ends are elastically restrained against rotation. Values of various integrals of these functions and their derivatives are established. Frequencies are obtained from a set of linear simultaneous equations which may be solved by a simple iterative process. Based on the generalized Green Function, Lin (1998) gave the exact solution for static analysis of an extensible circular curved Timoshenko beam with non-homogeneous elastic boundary conditions. A finite element method can be developed based on the results for the dynamic analysis. Liew and Feng (2000) used energy method for the three dimensional elasticity solutions for free vibrations of conical shell panels with cantilevered and clamped boundary conditions.

- Asymptotic method

As one of the asymptotic method, perturbation method has the advantage in obtaining

approximate theoretical solutions. The governing equations involve the variable parameter of curvature which introduces the nonlinear terms. When the equations of motion or boundary conditions have the nature of nonlinearity, closed form solutions cannot be found. Perturbation techniques like the method of multiple scales are used to study local dynamics of weakly nonlinear systems about an equilibrium state. To obtain an approximate analytical solution of a weakly nonlinear continuous system, one can either directly apply a perturbation method to the governing partial-differential equation of motion and boundary conditions, or first discretize the partial-differential system to obtain a reduced-order model and then apply a perturbation method to the nonlinear ordinary-differential equations of the reduced-order model (Pramod, 2003). In general, a limiting solution or a class of solutions are dependent on the parameter with a limiting value (Cole, 1968). Boyce and Goodwin (1964) used the perturbation approach for the solution of the eigenvalue problem of random strings and beams. Evensen (1968) solved the governing nonlinear differential equation of beams with various boundary conditions using the perturbation method. Tarnopolskaya *et al*. (1999) use the perturbation method to obtain the natural frequency and mode shape of circular and s-shaped curved beams. The features of mode transition phenomenon are revealed clearly and the effect of beam curvature is explained physically. However, the analytic approximations are up to the first order; therefore the analysis is limited to the low-frequency natural modes. Nayfeh and Arafat (2000) gave an overview of the perturbation methods used to obtain analytical solutions of nonlinear dynamical systems.

- Finite element method

There are many practical engineering problems for which we cannot obtain exact solutions. This inability to obtain an exact solution may be attributed to either the complex nature of governing differential equations or the difficulties that arise from dealing with the boundary and initial conditions. To deal with such problems, we resort to numerical approximations In contrast to analytical solutions, which show the exact behaviour of a system at any point within the system, numerical solutions approximate exact solutions only at discrete points, called nodes. The first step of any numerical procedure is discretization. This process divides the medium of interest into a number of

small sub-regions and nodes. There are two common classes of numerical methods: the finite difference method and the finite element method. With finite difference methods, the differential equation is written for each node, and the derivatives are replaced by difference equations. This approach results in a set of simultaneous linear equations. Although finite difference methods are easy to understand and employ in simple problems, they become difficult to apply to problems with complex boundary conditions. This situation is also true for problems with non-isotropic material properties. In contrast, the finite element method uses integral formulations rather than difference equations to create a system of algebraic equations. Moreover, an approximate continuous function is assumed to represent the solution for each element. The complete solution is then generated by connecting or assembling the individual solutions, allowing for continuity at the inter-elemental boundaries.

Yang and Sin (1995) created the two-, three-, four- and five-node Timoshenko beam elements which include the effects of shear deformation and rotary inertia. The elements are formulated in terms of curvature, and hence can present fully the total potential energy including the bending energy and the shear energy. Hinton, *et al*. (1995) derived finite strip method which uses a combination of finite elements and Fourier series to analyze curved shell panels with uniform geometrical and material properties in a particular direction. Jones (1996) described the extension of an existing isotropic thin shell element to a new element. This new element is formulated based upon Flügge's thin shell theory, with the capability of modelling curved laminated orthotropic structures. The proposed element is found to yield consistently accurate results in the inextensional and extensional regimes of flexural motion without membrane locking. Chakravorty *et al*. (1996) applied a finite element analysis to the free vibration behaviour of doubly curved laminated composite shells. They investigated the effects of various composite parameters such as fibre orientations and lamination schemes and several geometrical parameters like aspect ratio, smaller height to greater height ratio, thickness to radius ratio, and radii of curvature ratio. Bardell *et al*. (1997) used the finite element method to furnish a detailed study of vibration characteristics of completely free, open, cylindrically curved, isotropic shell panels. Reddy *et al*. (1997) demonstrated an elementary exposition

of locking-free shear deformable beam finite element models based on different beam theories. Friedman and Kosmatka (1998) created a two-node finite element with capability to model curved geometry exactly and obtain exact results in static and dynamic analysis. Bardell, *et al*. (1997) gave the *h*-*p* version of the finite element method to furnish a detailed study of the vibration characteristics of completely free, open, cylindrically curved, isotropic shell panels. Results illustrated interesting features of the natural behaviour of curved panels due to the increase in the curvature. Moser *et al*. (1999) illustrated the effectiveness of using the FE method to model guided wave propagation problems. In recent years, Raveendranath *et al*. (2000) investigated the performance of a curved beam finite element with a coupled polynomial displacement field. Cunningham, *et al*. (2000) used commercial FEM codes to validate the experimental results of free vibration of doubly curved sandwich panels and investigated the effects of changing radii of curvature on the natural frequencies of vibration. Raveendranath *et al*. (2000), in order to avoid the membrane locking phenomenon, developed two nodes curved beam element based on a coupled polynomial displacement field. Litewka and Rakowski (2000) created a new element by making use of the exact static shape functions in the stiffness matrix and the mass matrix to analyze the shear and compressibility effects on the natural frequency of arches. Nayak *et al*. (2002) developed new element based on Reddy's higher-order theory. Wu and Chiang (2003, 2004) reviewed various curved beam elements for natural vibration analysis and derived the simple implicit shape functions, which are associated with the tangential, radial and rotational displacements of the arch element. Ribeiro (2004) applied a *p*-version, hierarchical finite element to the curved, moderately thick, elastic and isotropic beam. Geometrically non-linear vibrations due to finite deformations are investigated. The influence of the thickness, longitudinal inertial and curvature radius on the dynamic behaviour of curved beams are studied. Wu and Chiang (2004) presented a simple approach to obtain the 18 unknown constants for the three displacement functions. By means of the displacement functions, the stiffness and mass matrices of each arch element are calculated and then the free vibration analysis of the arches is performed. Chen (2005) gave full review and demonstration of the development of differential quadrature element method (DQEM) in-plane vibration analysis model of arbitrarily

curved beam structures.

1.3 The Present Work

The present thesis locates the research emphasis on the impact of arbitrary and variable curvatures on the natural behaviour of the curved beam and the curved plate. Based on the comprehensive literature reviews, summations and achievements of the present research are given as follows:

Firstly, many researches demonstrated behaviours of the curved structures as results but seldom found the deep relationship between changes in the curvature with natural vibration behaviours. The present work proves this relationship which shows mode transition behaviours with kinds of regulations. Further, this relationship is substantially impacted by various boundary conditions, which is also proved by both theoretical and numerical solutions.

Secondly, analytical methods are hardly used to solve equations of motion of curved beams with variable parameters until the perturbation technology are used to decouple the flexure vibration and the extensional vibration. The present research further develops the Tarnopolskaya and Hoog's work (1999) to the second order perturbation approximations which gives more accurate results.

Thirdly, the curved plate problem are solved based on thin shell theories in the published works, but analytical solutions are only limited to the specific curvature and boundary condition. In the present thesis, the perturbation approximations of curved beams are adopted by the energy method to obtain the natural frequencies of curved plates with variable curvatures.

Fourthly, it is shown that the present method is not only applicable to the continuous varying curvature problem but also to the curved beam with other kind of curvatures.

Finally, the investigation is extended to the laminated curved beams with different lamina orientation and stacking sequence, which reveals extra characteristics brought by the composite materials.

1.4 Layout of the Thesis

The present research comprises both analytical and numerical methods. From the derivation of governing equations to the post-process solutions, the procedure is organised in the following manner. Chapter One introduces the research background, reviews the publications on the dynamic and static behaviour of curved structures, summarizes the analytical approaches and proposes the motivation and achievements of this work. Chapter Two develops the fundamental formulations of a curved surface. The equations of motion are derived for the curved beam with variable curvature. The non-dimensional equations and boundary conditions are demonstrated as well. Chapter Three demonstrates the solution procedure. The perturbation method is used to simplify the equations to obtain their approximate solutions. The relationship between eigenvalue and curvature is formulated. The simplified equations are used to interpret mode transition phenomena physically due to the changes of curvatures. Finite element method is introduced in Chapter Four. Numerical models are established by using the commercial code ANSYS (2002). In Chapter Five, examples of the curved beams with various types of curvatures are given to illustrate the effects of curvature on the natural characteristic. Curved beams with constant curvature and varying curvature are calculated respectively. Different boundary conditions are also considered. Numerical results from ANSYS code support analytical ones. Some new characteristics of curved beams revealed by numerical results are demonstrated, which leads to the limitation of the current analytical solutions. Chapter Six gives examples for curved beam with arbitrary curvatures. The analysis is extended to the curved plate through the Rayleigh energy method in Chapter Seven. The two-dimensional natural modes are demonstrated. Chapter Eight investigates the effects on the laminated composite curved beams by taking orthotropic laminated material properties back into the dimensionless solutions. Chapter Nine concludes on the present work and summarizes the effects of curvature on the natural characteristics of the curved beam and the curved plates. Recommendations for future work are proposed.

The structure of the present thesis is illustrated in Figure 1.2.

Figure 1.1 Structure of the thesis

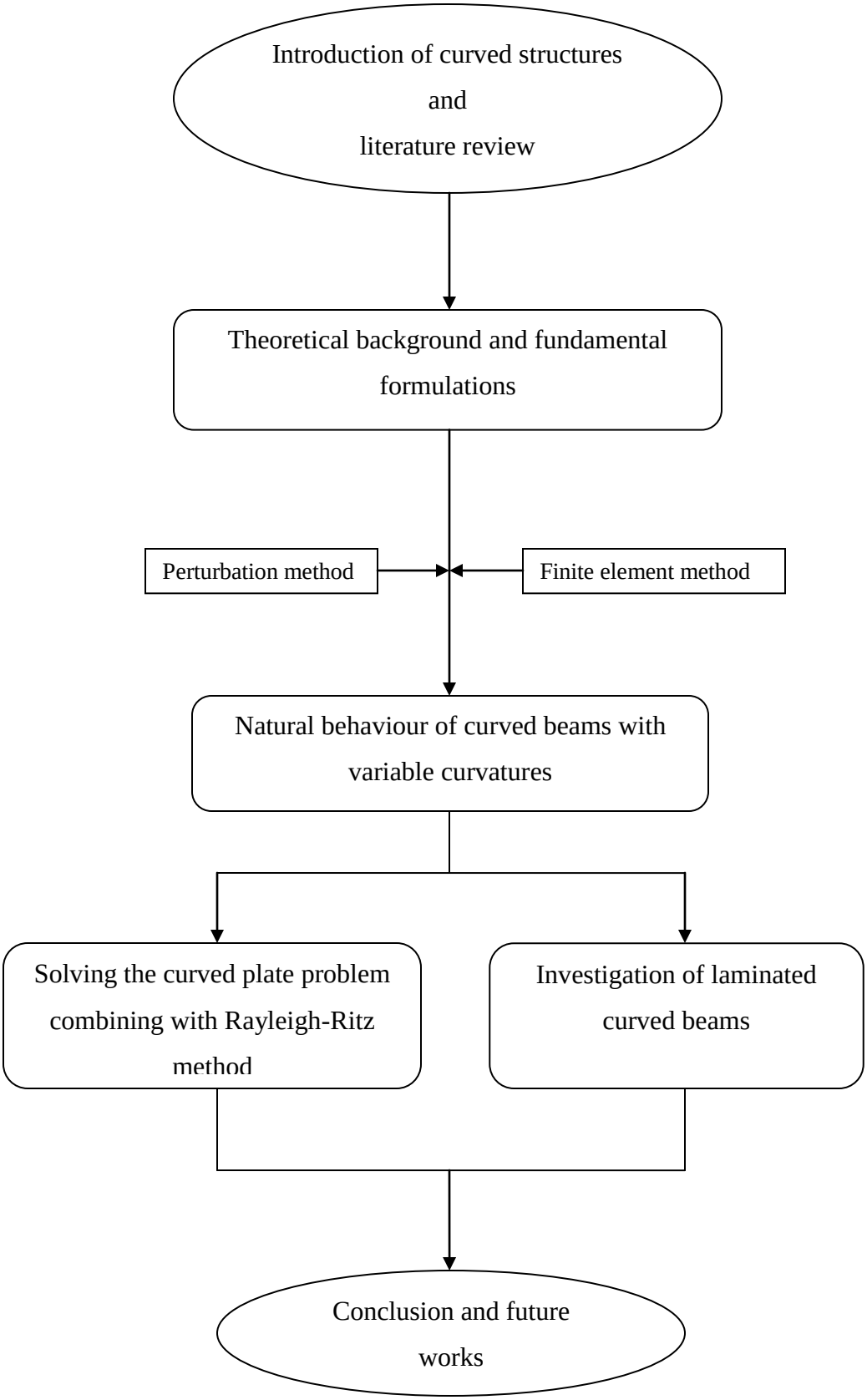

Chapter 2
Theoretical Formulations

The deformation of a curved body may be described geometrically by means of its middle surface, its edge-line and its thickness. In the three-dimensional coordinate system, the curved body is bounded by two closely spaced curved surfaces, the distance between the surfaces being small in comparison with the other dimensions. For the purpose of developing a general method of treatment of the problem of curved beams and curved plates, this chapter presents straightforward derivations of the sets of general formulations relating to the element of the theory of the curvature of surfaces (Huang *et al*. 1988). The equations of motion are derived based on these theoretical formulations.

2.1 Brief Outline of the Theory of Surfaces

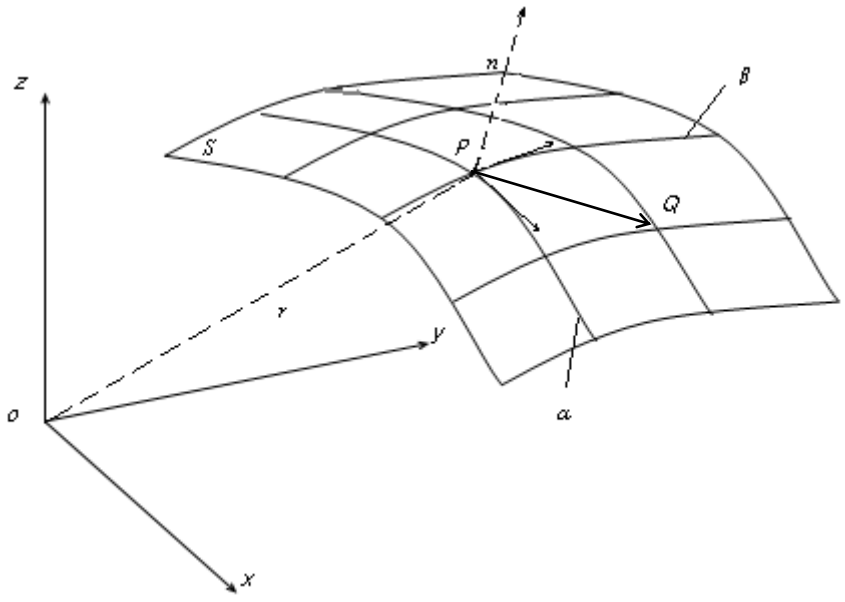

Figure 2.1 sketch of the curved surface

As shown in Figure 2.1, a surface *S* is defined, in a rectangular coordinate system o-*xyz* as follows:

$$x = x(\alpha, \beta), y = y(\alpha, \beta), z = z(\alpha, \beta). \quad (2\text{-}1)$$

where the coordinates *x*, *y*, *z* are the functions of the curvilinear coordinates (α, β) of the surface. Assume that the parameters α and β always vary within a definite region, the position vector of a point *P* on the un-deformed surface is represented by:

$$\vec{r} = \vec{r}(\alpha, \beta). \quad (2\text{-}2)$$

For a neighbouring point *Q* near to the point *P*, the vector $\overrightarrow{PQ}$ can be obtained using Taylor formulation,

$$\overrightarrow{PQ} = \left\{\frac{\partial \vec{r}}{\partial \alpha}d\alpha + \frac{\partial \vec{r}}{\partial \beta}d\beta + \frac{1}{2!}\left[\frac{\partial^2 \vec{r}}{\partial \alpha^2}(d\alpha)^2 + 2\frac{\partial^2 \vec{r}}{\partial \alpha \partial \beta}d\alpha d\beta + \frac{\partial^2 \vec{r}}{\partial \beta^2}(d\beta)^2\right] + \cdots\right\}, \quad (2\text{-}3)$$

which is approximately,

$$\overrightarrow{PQ} \approx d\vec{r} = \frac{\partial \vec{r}}{\partial \alpha}d\alpha + \frac{\partial \vec{r}}{\partial \beta}d\beta. \quad (2\text{-}4)$$

Assume that $\overrightarrow{e_\alpha}$ and $\overrightarrow{e_\beta}$ are two unit vectors or base vectors along α and β directions, respectively, and $\boldsymbol{e}_n$ (α, β) a unit normal vector at point *P*.

$$\frac{\partial \vec{r}}{\partial \alpha} = A\overrightarrow{e_\alpha}, \quad \frac{\partial \vec{r}}{\partial \beta} = B\overrightarrow{e_\beta}, \quad \overrightarrow{e_\alpha} \cdot \overrightarrow{e_\beta} = \cos\chi, \quad \overrightarrow{e_n} = \frac{\overrightarrow{e_\alpha} \times \overrightarrow{e_\beta}}{\sin\chi}. \quad (2\text{-}5)$$

We can define χ as the angle between these two base vectors, where *A* and *B* represent the length of related vectors, respectively.

2.1.1 The first quadratic form of the surface

The square of the length of a line element $d\vec{r}$ is defined as the first quadratic form of the surface, that is,

$$\mathrm{I} = (ds)^2$$

$$= d\vec{r} \cdot d\vec{r}$$

$$= \left(\frac{\partial \vec{r}}{\partial \alpha} d\alpha + \frac{\partial \vec{r}}{\partial \beta} d\beta\right) \cdot \left(\frac{\partial \vec{r}}{\partial \alpha} d\alpha + \frac{\partial \vec{r}}{\partial \beta} d\beta\right)$$

$$= A^2 (d\alpha)^2 + 2AB\cos\chi d\alpha d\beta + B^2 (d\beta)^2$$

$$= [d\alpha \quad d\beta] \begin{bmatrix} A^2 & AB\cos\chi d\alpha d\beta \\ AB\cos\chi d\alpha d\beta & B^2 \end{bmatrix} \begin{bmatrix} d\alpha \\ d\beta \end{bmatrix}. \tag{2-6}$$

2.1.2 The second quadratic form

To the curvature of a curve on the surface, the second quadratic form is introduced, i.e.

$$\mathrm{II} = 2\overrightarrow{PQ} \cdot \overrightarrow{e_n} = \left\{\frac{\partial \vec{r}}{\partial \alpha} d\alpha + \frac{\partial \vec{r}}{\partial \beta} d\beta + \frac{1}{2!}\left[\frac{\partial^2 \vec{r}}{\partial \alpha^2} (d\alpha)^2 + 2\frac{\partial^2 \vec{r}}{\partial \alpha \partial \beta} d\alpha d\beta + \frac{\partial^2 \vec{r}}{\partial \beta^2} (d\beta)^2\right] + \cdots\right\} \cdot \overrightarrow{e_n}$$

$$= L(d\alpha)^2 + 2Md\alpha d\beta + N(d\beta)^2. \tag{2-7}$$

Here, the higher order terms are neglected and the definitions

$$L = \frac{\partial^2 \vec{r}}{\partial \alpha^2} \cdot \overrightarrow{e_n}, \quad M = \frac{\partial^2 \vec{r}}{\partial \alpha \partial \beta} \cdot \overrightarrow{e_n}, \quad N = \frac{\partial^2 \vec{r}}{\partial \beta^2} \cdot \overrightarrow{e_n}. \tag{2-8}$$

are introduced.

2.1.3 Curvature of a curve

As shown in Figure 2.2, an intersection curve of the surface *S* with the plane *nPQ* is drawn. The curvature at point P of the intersection curve is defined as follows:

$$K = \frac{1}{R} = \frac{d\alpha}{dS}, \tag{2-9}$$

where,

$$\overrightarrow{PQ} \cdot n = \overline{PQ} \cos\left(\frac{\pi}{2} + \frac{d\alpha}{2}\right) = -|\overline{PQ}| \sin\frac{d\alpha}{2} \approx -\frac{1}{2}|\overline{PQ}| \cdot d\alpha, \tag{2-10}$$

Assume τ is the tangent to a curve on the surface

and,

$$dS = \sqrt{\overrightarrow{PQ} \cdot \overrightarrow{PQ}} = |\overrightarrow{PQ}|, \tag{2-11}$$

Then,

$$K = -\frac{2\overrightarrow{PQ}\cdot n}{|\overrightarrow{PQ}|\cdot|\overrightarrow{PQ}|}$$

$$= -\frac{\mathrm{II}}{\mathrm{I}} = -\frac{L(d\alpha)^2+2Md\alpha d\beta+N(d\beta)^2}{A^2(d\alpha)^2+2AB\cos\chi d\alpha d\beta+B^2(d\beta)^2}. \tag{2-12}$$

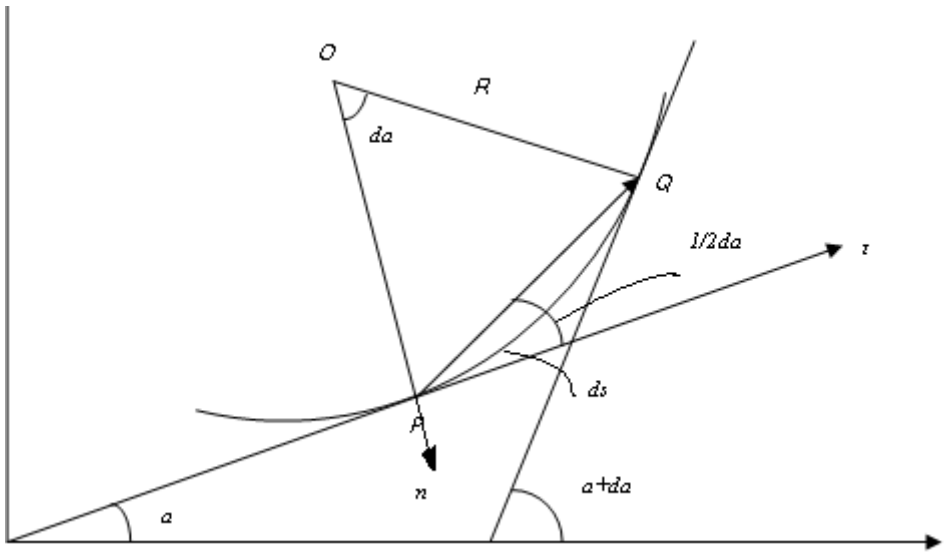

Figure 2.2 definition of curvature

2.2 Deformation of the Surface

2.2.1 Displacement field

Using the Kirchhoff hypothesis, the class of displacements is restricted to the following linear relationships:

$$U(\alpha,\beta,z) = u(\alpha,\beta) + z\theta_{\alpha}(\alpha,\beta), \tag{2-13a}$$

$$V(\alpha,\beta,z) = v(\alpha,\beta) + z\theta_{\beta}(\alpha,\beta), \tag{2-13b}$$

$$W(\alpha,\beta) = w(\alpha,\beta). \tag{2-13c}$$

where *u*, *v* and *w* are the components of displacements at the mid-plane (i.e. *z=0*) in the α, β and normal directions, respectively, and θ_{α} and θ_{β} are the rotations of the normal to the middle surface during deformation about the α and β axes, respectively. Assuming the shear strains are equal to zero, then θ_{α} and θ_{β} are expressed as follows:

$$\theta_{\alpha} = \frac{u}{R_{\alpha}} - \frac{1}{A}\frac{\partial w}{\partial \alpha}, \tag{2-14a}$$

$$\theta_{\beta} = \frac{v}{R_{\beta}} - \frac{1}{B}\frac{\partial w}{\partial \beta}. \tag{2-14b}$$

Figure 2.3 shows a general body in its initial configuration and in its current configuration. Let the body in its un-deformed configuration be Γ_0 and denote the deformed configuration by Γ_1. The initial position of a point *P*, is given by the position vector *r*, and the current point *P'* is given by the position vector *R*. When the surface *S* has strain, a displacement vector of *P* exists as follows:

$$\vec{\Delta}(\alpha,\beta) = U\overrightarrow{e_{\alpha}} + V\overrightarrow{e_{\beta}} + W\overrightarrow{e_{n}}. \tag{2-15}$$

The distance from the origin to a point *P'* of strained surface is as follows:

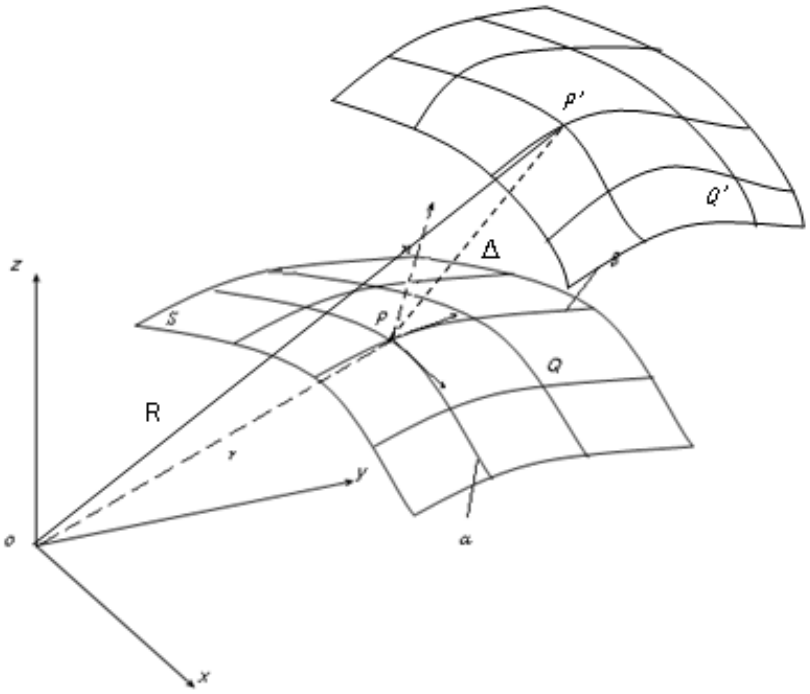

Figure 2.3 the deformation of the curved body from the initial configuration to the current configuration

$$\vec{R}(\alpha,\beta) = \vec{r}(\alpha,\beta) + \vec{\Delta}(\alpha,\beta). \tag{2-16}$$

2.2.2 Strain-displacement equation

The well-known strain-displacement equations of the three-dimensional theory of elasticity in orthogonal curvilinear coordinates are derived in Appendix I shown as follows:

$$\epsilon_\alpha = \frac{P'Q'_\alpha - PQ_\alpha}{PQ_\alpha} = \frac{A'-A}{A} = \frac{1}{A}\frac{\partial U}{\partial \alpha} + \frac{V}{AB}\frac{\partial A}{\partial \beta} + \frac{W}{R_\alpha}, \tag{2-17a}$$

$$\epsilon_\beta = \frac{P'Q'_\beta - PQ_\beta}{PQ_\beta} = \frac{B'-B}{B} = \frac{1}{AB}\frac{\partial B}{\partial \alpha} + \frac{U}{B}\frac{\partial V}{\partial \beta} + \frac{W}{R_\beta}, \tag{2-17b}$$

$$\epsilon_{\alpha\beta} = \frac{A}{B}\frac{\partial}{\partial \beta}\left(\frac{U}{A}\right) + \frac{B}{A}\frac{\partial}{\partial \alpha}\left(\frac{V}{B}\right). \tag{2-17c}$$

where e_α, $e_\beta$and $e_{\alpha\beta}$ are strains at an arbitrary point of the curved body. Substituting the

displacement field into above equations, strains at any arbitrary point of the curved thin shell based on Love and Timoshenko theories (Reddy and Wang 1997) are expressed as follows:

$$\epsilon_\alpha = \varepsilon_\alpha + z\kappa_\alpha, \tag{2-18a}$$

$$\epsilon_\beta = \varepsilon_\beta + z\kappa_\beta, \tag{2-18b}$$

$$\epsilon_{\alpha\beta} = \varepsilon_{\alpha\beta} + z\tau. \tag{2-18c}$$

where ε_α, ε_β and $\varepsilon_{\alpha\beta}$ represent strains on the middle surface; κ_α and κ_β are the middle surface changes in curvature and $\kappa_{\alpha\beta}$ is the middle surface twist, given by (Qu and Tang 2000)

$$\kappa_\alpha = \frac{1}{A}\frac{\partial \theta_\alpha}{\partial \alpha} + \frac{1}{AB}\frac{\partial A}{\partial \beta}\theta_\beta = \frac{1}{A}\frac{\partial}{\partial \alpha}\left(\frac{u}{R_\alpha} - \frac{1}{A}\frac{\partial w}{\partial \alpha}\right) + \frac{1}{AB}\frac{\partial A}{\partial \beta}\left(\frac{v}{R_\beta} - \frac{1}{B}\frac{\partial w}{\partial \beta}\right), \tag{2-19a}$$

$$\kappa_\beta = \frac{1}{B}\frac{\partial \theta_\beta}{\partial \beta} + \frac{1}{AB}\frac{\partial B}{\partial \alpha}\theta_\alpha = \frac{1}{B}\frac{\partial}{\partial \beta}\left(\frac{v}{R_\beta} - \frac{1}{B}\frac{\partial w}{\partial \beta}\right) + \frac{1}{AB}\frac{\partial B}{\partial \alpha}\left(\frac{u}{R_\alpha} - \frac{1}{A}\frac{\partial w}{\partial \alpha}\right), \tag{2-19b}$$

$$\kappa_{\alpha\beta} = \frac{1}{A}\frac{\partial \theta_\beta}{\partial \alpha} + \frac{1}{A}\frac{\partial \theta_\beta}{\partial \alpha} + \frac{1}{R_\alpha}\left(\frac{1}{B}\frac{\partial u}{\partial \beta} - \frac{v}{AB}\frac{\partial B}{\partial \alpha}\right) + \frac{1}{R_\beta}\left(\frac{1}{A}\frac{\partial v}{\partial \alpha} - \frac{u}{AB}\frac{\partial A}{\partial \beta}\right). \tag{2-19c}$$

2.2.3 Constitutive equations

The integration of the stresses through the thickness leads to the constitutive equation, which is expressed in terms of the 3×3 extensional, extensional-bending coupling, and bending stiffness matrices as follows:

$$\mathbf{N} = \mathbf{A}\boldsymbol{\varepsilon} + \mathbf{B}\boldsymbol{\kappa}, \tag{2-20a}$$

$$\mathbf{M} = \mathbf{B}\boldsymbol{\varepsilon} + \mathbf{D}\boldsymbol{\kappa}. \tag{2-20b}$$

where **N** and **M** are the resultant force matrix and moment matrix, respectively. Considering the general single layer equivalent theory, the stiffness matrices **A**, **B, D** for the *n* layers laminates are derived in Appendix II.

2.3 Equilibrium Equations

The equations of equilibrium are formed by equating to zero the resultant force and resultant moment of all the forces applied to a portion of the shell. Define the force and moment vector on a shell element shown in Figures 2.4 and 2.5 as follows:

$$\overrightarrow{N_\alpha} = N_\alpha \overrightarrow{e_\alpha} + N_{\alpha\beta}\overrightarrow{e_\beta} + Q_\alpha \overrightarrow{e_n}, \qquad \overrightarrow{N_\beta} = N_\beta \overrightarrow{e_\beta} + N_{\beta\alpha}\overrightarrow{e_\alpha} + Q_\beta \overrightarrow{e_n}, \tag{2-21a}$$

$$\overrightarrow{M_\alpha} = M_{\alpha\beta}\overrightarrow{e_\alpha} - M_\alpha \overrightarrow{e_\beta}, \qquad \overrightarrow{M_\beta} = M_\beta \overrightarrow{e_\alpha} - M_{\beta\alpha}\overrightarrow{e_\beta}. \tag{2-21b}$$

Assuming $\vec{q}$ is the contribution force on the unit area, the equilibrium of the force and moment on this element are expressed as follows:

$$\frac{\partial}{\partial\alpha}\left(\overrightarrow{N_\alpha}B\right) + \frac{\partial}{\partial\beta}\left(\overrightarrow{N_\beta}A\right) + \vec{q}AB = 0, \tag{2-22a}$$

$$\frac{\partial}{\partial\alpha}\left(\overrightarrow{M_\alpha}B\right) + \frac{\partial}{\partial\beta}\left(\overrightarrow{M_\beta}A\right) + A\overrightarrow{e_\alpha} \times \overrightarrow{N_\alpha}B + B\overrightarrow{e_\beta} \times \overrightarrow{N_\beta}A = 0. \tag{2-22b}$$

Substituting equations (2-21) into equation (2-22), six equilibrium equations projected in three directions can be obtained as follows:

$$\frac{1}{AB}\left(\frac{\partial BN_\alpha}{\partial\alpha} + \frac{\partial AN_{\beta\alpha}}{\partial\beta} + \frac{\partial A}{\partial\beta}N_{\alpha\beta} - \frac{\partial B}{\partial\alpha}N_\beta\right) + \frac{Q_\alpha}{R_\alpha} + q_\alpha = 0, \tag{2-23a}$$

$$\frac{1}{AB}\left(\frac{\partial BN_{\alpha\beta}}{\partial\alpha} + \frac{\partial AN_\beta}{\partial\beta} + \frac{\partial B}{\partial\alpha}N_{\beta\alpha} - \frac{\partial A}{\partial\beta}N_\alpha\right) + \frac{Q_\beta}{R_\beta} + q_\beta = 0, \tag{2-23b}$$

$$\frac{1}{AB}\left(\frac{\partial BQ_\alpha}{\partial\alpha} + \frac{\partial AQ_\beta}{\partial\beta}\right) - \frac{N_\alpha}{R_\alpha} - \frac{N_\beta}{R_\beta} + q_n = 0, \tag{2-23c}$$

$$\frac{1}{AB}\left(\frac{\partial BM_\alpha}{\partial\alpha} + \frac{\partial AM_{\beta\alpha}}{\partial\beta} + \frac{\partial A}{\partial\beta}M_{\alpha\beta} - \frac{\partial B}{\partial\alpha}M_\beta\right) - Q_\alpha = 0, \tag{2-23d}$$

$$\frac{1}{AB}\left(\frac{\partial BM_{\alpha\beta}}{\partial\alpha} + \frac{\partial AM_\beta}{\partial\beta} + \frac{\partial B}{\partial\alpha}M_{\beta\alpha} - \frac{\partial A}{\partial\beta}M_\alpha\right) - Q_\beta = 0, \tag{2-23e}$$

$$N_{\alpha\beta} - N_{\beta\alpha} - \frac{M_{\alpha\beta}}{R_\alpha} + \frac{M_{\beta\alpha}}{R_\beta} = 0. \tag{2-23f}$$

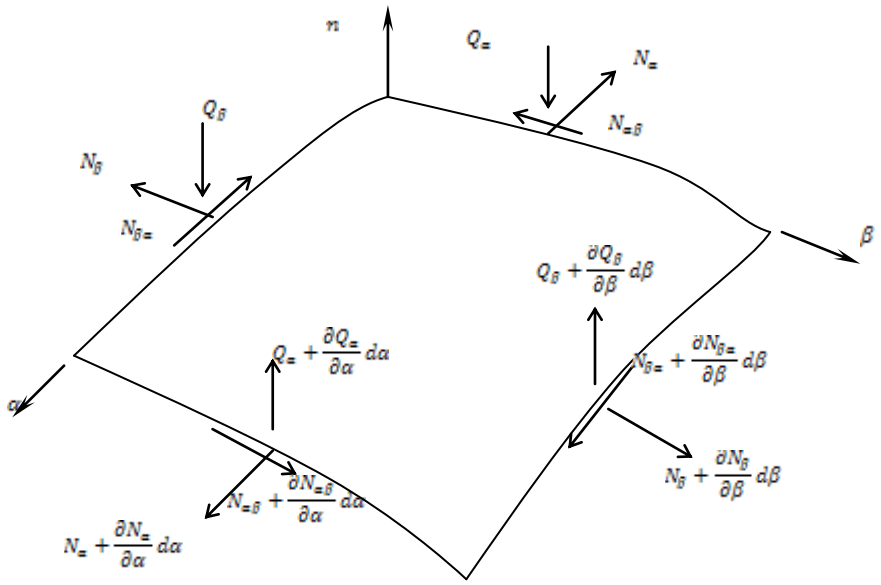

Figure 2.4 notation and positive directions of force resultants in shell coordinates

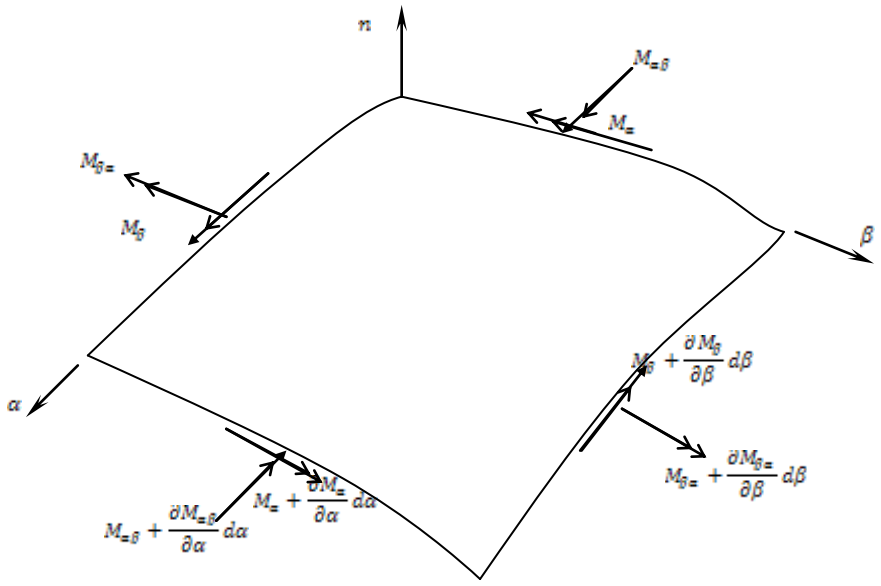

Figure 2.5 notation and positive directions of moment resultants in shell coordinates

Considering the natural vibration of a single curved beam, in the planar coordinate system shown in Figure 2.4 and Figure 2.5, let $\alpha = s$, $\beta = x$ and $A = B = 1$, where *s is* the circumferential coordinate measured around the centreline; *x* and *z* are the principal axis of the beam cross-section; *r* is the general radial coordinate. Assume there is no strain in the lateral *x* direction and consider the equilibrium of the forces on an element of the

beam shown in Figure 2.6, the following equations can be obtained:

In tangential direction $$\frac{\partial N_s}{\partial s} + \frac{Q_s}{R_s} = \rho A' \frac{\partial^2 u}{\partial t^2}\,, \tag{2-24a}$$

In radial direction $$\frac{\partial Q_s}{\partial s} - \frac{N_s}{R_s} = \rho A' \frac{\partial^2 w}{\partial t^2}\,, \tag{2-24b}$$

Moment equilibrium $$\frac{\partial M_s}{\partial s} = Q_s\,. \tag{2-24c}$$

where ρ is the density, *A'* is the area of the cross section per unit width, *u* is the tangential displacement, *w* is the radial displacement of the mid-surface, M_s is the bending moment, N_s is the tensile force and Q_s is the shear force. The second derivative of the displacement about time *t* gives the acceleration, which shows inertia after multiply by the mass ρ*A'*. Substituting the curvature *k*, defined as $k = \frac{1}{R_s}$, and equation (2-24c) into equation (2-24a) and (2-24b), results in:

$$k\frac{\partial M_s}{\partial s} + \frac{\partial N_s}{\partial s} = \rho A' \frac{\partial^2 u}{\partial t^2}\,, \tag{2-25a}$$

$$\frac{\partial^2 M_s}{\partial s^2} - kN_s = \rho A' \frac{\partial^2 w}{\partial t^2}\,. \tag{2-25b}$$

It is also assumed that velocity in *x* direction is zero, which leads to resultant forces N_x, N_{xs} and moments M_x, M_{xs} being equal to zero. Therefore, the constitutive behaviour of the curved beam, in terms of mid-plane values and resultant quantities is expressed as follows:

$$\begin{bmatrix} N_s \\ M_s \end{bmatrix} = \begin{bmatrix} A_{11} & B_{11} \\ B_{11} & D_{11} \end{bmatrix} \begin{bmatrix} \varepsilon_s \\ \kappa_s \end{bmatrix}. \tag{2-26}$$

where A_{11} is the tension stiffness, B_{11} is the coupling stiffness and D_{11} is the flexible stiffness respectively. For an isotropic beam, A_{11} and D_{11} in the governing equations are replaced by the extensional rigidity *A* and flexural rigidity *D*.

According to equations (2-17)-(2-19), for the thin curved beam, when $z \ll R_s$, the

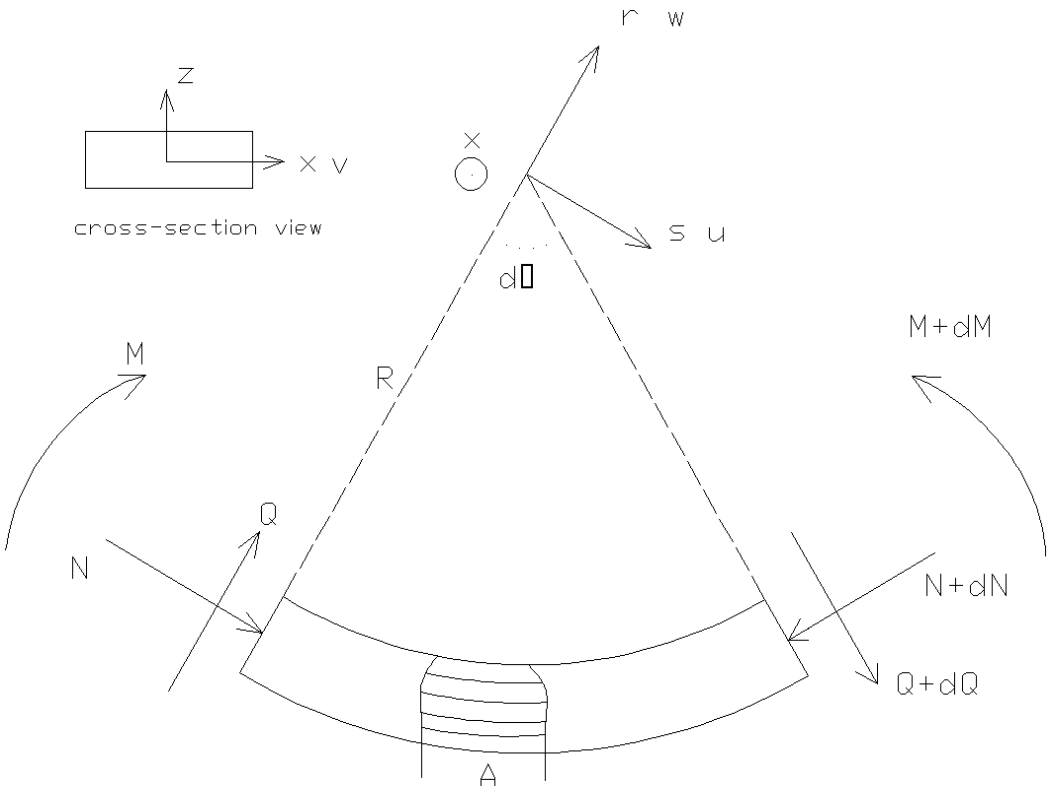

Figure 2.6 sketch of forces on a beam element

strain in *s* direction in terms of the middle surface is express as follows:

$$\varepsilon_s = \frac{\partial u}{\partial s} + kw\,, \tag{2-27a}$$

$$\kappa_s = u\frac{\partial k}{\partial s} + k\frac{\partial u}{\partial s} - \frac{\partial^2 w}{\partial s^2}\,. \tag{2-27b}$$

Assuming the material of the curved beam is balanced and symmetrical in terms of the middle surface, which leads to $B_{11} = 0$, the constitutive equations are thus simplified as follows:

$$N_s = A_{11}\left(\frac{\partial u}{\partial s} + kw\right), \tag{2-28a}$$

$$M_s = D_{11}\left(u\frac{\partial k}{\partial s} + k\frac{\partial u}{\partial s} - \frac{\partial^2 w}{\partial s^2}\right). \tag{2-28b}$$

Omiting the index‘s’ in notations, substituting equation (2-28) into equation (2-25),

equations (2-25) is expanded as follows:

$$D_{11}k\frac{\partial}{\partial s}\left(u\frac{\partial k}{\partial s}+k\frac{\partial u}{\partial s}-\frac{\partial^2 w}{\partial s^2}\right)+A_{11}\frac{\partial}{\partial s}\left(\frac{\partial u}{\partial s}+kw\right)=\rho A'\frac{\partial^2 u}{\partial t^2}, \qquad \text{(2-29a)}$$

$$D_{11}\frac{\partial^2}{\partial s^2}\left(u\frac{\partial k}{\partial s}+k\frac{\partial u}{\partial s}-\frac{\partial^2 w}{\partial s^2}\right)-A_{11}k\left(\frac{\partial u}{\partial s}+kw\right)=\rho A'\frac{\partial^2 w}{\partial t^2}. \qquad \text{(2-29b)}$$

2.4 Dimensionless Governing Equations

In many problems, we are interested in comparing the dimensionless response rather than the actual values, which is of great help when we are comparing results with different properties and performing parametric studies. A transformation to dimensionless variables of the coordinate *s* and the curvature *k* can be made as follows:

$$\bar{s} = \frac{s}{l},\ \bar{k} = kl\ . \tag{2-30}$$

Moreover, the dimensionless axial and transverse displacements are shown as follows:

$$\bar{u} = \frac{u}{l}, \bar{w} = \frac{w}{l}\ . \tag{2-31}$$

where *l* is the length of the beam.

For the sake of convenience, a dimensionless parameter η is introduced by dividing A_{11} at both sides of governing equations,

$$\eta = \frac{1}{l^2}\frac{D_{11}}{A_{11}}\ . \tag{2-32}$$

From equation (2-32) it can be seen that η is the ratio of the flexural stiffness to the tension stiffness. For the isotropic curved beam, it represents the geometrical properties. For the composite material, it also includes the impact of the material property.

Expressing the displacements as harmonic functions of time with frequency ω, i.e. $\bar{u} = \bar{u}e^{i\omega t}$ and $\bar{w} = \bar{w}e^{i\omega t}$, the dimensionless governing equations of the curved beam with variable curvature is then expressed as follows:

$$\eta\bar{k}\frac{\partial}{\partial\bar{s}}\left(\bar{u}\frac{\partial\bar{k}}{\partial\bar{s}} + \bar{k}\frac{\partial\bar{u}}{\partial\bar{s}} - \frac{\partial^2\bar{w}}{\partial\bar{s}^2}\right) + \frac{\partial}{\partial\bar{s}}\left(\frac{\partial\bar{u}}{\partial\bar{s}} + \bar{k}\bar{w}\right) = -\lambda\bar{u}\ , \tag{2-33a}$$

$$\eta\frac{\partial^2}{\partial\bar{s}^2}\left(\bar{u}\frac{\partial\bar{k}}{\partial\bar{s}} + \bar{k}\frac{\partial\bar{u}}{\partial\bar{s}} - \frac{\partial^2\bar{w}}{\partial\bar{s}^2}\right) - \bar{k}\left(\frac{\partial\bar{u}}{\partial\bar{s}} + \bar{k}\bar{w}\right) = -\lambda\bar{w}\ . \tag{2-33b}$$

where λ is the square of the non-dimensional frequency or the non-dimensional

eigenvalue of the system. It is defined as follows:

$$\lambda = \frac{\rho A' l^2 \omega^2}{A_{11}} . \tag{2-34}$$

This non-dimensional eigenvalue is the ratio of the square of natural frequency ω to the square of vibration frequency $\sqrt{A_{11}/\rho A' l^2}$ in tension motion. For our convenience in the following description, we may simply say the non-dimensional frequency λ of the beam in stead of its full definition description mentioned herein.

Equation (2-33) represents the extensional and flexural coupled vibrations of curved beams with general curvature. Since curvature is not limited to constant, non-linear terms are involved in the flexural deformation part of above equations. In the following chapters, the perturbation method is used to simplify the governing equations.

2.5 Boundary Conditions

In addition to the equations of equilibrium and compatibility, the governing equations must satisfy certain boundary conditions. To complete the formulation of the problem where a fourth order differential equation is involved, such conditions corresponding to the edge constraints must be specified. Boundary conditions are applied at both ends of the curved beam, i.e. when $s = 0$ and $s = l$. Following boundary conditions are considered in the present studies. They are:

1. Free end

There is no constraint applied at the end. All DOFs are free. The moment, shear and axial force at the end are equal to zero, shown as follows:

$$M = 0, N = 0, Q = 0, \tag{2-35}$$

according to equation (2-24c) and equation (2-28), equation (2-35) is equivalent to

$$u\frac{\partial k}{\partial s} + k\frac{\partial u}{\partial s} - \frac{d^2 w}{d s^2} = 0, \tag{2-36a}$$

$$\frac{\partial u}{\partial s} + kw = 0, \tag{2-36b}$$

$$\frac{\partial}{\partial s}\left(u\frac{\partial k}{\partial s} + k\frac{\partial u}{\partial s} - \frac{d^2 w}{d s^2}\right) = 0. \tag{2-36c}$$

2. Hinged end

The end of the beam can freely rotate but all displacements are equal to zero, shown as follows:

$$u = 0, w = 0, \tag{2-37a}$$

The moment at the end is also equal to zero, shown as follows:

$$M = 0, \tag{2-37b}$$

according to equation (2-28b), which results in,

$$\left(u\frac{\partial k}{\partial s}+k\frac{\partial u}{\partial s}-\frac{d^2w}{ds^2}\right)=k\frac{\partial u}{\partial s}-\frac{d^2w}{ds^2}=0\,. \tag{2-37c}$$

3. Clamped end

All DOFs are constrained at the end of the beam, shown as follows:

$$u=0,\,w=0. \tag{2-38a}$$

Additionally, the rotation of the mid-surface during the deformation is equal to zero. From equation (2-14), it results in

$$\phi=-\frac{dw}{ds}+uk=0\,. \tag{2-38b}$$

The hinged and clamped conditions provide the extensional constraints on the beam, which is vital to the effects of changing curvatures and will be explained in Chapter Three, section 3.2.

2.6 Summary

The governing equations of curved beams are derived based on the deformation of a curved surface. The curvature k is not limited to a constant value; therefore, the governing equations can be used to solve the natural vibration problem for the curved beam with variable curvature. On the other hand, the variation in curvature brings the extra unknown parameter into the equations. Therefore, the key issue in solving the equations is how to treat the curvature parameter. In the following chapters, the perturbation method is adopted to deal with variable curvature problem.

Chapter 3
Perturbation Analysis

In Chapter two, the non-dimensional governing equations of the curved beam were derived, which is coupled flexural and extensional vibration and also includes the variable curvature parameter. Therefore, it is difficult to solve by the classical analytical methods. By using perturbation techniques, in general, one expects analytic dependence on a small parameter. A solution or a class of solutions are dependent on this parameter with a limiting value. In physical problems, it is important to discover the nature of this dependence by working with various approximate differential equations and to investigate the nature of solutions from perturbation procedures. This chapter will demonstrate the process of using the perturbation technique on the vibration analysis of curved beams.

3.1 Transformation of Governing Equations

The eigenvalue of the vibration beam problem can also be expressed as follows (Qu and Tang 2000):

$$\Lambda = \frac{\rho A' l^4 \omega^2}{D_{11}}. \tag{3-1}$$

This non-dimensional eigenvalue is the ratio of the square of natural frequency ω to the square of vibration frequency $\sqrt{D_{11}/\rho A' l^4}$ in bending motion.

Considering equation (2-34), one can establish the relationship between the eigenvalue and the square of non-dimensional natural frequency as follows:

$$\Lambda = \frac{\lambda}{\eta}. \tag{3-2}$$

Based on the number of oscillations in the non-dimensional amplitude of transverse and longitudinal displacement, estimate for the order of magnitude of terms is as follows:

$$\Lambda \sim O\left(\hat{k}^2\right),\ \hat{u} \sim O\left(\hat{k}^{\frac{1}{2}}\right),\ \hat{w} \sim O(1). \tag{3-3}$$

and leads to the scaled parameters as follows:

$$\hat{k} = \frac{\bar{k}}{\sqrt{\eta}},\ \hat{u} = \frac{\bar{u}}{\sqrt{\eta}},\ \hat{w} = \frac{\bar{w}}{\eta^0}. \tag{3-4}$$

In the dimensionless coordinates, for the sake of keeping the same order of magnitude of terms in the governing equations, substituting equations (3-2) and equation (3-4) into the equation (2-33), results in

$$\eta\hat{k}\frac{\partial}{\partial\bar{s}}\left(\eta\hat{u}\frac{\partial\hat{k}}{\partial\bar{s}} + \eta\hat{k}\frac{\partial\hat{u}}{\partial\bar{s}} - \frac{\partial^2\hat{w}}{\partial\bar{s}^2}\right) + \frac{\partial}{\partial\bar{s}}\left(\frac{\partial\hat{u}}{\partial\bar{s}} + \hat{k}\hat{w}\right) = -\eta\Lambda\hat{u}, \tag{3-5a}$$

$$\frac{\partial^2}{\partial\bar{s}^2}\left(\eta\hat{u}\frac{\partial\hat{k}}{\partial\bar{s}} + \eta\hat{k}\frac{\partial\hat{u}}{\partial\bar{s}} - \frac{\partial^2\hat{w}}{\partial\bar{s}^2}\right) - \hat{k}\left(\frac{\partial\hat{u}}{\partial\bar{s}} + \hat{k}\hat{w}\right) = -\Lambda\hat{w}. \tag{3-5b}$$

The solution to the transformed non-dimensional governing equations (3-5) depends on the parameter ξ defined as follows:

$$\xi = \hat{k}\eta = \hat{k}\frac{1}{l^2}\frac{D_{11}}{A_{11}}. \tag{3-6}$$

which is a dimensionless quantity, determined by both the curvature and the ratio of the flexural stiffness to the extensional stiffness. It is not like η which represents the geometric and material properties. This small parameter ξ also includes the impact from the curvature. For the straight beam, ξ is equal to zero, then equation (3-5) turns out to be the Euler-Bernoulli beam equations. The interesting thing is that the parameter ξ is not linear with the curvature. When the curvature is very small, the flexural stiffness is larger than the extensional stiffness. With the increase in the curvature, a critical point exists when the extensional stiffness predominates the vibration. In consequence, the parameter ξ is controlled in the region of $[0, \xi^0]$. Thus ξ has the feature to be taken as the small parameter to obtain an approximate solution of the eigenvalue problem. This leads to the

change in characteristics of the natural vibration, which will be examined mathematically in the following sections.

Substituting equation (3-6) into equation (3-5), one obtains the following equations:

$$\xi \frac{\partial}{\partial \bar{s}}\left(\frac{\xi \hat{u}}{\hat{k}}\frac{\partial \hat{k}}{\partial \bar{s}} + \xi \frac{\partial \hat{u}}{\partial \bar{s}} - \frac{\partial^2 \hat{w}}{\partial \bar{s}^2}\right) + \frac{\partial}{\partial \bar{s}}\left(\frac{\partial \hat{u}}{\partial \bar{s}} + \hat{k}\hat{w}\right) = -\frac{\xi \Lambda \hat{u}}{\hat{k}}, \tag{3-7a}$$

$$\frac{1}{\hat{k}}\frac{\partial^2}{\partial \bar{s}^2}\left(\frac{\xi \hat{u}}{\hat{k}}\frac{\partial \hat{k}}{\partial \bar{s}} + \xi \frac{\partial \hat{u}}{\partial \bar{s}} - \frac{\partial^2 \hat{w}}{\partial \bar{s}^2}\right) - \left(\frac{\partial \hat{u}}{\partial \bar{s}} + \hat{k}\hat{w}\right) = -\frac{\Lambda \hat{w}}{\hat{k}}. \tag{3-7b}$$

Applying the perturbation technique into equation (3-7), the solution is assumed in the following expansion form:

$$\Lambda(\xi) = \sum_{n=0}^{\infty} \xi^n \Lambda_n, \tag{3-8a}$$

$$\hat{u}(\bar{s}, \xi) = \sum_{n=0}^{\infty} \xi^n \hat{u}_n(\bar{s}), \tag{3-8b}$$

$$\hat{w}(\bar{s}, \xi) = \sum_{n=0}^{\infty} \xi^n \hat{w}_n(\bar{s}). \tag{3-8c}$$

3.2 Zero Order Approximations

The zero order perturbation solutions are easily written as follows:

$$\Lambda(\xi) = \Lambda_0 \, , \hat{u}(\bar{s}, \xi) = \hat{u}_0(\bar{s}) \, , \quad \hat{w}(\bar{s}, \xi) = \hat{w}_0(\bar{s}). \tag{3-9}$$

Substituting the perturbation solutions into equation (3-7), the zero order perturbation equations are obtained as follows:

$$\xi \frac{\partial}{\partial \bar{s}} \left(\frac{\xi}{\hat{k}} \hat{u}_0 \frac{\partial \hat{k}}{\partial \bar{s}} + \xi \frac{\partial \hat{u}_0}{\partial \bar{s}} - \frac{\partial^2 \hat{w}_0}{\partial \bar{s}^2} \right) + \frac{\partial}{\partial \bar{s}} \left(\frac{\partial \hat{u}_0}{\partial \bar{s}} + \hat{k} \hat{w}_0 \right) = - \frac{\xi \Lambda_0 \hat{u}_0}{\hat{k}} \, , \tag{3-10a}$$

$$\frac{1}{\hat{k}} \frac{\partial^2}{\partial \bar{s}^2} \left(\frac{\xi}{\hat{k}} \hat{u}_0 \frac{\partial \hat{k}}{\partial \bar{s}} + \xi \frac{\partial \hat{u}_0}{\partial \bar{s}} - \frac{\partial^2 \hat{w}_0}{\partial \bar{s}^2} \right) - \left(\frac{\partial \hat{u}_0}{\partial \bar{s}} + \hat{k} \hat{w}_0 \right) = - \frac{\Lambda_0 \hat{w}_0}{\hat{k}} \, . \tag{3-10b}$$

Since the leading power of ξ is zero, equations (3-10) are reduced by setting $\xi^{n \geq 1} = 0$ as follows:

$$\frac{\partial}{\partial \bar{s}} \left(\frac{\partial \hat{u}_0}{\partial \bar{s}} + \hat{k} \hat{w}_0 \right) = 0 \, , \tag{3-11a}$$

$$\frac{1}{\hat{k}} \frac{\partial^4 \hat{w}_0}{\partial \bar{s}^4} + \left(\frac{\partial \hat{u}_0}{\partial \bar{s}} + \hat{k} \hat{w}_0 \right) = \frac{\Lambda_0 \hat{w}_0}{\hat{k}} \, . \tag{3-11b}$$

Equations (3-11) are the zero order approximation equations, which eliminate non-linear terms in governing equations (3-5). In equation (3-11), the differential of the term $\left(\frac{\partial \hat{u}_0}{\partial \bar{s}} + \hat{k} \hat{w}_0 \right)$ is equal to zero, which indicates that the mean axial tension along the mid-surface of the curved beam is constant and independent of the length *s*.

In order to obtain the solutions of the transverse displacement, substituting the differential of equation (3-11b) into equation (3-11a), the fifth order differential equation can be obtained as follows:

$$\frac{\partial}{\partial \bar{s}} \left[\frac{1}{\hat{k}} \left(\frac{\partial^4 \hat{w}_0}{\partial \bar{s}^4} - \Lambda_0 \hat{w}_0 \right) \right] = 0 \, . \tag{3-12}$$

The solution of the equation (3-12) is obtained as follows:

$$\hat{w}_0 = \hat{k}\hat{w}_{s0} + P_0 . \tag{3-13}$$

where P_0 is a constant. The closed form solution to the homogeneous equation of the straight beam $\hat{w}_{s0}$ is shown as follows (Qu and Tang 2000):

$$\hat{w}_{s0} = C_1\left[C_2\sin\left(\Lambda^{\frac{1}{4}}\bar{s}\right) + C_3\cos\left(\Lambda^{\frac{1}{4}}\bar{s}\right) + C_4\sinh\left(\Lambda^{\frac{1}{4}}\bar{s}\right) + \cosh\left(\Lambda^{\frac{1}{4}}\bar{s}\right)\right]. \tag{3-14}$$

where C_1, C_2, C_3 and C_4 are unknown constants. For the clamped or hinged boundary conditions, there are four boundary conditions respectively as follows:

Hinged: $$\hat{w}_0(0) = 0,\ \hat{w}_0(1) = 0,\ \frac{\partial \hat{w}_0^2(0)}{\partial \bar{s}^2} = 0, \frac{\partial \hat{w}_0^2(1)}{\partial \bar{s}^2} = 0. \tag{3-15a}$$

Clamped: $$\hat{w}_0(0) = 0,\ \hat{w}_0(1) = 0,\ \frac{\partial \hat{w}_0(0)}{\partial \bar{s}} = 0, \frac{\partial \hat{w}_0(1)}{\partial \bar{s}} = 0. \tag{3-15b}$$

Applying the boundary conditions into the transverse displacement $\hat{w}_0$, the unknown constant C_2, C_3, C_4 and P_0 can be obtained. C_1 is not important in terms of the normalization of the transverse displacement.

Furthermore, equation (3-11a) leads to another equation, which is expressed as follows:

$$\frac{\partial \hat{u}_0}{\partial \bar{s}} + \hat{k}\hat{w}_0 = \tau. \tag{3-16}$$

where τ is a constant. Substituting equation (3-16) into equation (3-11b), it gives that:

$$\frac{\partial^4 \hat{w}_0}{\partial \bar{s}^4} - \Lambda_0 \hat{w}_0 = -\hat{k}\tau. \tag{3-17}$$

Equation (3-17) shows physically the nature of free vibration problems for curved beams. Where on the right side of equation (3-17), if either $\hat{k}$ or τ is assumed equal to zero, the equation can be reduced to the form as follows:

$$\frac{\partial^4 \hat{w}_0}{\partial \bar{s}^4} - \Lambda_0 \hat{w}_0 = 0. \tag{3-18}$$

It is obvious that equation (3-18) represents the flexural vibration of the straight beam.

Hence, equation (3-17) is taken as a straight beam flexural vibration plus the additional term $\hat{k}\tau$ which represents the coupling effects from the curvature and the tension.

Consider the boundary conditions of the curved beam. If either end of the curved beam is free, there will be no tension in the beam provided by boundary conditions which leads to $\tau = 0$. Therefore, it does not matter how curvature changes, as if either end is free, these changes in curvature will not affect the natural behaviour of the curved beam. Based on this conclusion, the following analysis only considers the clamped and hinged boundary conditions. The easy way to express the solution of equation (3-17) in another form shown as follows:

$$\hat{w}_0 = \hat{w}_{s0} + \hat{w}_{p0}. \tag{3-19}$$

where $\hat{w}_{s0}$ is the eigenvector of the straight beam, and $\hat{w}_{p0}$ is the particular solution.

The eigenvalue can be derived based on equation (3-17), from which the particular solution $\hat{w}_{p0}$ can be also expressed as follows:

$$\hat{w}_{p0} = \frac{\hat{k}\tau}{\Lambda}. \tag{3-20}$$

where considering a curved beam with specific curvature, the non-dimensional curvature $\hat{k}$ is defined as the function of $\bar{s}$, which can be expressed as follows:

$$\hat{k} = b\bar{K}(\bar{s}). \tag{3-21}$$

where *b* represents the amplitude of curvature and $\bar{K}(\bar{s})$ represents the shape function of curvature.

The constant τ can be derived by adopting the following procedure. Integrating equation (3-16) with respect to $\bar{s}$, $0 \leq \bar{s} \leq 1$ it results in:

$$\tau \cdot \bar{s}|_0^1 = \hat{u}(\bar{s})|_0^1 + \int_0^1 \hat{k}\hat{w}_0 \, d\bar{s}. \tag{3-22}$$

and in either case of clamped or hinged boundary condition,

$$\hat{u}_0(0) = \hat{u}_0(1) = 0\,. \tag{3-23}$$

Thus, substituting equation (3-23) into equation (3-22), it results in:

$$\tau = \int_0^1 \hat{k}\hat{w}_0 d\bar{s}\,. \tag{3-24}$$

Hence, equation (3-20) can be rewritten as follows:

$$\hat{w}_{p0} = \frac{\hat{k}}{\Lambda}\int_0^1 \hat{k}\hat{w}_0 d\bar{s}\,, \tag{3-25}$$

where,

$$\int_0^1 \hat{k}\hat{w}_0 d\bar{s} = \int_0^1 \hat{k}\hat{w}_{s0} d\bar{s} + \int_0^1 \hat{k}\hat{w}_{p0} d\bar{s}, \tag{3-26}$$

Substituting equation (3-26) into equation (3-25), it results in

$$\int_0^1 \hat{k}\hat{w}_0 d\bar{s} = \int_0^1 \hat{k}\hat{w}_{s0} d\bar{s} + \frac{1}{\Lambda}\int_0^1 \hat{k}^2 \int_0^1 \hat{k}\hat{w}_0 d\bar{s}\, d\bar{s}\,, \tag{3-27}$$

then,

$$\int_0^1 \hat{k}\hat{w}_0 d\bar{s} = \frac{\Lambda_0 \int_0^1 \hat{k}\hat{w}_{s0} d\bar{s}}{\Lambda_0 - \int_0^1 \hat{k}^2 d\bar{s}}\,, \tag{3-28}$$

Therefore,

$$\hat{w}_0 = \hat{w}_{s0} + \frac{\hat{k}\int_0^1 \hat{k}\hat{w}_{s0} d\bar{s}}{\Lambda_0 - \int_0^1 \hat{k}^2 d\bar{s}}\,. \tag{3-29}$$

Substituting equation (3-14) into equation (3-29) and applying the boundary condition, the eigenvalue can be obtained, which also indicates the relationship between the curvature and the natural frequency. Examples of curved beams with various curvatures and with different boundary conditions will be demonstrated in the Chapter five.

3.3 First Order Approximation Equations

The zero order perturbation solutions give the approximate results, though it can explain physical meaning of the vibration characteristics. In this section, the accuracy of the results will be improved by the first order perturbation equations. The first order perturbation solutions are written as follows:

$$\Lambda(\xi) = \Lambda_0 + \xi\Lambda_1 ,$$

$$\hat{u}(\bar{s},\xi) = \hat{u}_0(\bar{s}) + \xi\hat{u}_1(\bar{s}) ,$$

$$\hat{w}(\bar{s},\xi) = \hat{w}_0(\bar{s}) + \xi\hat{w}_1(\bar{s}). \tag{3-30}$$

Substituting equation (3-30) into equation (3-7), the first order perturbation equations can be obtained as follows:

$$\xi\frac{\partial}{\partial\bar{s}}\left(\frac{\xi}{\hat{k}}(\hat{u}_0+\xi\hat{u}_1)\frac{\partial\hat{k}}{\partial\bar{s}}+\xi\frac{\partial(\hat{u}_0+\xi\hat{u}_1)}{\partial\bar{s}}-\frac{\partial^2(\hat{w}_0+\xi\hat{w}_1)}{\partial\bar{s}^2}\right)+\frac{\partial}{\partial\bar{s}}\left(\frac{\partial(\hat{u}_0+\xi\hat{u}_1)}{\partial\bar{s}}+\hat{k}(\hat{w}_0+\xi\hat{w}_1)\right)=-\frac{\xi(\hat{\Lambda}_0+\xi\hat{\Lambda}_1)(\hat{u}_0+\xi\hat{u}_1)}{\hat{k}}, \tag{3-31a}$$

$$\frac{1}{\hat{k}}\frac{\partial^2}{\partial\bar{s}^2}\left(\frac{\xi}{\hat{k}}(\hat{u}_0+\xi\hat{u}_1)\frac{\partial\hat{k}}{\partial\bar{s}}+\xi\frac{\partial(\hat{u}_0+\xi\hat{u}_1)}{\partial\bar{s}}-\frac{\partial^2(\hat{w}_0+\xi\hat{w}_1)}{\partial\bar{s}^2}\right)-\left(\frac{\partial(\hat{u}_0+\xi\hat{u}_1)}{\partial\bar{s}}+\hat{k}(\hat{w}_0+\xi\hat{w}_1)\right)=-\frac{(\hat{\Lambda}_0+\xi\hat{\Lambda}_1)(\hat{w}_0+\xi\hat{w}_1)}{\hat{k}}. \tag{3-31b}$$

Since the leading power of ξ is equal to one, equations (3-31) are reduced by setting $\xi^{n\geq 2}=0$ as follows:

$$\frac{\partial}{\partial\bar{s}}\left(\frac{\partial\hat{u}_1}{\partial\bar{s}}+\hat{k}\hat{w}_1\right)=\frac{\partial^3\hat{w}_0}{\partial\bar{s}^3}-\frac{\hat{\Lambda}_0\hat{u}_0}{\hat{k}}, \tag{3-32a}$$

$$\frac{1}{\hat{k}}\frac{\partial^2}{\partial\bar{s}^2}\left(\frac{\partial\hat{k}}{\partial\bar{s}}\frac{\hat{u}_0}{\hat{k}}+\frac{\partial\hat{u}_0}{\partial\bar{s}}-\frac{\partial^2\hat{w}_1}{\partial\bar{s}^2}\right)-\left(\frac{\partial\hat{u}_1}{\partial\bar{s}}+\hat{k}\hat{w}_1\right)=-\frac{(\hat{\Lambda}_0\hat{w}_1+\hat{\Lambda}_1\hat{w}_0)}{\hat{k}}. \tag{3-32b}$$

It is obvious that the tension along the curved beam is not constant anymore. It takes

account of the effects from the initial rotation and the linear momentum in the longitudinal direction, which can be observed by integrating equation (3-32a) as follows:

$$\frac{\partial \hat{u}_1}{\partial \bar{s}} + \hat{k}\hat{w}_1 = \underbrace{\int_0^{\bar{s}} \frac{\partial^3 \hat{w}_0}{\partial \bar{s}^3} d\bar{s}}_{\text{effect of rotation}} - \underbrace{\int_0^{\bar{s}} \frac{\hat{\Lambda}_0 \hat{u}_0}{\hat{k}} d\bar{s}}_{\text{effect of linear momentum}} + \tau_1. \tag{3-33}$$

where τ_1 can be obtained by integrating equation (3-33) and using the boundary conditions $\hat{u}_1(0) = 0$ and given as follows:

$$\tau_1 = \int_0^1 \int_0^{\bar{s}} \hat{\Lambda}_0 \hat{u}_0 \, d\bar{s} \, d\bar{s} - \int_0^1 \int_0^{\bar{s}} \hat{k} \frac{\partial^3 \hat{w}_0}{\partial \bar{s}^3} d\bar{s} \, d\bar{s} + \int_0^1 \hat{k}\hat{w}_1 \, d\bar{s} \, . \tag{3-34}$$

Substituting equation (3-34) into equation (3-32b), one obtains the following equation:

$$\frac{\partial^4 \hat{w}_1}{\partial \bar{s}^4} - \hat{\Lambda}_0 \hat{w}_1 = \frac{\hat{\Lambda}_1 \hat{w}_0}{\hat{k}} + \frac{1}{\hat{k}} \frac{\partial^2}{\partial \bar{s}^2} \left(\frac{\partial \hat{k}}{\partial \bar{s}} \frac{\hat{u}_0}{\hat{k}} + \frac{\partial \hat{u}_0}{\partial \bar{s}} \right) - \left(\int_0^{\bar{s}} \frac{\hat{k}(\partial^3 \hat{w}_0)}{\partial \bar{s}^3} d\bar{s} - \int_0^{\bar{s}} \hat{\Lambda}_0 \hat{u}_0 \, d\bar{s} + \int_0^1 \int_0^{\bar{s}} \hat{\Lambda}_0 \hat{u}_0 \, d\bar{s} \, d\bar{s} - \int_0^1 \int_0^{\bar{s}} \frac{\hat{k}(\partial^3 \hat{w}_0)}{\partial \bar{s}^3} d\bar{s} \, d\bar{s} + \int_0^1 \hat{k}\hat{w}_1 \, d\bar{s} \right). \tag{3-35}$$

The solution of the equation is easily written as follows:

$$\hat{w}_1 = \hat{w}_{s1} + \hat{w}_{p1}. \tag{3-36}$$

where $\hat{w}_{s1}$ is the eigenvector of the straight beam expressed as follows:

$$\hat{w}_{s1} = D_1 \left[D_2 \sin\left(\Lambda^{\frac{1}{4}} \bar{s}\right) + D_3 \cos\left(\Lambda^{\frac{1}{4}} \bar{s}\right) + D_4 \sinh\left(\Lambda^{\frac{1}{4}} \bar{s}\right) + \cosh\left(\Lambda^{\frac{1}{4}} \bar{s}\right) \right]. \tag{3-37}$$

and $\hat{w}_{p1}$ is the particular solutions. It is complex to obtain $\hat{w}_1$ directly from equation (3-36), thus using similar procedure with the zero order perturbation, differentiate equation (3-32b) and then substitute into equation (3-32a), the fifth order differential equation can be obtained as follows:

$$\frac{\partial}{\partial \bar{s}} \left[\frac{1}{\hat{k}} \left(\frac{\partial^4 \hat{w}_1}{\partial \bar{s}^4} - \hat{\Lambda}_0 \hat{w}_1 \right) \right] = \frac{\partial}{\partial \bar{s}} \left\{ \frac{1}{\hat{k}} \left[\frac{\partial^2}{\partial \bar{s}^2} \left(\frac{\partial \hat{k}}{\partial \bar{s}} \frac{\hat{u}_0}{\hat{k}} \right) + \frac{\partial^3 \hat{u}_0}{\partial \bar{s}^3} \right] \right\} - \left(\frac{\partial^3 \hat{w}_0}{\partial \bar{s}^3} - \frac{\hat{\Lambda}_0 \hat{u}_0}{\hat{k}} \right) + \frac{\partial}{\partial \bar{s}} \left(\frac{\hat{\Lambda}_1 \hat{w}_0}{\hat{k}} \right). \tag{3-38}$$

which can be further simplified as follows:

$$\frac{\partial}{\partial \bar{s}}\left[\frac{1}{\hat{k}}\left(\frac{\partial^4 \hat{w}_1}{\partial \bar{s}^4} - \hat{\Lambda}_0 \hat{w}_1\right)\right] = \Gamma(\bar{s}), \tag{3-39}$$

where

$$\Gamma(\bar{s}) = \frac{\partial}{\partial \bar{s}}\left\{\frac{1}{\hat{k}}\left[\frac{\partial^2}{\partial \bar{s}^2}\left(\frac{\partial \hat{k}}{\partial \bar{s}}\frac{\hat{u}_0}{\hat{k}}\right) + \frac{\partial^3 \hat{u}_0}{\partial \bar{s}^3}\right]\right\} - \left(\frac{\partial^3 \hat{w}_0}{\partial \bar{s}^3} - \frac{\hat{\Lambda}_0 \hat{u}_0}{\hat{k}}\right) + \frac{\partial}{\partial \bar{s}}\left(\frac{\hat{\Lambda}_1 \hat{w}_0}{\hat{k}}\right). \tag{3-40}$$

Then, using similar derivation procedure as zero order, find $\hat{w}_{p1}$ and substituting into equation (3-36). Let $\hat{w}_1$ is expressed by equations only including $\hat{w}_{s1}$. The whole procedure is processed by using the commercial code MAPLE, the unknown constant D_2, D_3, D_4 and the eigenvalue Λ_1 are also solved.

Finally, the eigenvalue is solved as follows:

$$\Lambda = \Lambda_0 + \xi \Lambda_1. \tag{3-41}$$

3.4 Second Order Approximation Equations

Comparing to the zero order perturbation equations, the first order equations have advantages of taking account of the coupling effect which is controlled by the small parameter ξ. However, there is still the simplification in perturbation equations. The accuracy of results could be improved by the second order perturbations.

The second order perturbation solutions are shown as follows:

$$\Lambda(\xi) = \Lambda_0 + \xi\Lambda_1 + \xi^2\Lambda_2, \tag{3-42a}$$

$$\hat{u}(\bar{s},\xi) = \hat{u}_0(\bar{s}) + \xi\hat{u}_1(\bar{s}) + \xi^2\hat{u}_2(\bar{s}), \tag{3-42b}$$

$$\hat{w}(\bar{s},\xi) = \hat{w}_0(\bar{s}) + \xi\hat{w}_1(\bar{s}) + \xi^2\hat{w}_2(\bar{s}). \tag{3-42c}$$

Substituting equation (3-42) into equation (3-7), the second order perturbation equations are obtained as follows:

$$\xi\frac{\partial}{\partial\bar{s}}\left(\frac{\xi}{\hat{k}}(\hat{u}_0+\xi\hat{u}_1+\xi^2\hat{u}_2)\frac{\partial\hat{k}}{\partial\bar{s}}+\xi\frac{\partial(\hat{u}_0+\xi\hat{u}_1+\xi^2\hat{u}_2)}{\partial\bar{s}}-\frac{\partial^2(\hat{w}_0+\xi\hat{w}_1+\xi^2\hat{w}_2)}{\partial\bar{s}^2}\right)+$$
$$\frac{\partial}{\partial\bar{s}}\left(\frac{\partial(\hat{u}_0+\xi\hat{u}_1+\xi^2\hat{u}_2)}{\partial\bar{s}}+\hat{k}(\hat{w}_0+\xi\hat{w}_1+\xi^2\hat{w}_2)\right)=-\frac{\xi(\hat{\Lambda}_0+\xi\hat{\Lambda}_1+\xi^2\Lambda_2)(\hat{u}_0+\xi\hat{u}_1+\xi^2\hat{u}_2)}{\hat{k}} \tag{3-43a}$$

$$\frac{1}{\hat{k}}\frac{\partial^2}{\partial\bar{s}^2}\left(\frac{\xi}{\hat{k}}(\hat{u}_0+\xi\hat{u}_1+\xi^2\hat{u}_2)\frac{\partial\hat{k}}{\partial\bar{s}}+\xi\frac{\partial(\hat{u}_0+\xi\hat{u}_1+\xi^2\hat{u}_2)}{\partial\bar{s}}-\frac{\partial^2(\hat{w}_0+\xi\hat{w}_1+\xi^2\hat{w}_2)}{\partial\bar{s}^2}\right)-$$
$$\left(\frac{\partial(\hat{u}_0+\xi\hat{u}_1+\xi^2\hat{u}_2)}{\partial\bar{s}}+\hat{k}(\hat{w}_0+\xi\hat{w}_1+\xi^2\hat{w}_2)\right)=-\frac{(\hat{\Lambda}_0+\xi\hat{\Lambda}_1+\xi^2\Lambda_2)(\hat{w}_0+\xi\hat{w}_1+\xi^2\hat{w}_2)}{\hat{k}} \tag{3-43b}$$

Equation (3-43) can be rewritten by setting $\xi^{n\geq 3}=0$ as follows:

$$\frac{\partial}{\partial\bar{s}}\left(\frac{\hat{u}_0}{\hat{k}}\frac{\partial\hat{k}}{\partial\bar{s}}+\frac{\partial\hat{u}_0}{\partial\bar{s}}-\frac{\partial^2\hat{w}_1}{\partial\bar{s}^2}\right)+\frac{\partial}{\partial\bar{s}}\left(\frac{\partial\hat{u}_2}{\partial\bar{s}}+\hat{k}\hat{w}_2\right)=-\frac{(\hat{\Lambda}_0\hat{u}_1+\hat{\Lambda}_1\hat{u}_0)}{\hat{k}}, \tag{3-44a}$$

$$\frac{1}{\hat{k}}\frac{\partial^2}{\partial\bar{s}^2}\left(\frac{\hat{u}_1}{\hat{k}}\frac{\partial\hat{k}}{\partial\bar{s}}+\frac{\partial\hat{u}_1}{\partial\bar{s}}-\frac{\partial^2\hat{w}_2}{\partial\bar{s}^2}\right)-\left(\frac{\partial\hat{u}_2}{\partial\bar{s}}+\hat{k}\hat{w}_2\right)=-\frac{(\hat{\Lambda}_0\hat{w}_2+\hat{\Lambda}_1\hat{w}_1+\Lambda_2\hat{w}_0)}{\hat{k}}. \tag{3-44b}$$

Equation (3-44) is in the same format with the original equations of motion (3-7), which means the second order perturbation approximations take account of all effects from the curvature and the coupling of stiffness. The solution procedure to obtain the eigenvalue and eigenvector is similar to the previous sections, namely

1. Combine two equations into one and integrate equation.
2. According to the beam shape define the curvature value.
3. Through derivation to find out the particular solution $\widehat{w}_{p2}$.
4. Let the displacement $\widehat{w}_2$ is expressed only by homogeneous solution $\widehat{w}_{s2}$.
5. Substituting lower order perturbation solutions into the second order equations.
6. Using boundary conditions to solve unknown constants.

3.5 Summary

This chapter demonstrated the perturbation approach applied the natural vibration analysis of curved beams. The reason for using perturbation method is to expand the unknown curvature parameter into a series equation, represented by the known factors. The non-dimensional governing equations are solved depending on a small parameter, which represents the geometric property, material property and the curvature and shows how these properties affect the natural vibration of a curved beam.

The zero order perturbation decouples the flexural and extensional vibration, which explains the physical meaning of the vibration characteristics of the curved beam. The transverse displacement of the curved beam is represented by the straight beam displacement combined with the special solution. This special solution generates the effects from curvatures. The first order perturbation improves the accuracy of the results and the second order solutions take account of all effects from the curvature, the stiffness and the coupling. The differences between different orders are observed from equations for extensional mode and bending mode. Mode transition phenomena will be explained by results of both eigenvalue and mode shapes. Examples will be given in Chapter five.

Table 3.1 Differences between different order perturbations, (observed from equations)

Perturbation	Zero order	First order	Second order
Extensional mode	Tension is constant equation (3-16)	Tension includes effect from initial rotation and linear momentum Equation (3-33)	Additional component added, the change of tension is not linear Equation (3-44a)
Bending mode	Particular solution W_p is linear to the curvature. Equation (3-25)	Couple the effect from tension Equation (3-32b)	Couple the effect from tension

Chapter 4 Finite Element Models

This chapter is presented to prove that numerical methods to establish the curved beam and the curved plate subjected to various variable curvatures are accepted as an alternative to the formulations presented in the previous chapter. One widely-accepted method relies on the use of Finite Element Analysis (FEA) which allows the designer to model the geometry; material properties; imperfections (such as out-of-roundness), fabrication-induced residual stresses, misalignment and corrosion defects, as well as boundary conditions. The primary advantage of the FEA is that there are numerous commercial FE codes available. Thus eliminating any need to develop actual code. These commercial FE codes have the additional advantages of being very user friendly, and providing sophisticated pre- and post-processing options.

4.1 General Procedure

The FEA analysis model is translated from the engineering model and key issues include the selection of the commercial code, the determination of the loads and boundary conditions, development of the mathematical model, choice of element types, design of the mesh, solution procedures and verification and validation. Numerous decisions are to be made during this analysis process as follows:

• *Extent of the model*. The use of a full model is preferred in FEA. Symmetric conditions may be utilized to reduce the size of finite element model, if appropriate. The model should include the main features of the physical structure related to dynamic behaviour and capture all relevant modes.

• *Material properties.* Material nonlinearity may have to be considered in some circumstances, particularly in order to account for the effects of residual stresses.

• *Loads*. All possible loads and their combinations are to be considered.

• *Boundary conditions*. Boundary conditions are the constraints applied to the model. The boundary conditions should suitably reflect the constraint relationship between the structural component and its surroundings.

• *Element types*. Finite element types are specialized and can only simulate a limited number of response types. The choice of element types should be best suited to the problem.

• *Mesh design*. The discretization of a structure into a number of finite elements is one of the most critical tasks in finite element modelling and often a difficult one. The following parameters need to be considered in designing the layout of elements: mesh density, mesh transitions and the stiffness ratio of adjacent elements. As a general rule, a finer mesh is required in areas of high stress gradient. The performance of elements degrades as they become more skewed. If the mesh is graded, rather than uniform, as is usually the case, the grading should be done in a way that minimizes the difference in size between adjacent elements.

The basic steps involved in any finite element analysis consist of the following procedures:

1 Pre-processing phase: Create and discretize the solution domain into finite elements; that is, subdivide the problem into nodes and elements. Assume a shape function to represent the physical behaviour of an element; that is, an approximate continuous function is assumed to represent the solution of an element. Develop equations for an element. Assemble the elements to present the entire problem. Construct the global stiffness matrix. Apply boundary conditions, initial conditions, and loading.

2 Solution phase: Solve a set of linear or nonlinear algebraic equations simultaneously to obtain nodal results, such as displacement values at different nodes or temperature values at different nodes in a heat transfer problem.

3 Post processing phase: Obtain other important information such as values of principal stresses, heat fluxes, etc.

4.2 FEA Solutions of Natural Vibration

In the dynamic problem of a structural system, using a finite element idealization, the dynamic equilibrium equation of the system is written in a matrix form as

$$\mathbf{M}\ddot{\mathbf{u}} + \mathbf{C}\dot{\mathbf{u}} + \mathbf{K}\mathbf{u} = \mathbf{F}, \tag{4-1}$$

where **M**, **C** and **K** denote respectively the mass, damping and stiffness matrices of the structural system. In general, **M** and **K** are symmetric matrices whilst **C** is non-symmetric. **u** is the displacement vector and **F** is the external force vector. To determine the natural vibrations of this structural system, damping and external loads are ignored and hence Equation (4-1) reduces to

$$\mathbf{M}\ddot{\mathbf{u}} + \mathbf{K}\mathbf{u} = 0. \tag{4-2}$$

It is assumed that the solution of Equation (4-2) has the harmonic form

$$\mathbf{u} = \mathbf{q}\, e^{i\omega t}, \tag{4-3}$$

which upon substitution into Equation (4-2) leads to

$$(\mathbf{K} - \omega^2\mathbf{M})\,\mathbf{q} = \mathbf{0}. \tag{4-4}$$

Equation (4-4) is a linear homogenous algebraic system of equations with unknown vector **q** and ω^2. This is known as the eigenvalue problem of the structural system, with ω and **q** representing the natural frequency and the corresponding principal mode vector respectively. A nontrivial solution of Equation (4-4) requires the determinant of the coefficient matrix to be zero, that is

$$\det(\mathbf{K} - \omega^2\mathbf{M}) = 0. \tag{4-5}$$

The expansion of the determinant in Equation (4-5) results in a polynomial equation of ω^2 designated as the characteristic equation of the structural system. If the system has *N* degrees of freedom, *N* solutions of ω^2 can be obtained from Equation (4-5).

4.3 The Choice of Element

In the present work, the commercial code ANSYS (2002) is adopted for modelling and analysis. There are three elements in ANSYS which are able to model the curved beam as shown in Table 4.1:

Table 4.1 Selected elements in ANSYS

BEAM4	PLAN42	SHELL93
a uniaxial element with tension, compression, torsion, and bending capabilities. The element has six degrees of freedom at each node: translations in the nodal x, y, and z directions and rotations about the nodal x, y, and z axes. Stress stiffening and large deflection capabilities are included.	used for 2-D modeling of solid structures. The element can be used either as a plane element (plane stress or plane strain) or as an axisymmetric element. The element is defined by four nodes having two degrees of freedom at each node: translations in the nodal x and y directions. The element has plasticity, creep, swelling, stress stiffening, large deflection, and large strain capabilities.	defined by eight nodes, four thicknesses, and the orthotropic material properties and particularly well suited to model curved shells. The element has six degrees of freedom at each node: translations in the nodal x, y, and z directions and rotations about the nodal x, y, and z axes. The deformation shapes are quadratic in both in-plane directions.
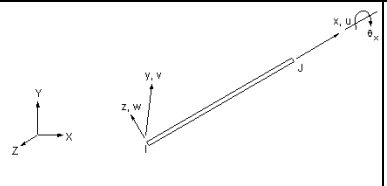	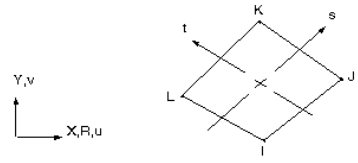	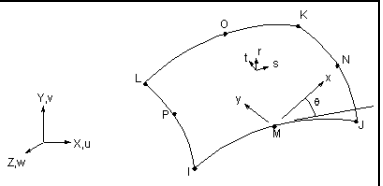

A simple test is made to find the accuracy of the chosen elements. Table 4.2 illustrates the natural frequency of a curved beam calculated using these three elements compared with the reference value also using FEA from (Fleischer 1974). The properties of the uniform curved beam are listed as follows:

l=10.16cm, a=7.62cm, t=0.033cm, r=76.2 cm, E=6.89e^{10} N/m^2, ρ =2660 Kg/m^3, μ=0.33

where ρ is the density, r is radius of curvature, l is the length, a is the width, t is the thickness, E is Young's modulus and μ is the Poisson' ratio. The curved edges are clamped.

Table 4.2 natural frequency of selected elements

Mode shape	BEAM4 Hz	PLAN42 Hz	SHELL93 Hz	Fleischer Hz
1	870.32	868.93	870	868.55
2	958.61	958.87	957.882	958.48
3	1292.01	1290.11	1291	1289.12

In order to compare the numerical results with analytical results, in some case the natural frequency is converted into dimensionless state. The following equation is used for this transformation. The non-dimensional frequency is defined as follows:

$$\lambda = \rho l^2(1-\mu^2)\omega^2/_E. \tag{4-6}$$

where ρ is the density, l is the length, E is Young's modulus and μ is the Poisson' ratio. A convergence study has also been carried out, shown in Figure 4.1. Due to the simple geometry, more than 20 elements ensure the results are accurate enough.

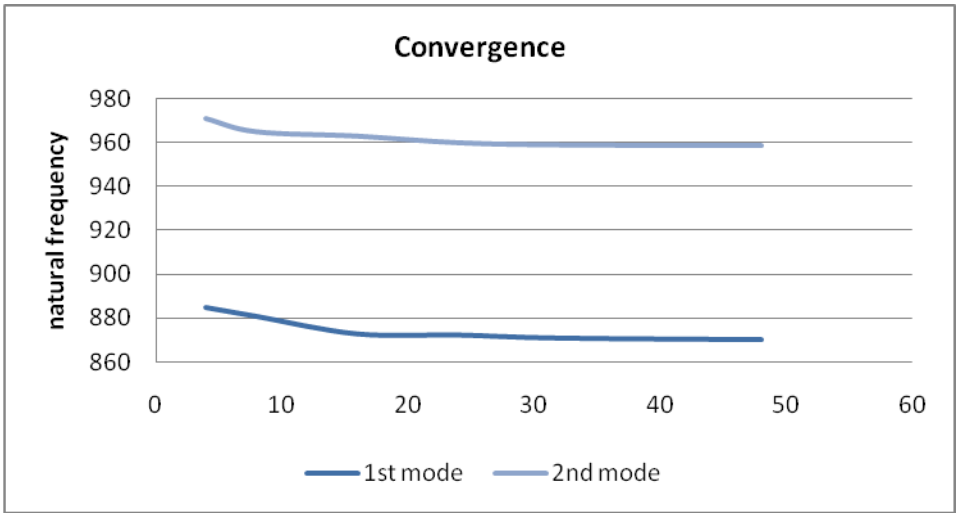

Figure 4.1 convergence study of SHELL93 element

Although all three elements are able to model the curved beam and show similar accuracy for the circular curved beam, based on all following reasons SHELL93 is taken as the numerical analysis of curved structures.

1. make the numerical simulation closer to the real structure
2. capable for two dimensional curved panels
3. easier to control boundary conditions
4. more accurate for larger curvatures
5. Avoid shear locking by using the designed stress-strain relationship (ANSYS Theory Reference)

4.4 FE model of Curved Beam

4.4.1 The circular curved beam

The equation of the curvature is derived in Chapter 2 and the curvature taken as a variable parameter is used in the perturbation equations in Chapter3. In order to model the curved beam or plate, the curvature need to be transformed into ANSYS coordinate system.

The first model shown in Figure 4.2 is the sketch of a circular curved beam with the properties as: the length is 1000 mm, the width is 150 mm, the thickness is 0.8 mm, the density ρ is 7770 kg/m^3, Young's modulus E is 200 *GPa*. The global coordinate system is represented by the Cartesian coordinate system *o-αβγ*. *oβ* is along the direction of the straight line between two ends of the beam; *oα* is normal to *oβ* direction, along the short edge of shell. *oγ* is normal to the plan *αoβ*. The geometry of the shell is that *l* denotes the length of curved edge; *a* denotes the length of short edge; *r* denotes the radius of curved edge.

The non-dimensional curvature denoted by $\bar{k}$ defined as follows:

$$\bar{k} = {}^{l}/_{r}\,. \tag{4-7}$$

where *l* is the length of the beam, r is the radius of curvature and *k* is the curvature.

The relation between the non-dimensional curvature and the subtended angle of the curved beam is defined as follows:

$$\theta = \bar{k} \times {}^{360}/_{2\pi}\,. \tag{4-8}$$

In present numerical studies, the changes in subtended angle are used to represent the changes in curvatures.

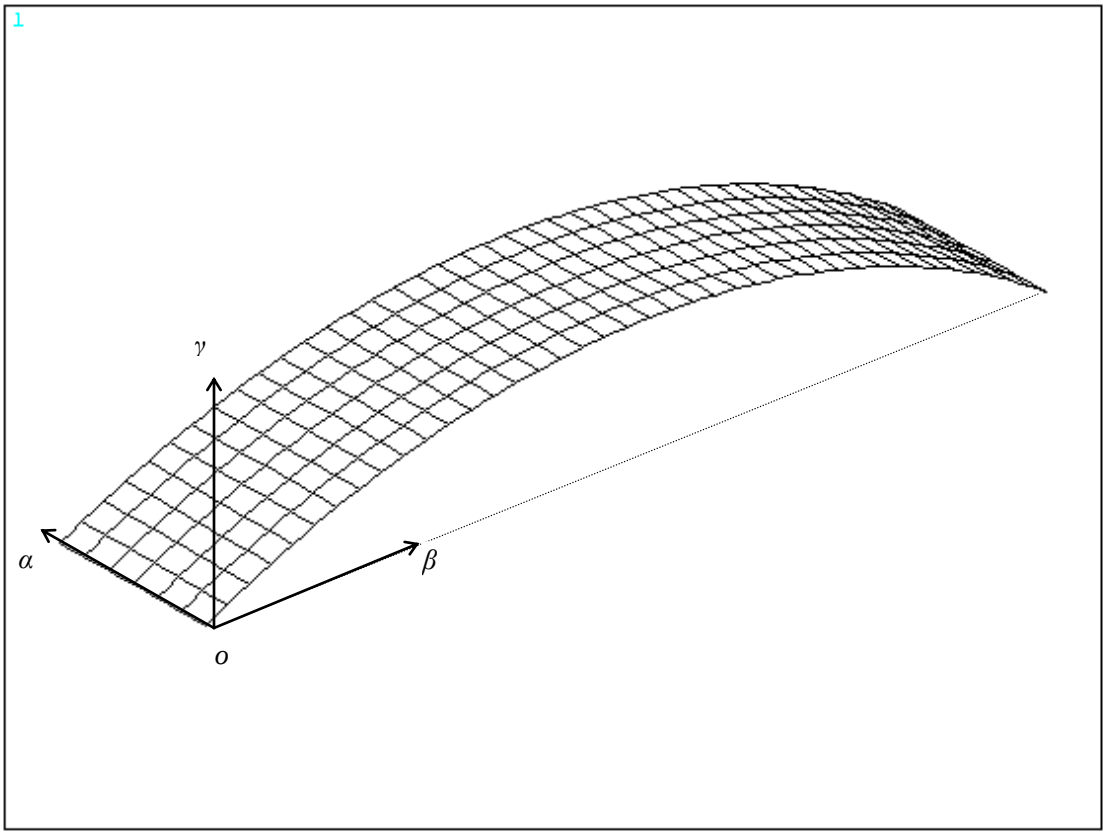

Figure 4.2 Geometry of curved beam with a constant curvature

4.4.2 The S-shape strip

The s-shape elastic strip has zero curvature at the inflection point; the curvature increases monotonically in magnitude away from that point in both directions. For the simple model of the strip as a uniform beam in static equilibrium under end moments, the curvature would vary linearly with axial distance.

The anti-symmetric linear curvature function can be defined as follows:

$$k = b(2s - 1). \tag{4-9}$$

where k denotes the curvature, b denotes the amplitude of curvature and s denotes the length of arch.

The global coordinate system is represented by the Cartesian coordinate system o-

$\alpha\beta\gamma$, shown in Figure 4.3. $o\beta$ along the zero curvature direction; $o\alpha$ is normal to $o\beta$ direction, along the short edge of shell. $o\gamma$ is normal to the plan $\alpha o\beta$. A code is developed in MATLAB to solve the function of $\alpha(k)$ and $\beta(k)$ which represents the

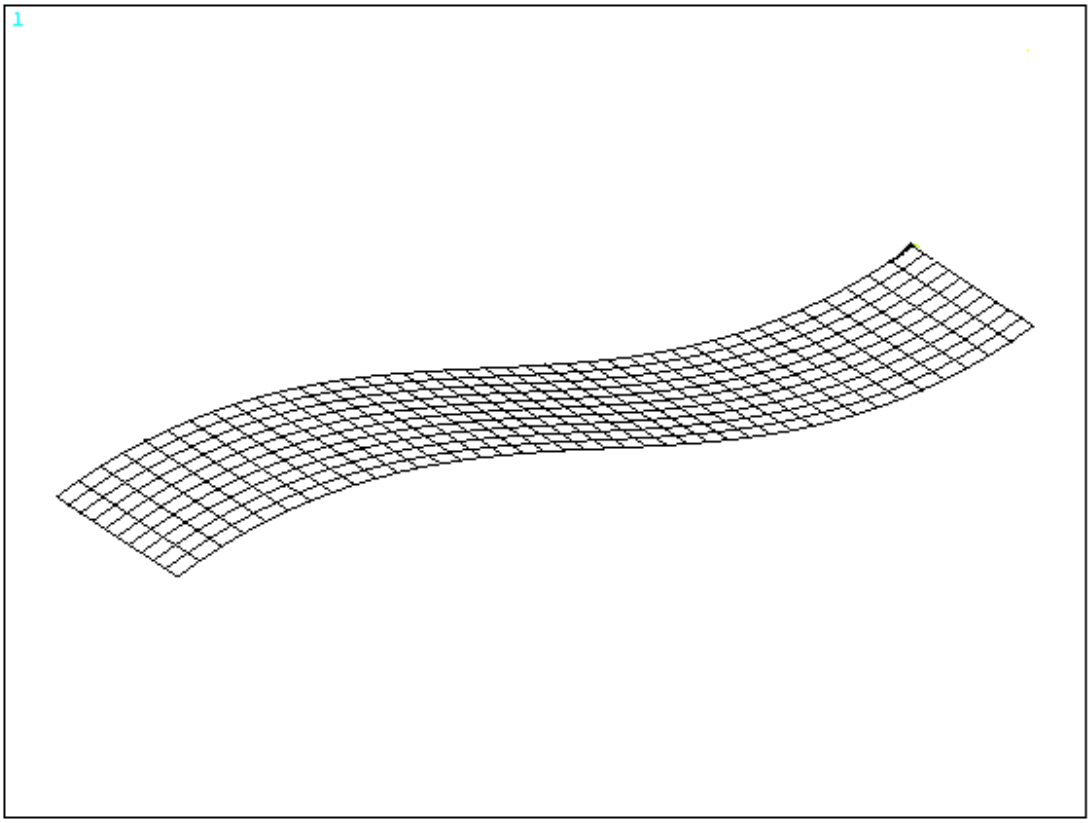

Figure 4.3 finite element models for the strip of varying curvature

coordinate of each point on the curved edges of the S-shape strip. In ANSYS the anti-symmetric linear curves are expanded into a two dimensional strip. The SHELL*93* element is used to mesh the strip.

4.4.3 Other curvatures

Similar to the circular curved and S-shape curved beam, through the curvature function, many kinds of geometry can be defined, shown in Table 4.3. Curved beams with these curvatures can also be modelled by creating curves of $\alpha(k)$ and $\beta(k)$ in the model.

Using the curvature function it is possible to solve the perturbation equations

demonstrated in Chapter 3; however, there are also some types of curved beams which are difficult to represent by such function. The example will be given in Chapter 6.

Table 4.3 Curvature function of various curves

k	Geometry of curved edge	Figure
1	circle	4-2
$2s$-1	S-shape	4-3
s	Euler ́s spiral	
s^2	double clothoid	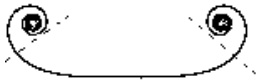
s^2-1	Polynomial spiral	

4.5 Boundary Conditions Treatment

Since both clamped and hinged boundary conditions provide the extensional restraint, changes of curvature will cause the mode transitions of the curved beams. Therefore to examine different boundary conditions is an important procedure in the numerical analysis. Boundary conditions demonstrated in Chapter three will be treated in the following forms in numerical analysis.

For the circular curved beams, various boundary conditions are introduced into the global coordinate system $o-\alpha\beta\gamma$. $o\alpha$ is along the direction of the straight line between two ends of the beam; $o\beta$ is normal to $o\alpha$ direction, along the short edge of the beam. $o\gamma$ is normal to the plan $\alpha o\beta$.

For the s-shaped strip, $o\alpha$ along the zero curvature direction; $o\beta$ is normal to $o\alpha$ direction, along the short edge of shell. $o\gamma$ is normal to the plan $\alpha o\beta$.

Case 1 Spin

The transverse displacement is fixed and no moment applied at the boundary.

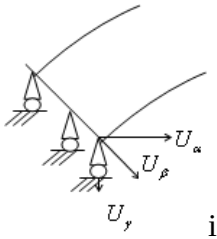

i.e. only $U_\gamma = 0$. (4-10)

Case 2 Clamped

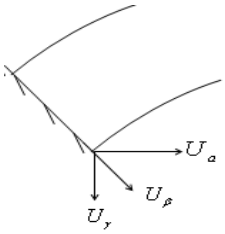

All DOFs = 0 . (4-11)

Case 3 Hinged

All the displacements are fixed at the boundary, but rotations are not fixed.

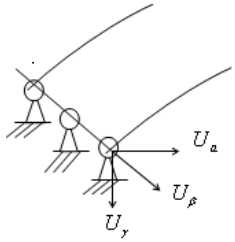

$$U_\alpha = 0, U_\beta = 0, U_\gamma = 0, M = 0. \tag{4-12}$$

Case 4 Free

No shear, axial force and moment at the boundary.

All DOFs are free (4-13)

Case 5 Rolling

Only the horizontal displacement is free.

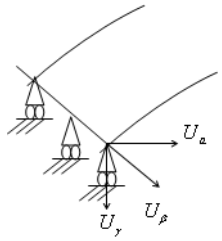

$$U_\alpha = 0, U_\gamma = 0, \emptyset_\alpha = 0, \emptyset_\beta = 0, \emptyset_\gamma = 0. \tag{4-14}$$

Chapter 5 Curved Beams with Variable Curvature

The natural vibration behaviour of the curved beam with variable curvatures is analyzed in Chapter three. The solution of the perturbation equations is derived. In order to investigate effects of curvature on the natural characteristics of curved beams, in this chapter, the relationship between eigenvalue and curvature are formulated by solving unknown constants in equation (3-29). The circular curved beam and S-shape strip are taken as examples. Results are obtained and plotted in MATLAB code. Some features caused by the curvature are revealed. Numerical results are also plot and explained.

5.1 Curved Beam with Constant Curvature

As defined in equation (3-21), non-dimensional curvature $\hat{k}$ is a function of the length of arch $\bar{s}$. The constant curvature is independent of $\bar{s}$, therefore the shape function $\hat{K}(\bar{s})$ is equal to 1 and then equation (3-21) can be rewritten as follows:

$$\hat{k}(\bar{s}) = b\hat{K}(\bar{s}) = b = 1/r \,. \tag{5-1}$$

where the curvature amplitude *b* is equal to constant that is the curvature of an arch with a constant radius *r*. Substituting equation (5-1) into equation (3-29), it results in:

$$\overline{w} = C\left\{\begin{array}{l}\left[C_1 \sin(\Lambda^{\frac{1}{4}}\bar{s}) + C_2\cos(\Lambda^{\frac{1}{4}}\bar{s}) + C_3\sinh(\Lambda^{\frac{1}{4}}\bar{s}) + \cosh(\Lambda^{\frac{1}{4}}\bar{s})\right] \\ + \dfrac{b^2\int_0^1\left[C_1 \sin(\Lambda^{\frac{1}{4}}\bar{s}) + C_2\cos(\Lambda^{\frac{1}{4}}\bar{s}) + C_3\sinh(\Lambda^{\frac{1}{4}}\bar{s}) + \cosh(\Lambda^{\frac{1}{4}}\bar{s})\right]d\bar{s}}{\Lambda - b^2}\end{array}\right\}. \tag{5-2}$$

where constant *C* can be eliminated by normalizing the transverse displacement and constants C_1, C_2 and C_3 need to be solved by using appropriate boundary conditions.

Firstly, hinged boundary conditions are processed as follows.

5.1.1 Hinged boundary conditions

According to equation (2-37), hinged boundary conditions can be treated as:

$$\overline{w}(0)=0\,,\ \overline{w}(1)=0\,,\ \frac{d^2\overline{w}(0)}{d\overline{s}^2}=0\,,\ \frac{d^2\overline{w}(1)}{d\overline{s}^2}=0\ . \tag{5-3}$$

Substituting boundary conditions shown in equation (5-3) into equation (5-2), it yields four equations. Three unknown constants C_1, C_2 and C_3 are obtained by solving these equations and shown as follows:

$$C_1=\frac{1-\cos\Lambda^{\frac{1}{4}}}{\sin\Lambda^{\frac{1}{4}}}\ , \tag{5-4}$$

$$C_2=1\ , \tag{5-5}$$

$$C_3=\frac{1-\cosh\Lambda^{\frac{1}{4}}}{\sinh\Lambda^{\frac{1}{4}}}\ . \tag{5-6}$$

Substituting the first condition in equation (5-3) and equation (5-4) – (5-6) into equation (5-2), the relationship between the eigenvalue and curvature can be formulated as follows:

$$\begin{aligned} b^2 &= \frac{\Lambda(C_2+1)}{(C_2+1)-\int_0^1\left[C_1\sin(\Lambda^{\frac{1}{4}}\overline{s})+C_2\cos(\Lambda^{\frac{1}{4}}\overline{s})+C_3\sinh(\Lambda^{\frac{1}{4}}\overline{s})+\cosh(\Lambda^{\frac{1}{4}}\overline{s})\right]d\overline{s}} \\ &= \frac{\Lambda(C_2+1)}{(C_2+1)-\Lambda^{-\frac{1}{4}}\left[C_1(1-\cos\Lambda^{\frac{1}{4}})+C_2\sin\Lambda^{\frac{1}{4}}+C_3(\cosh\Lambda^{\frac{1}{4}}-1)+\sinh\Lambda^{\frac{1}{4}}\right]} \\ &= \frac{\Lambda}{1-\Lambda^{-\frac{1}{4}}\left(\frac{1-\cos\Lambda^{\frac{1}{4}}}{\sin\Lambda^{\frac{1}{4}}}-\frac{1-\cosh\Lambda^{\frac{1}{4}}}{\sinh\Lambda^{\frac{1}{4}}}\right)} \end{aligned} \tag{5-7}$$

The code to solve equation (5-7) is written in MATLAB; the result is obtained and illustrated in Figure 5-1. The horizontal coordinates is amplitude of the curvature *b*. The vertical coordinates the non-dimensional eigenvalue Λ.

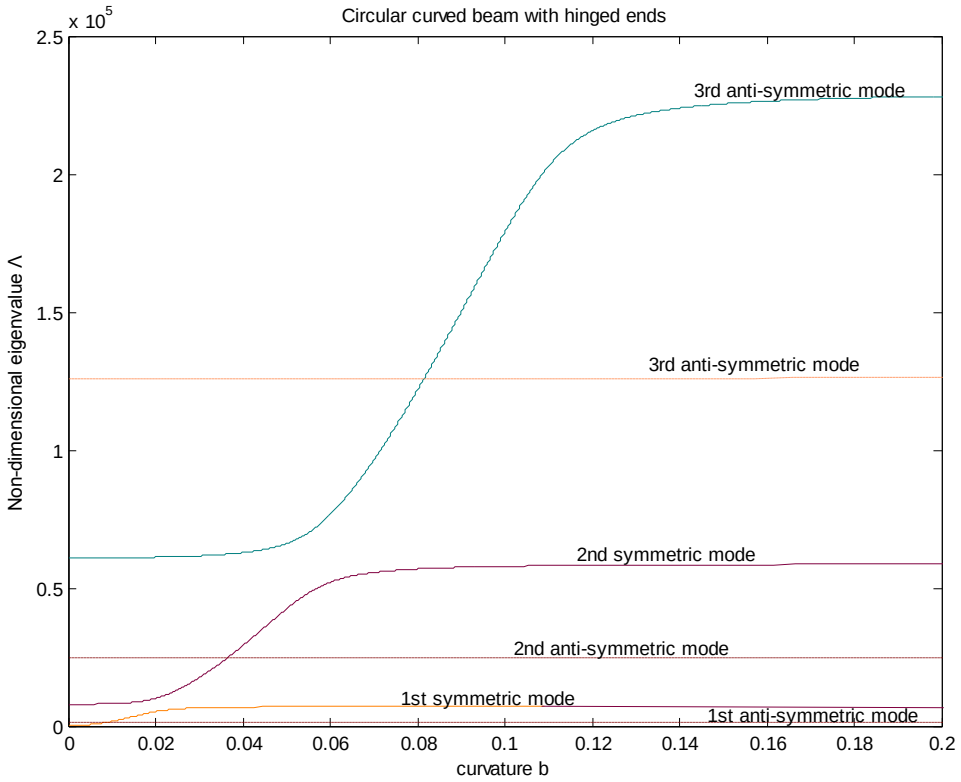

Figure 5.1 Non-dimensional eigenvalue of a circular beam with hinged boundary conditions

The symmetric modes and the anti-symmetric modes are labelled on the curves. The definition of symmetric modes and anti-symmetric modes can be easily demonstrated by the mode shapes. When the deflection of the left half of the beam is the same with the right half of the beam, it can be called symmetric mode. If the deflection of the left half of the beam is of the opposite sign to that of the right half, it is called anti-symmetric mode.

From Figure 5.1, it can be seen that with the increase in curvature, frequencies of symmetric modes rise dramatically and frequencies in anti-symmetric modes remain almost constant. As curvature increase from zero, the frequency of first symmetric mode starts rising. The rising will stop when curvature reaches a certain large value, and from

which the frequency of second symmetric mode start to increase. It will stop rising when it reaches another larger value of curvature. The trends continue in higher symmetric modes.

The analysis is also processed by finite element method in ANSYS.

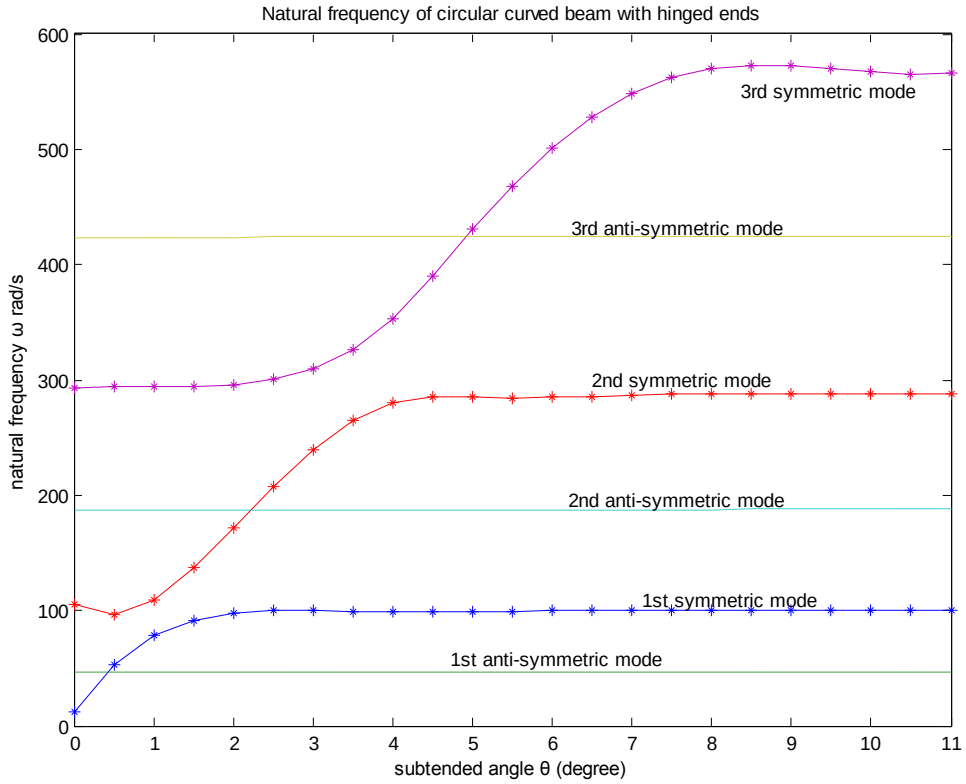

Figure 5.2 Natural frequency of circular curved beam with hinged ends

The natural frequency of the circular curved beam with hinged boundary conditions is shown in Figure 5.2. The circular curved beam has the properties as the length of the beam is 1000 mm, the width is 150 mm, the thickness is 0.8 mm, the density ρ is 7770 kg/m^3, Young's modulus E is 200 *GPa*. A is the area of cross section and I is second moment of inertia. *f* is the frequency (Hz) obtained from ANSYS and ω is angular frequency (rad/s).

Natural frequencies obtained from ANSYS are converted to the non-dimensional eigenvalue using the following equations:

$$\Lambda = \frac{\rho A l^4 \omega^2}{EI}, \tag{5-8a}$$

$$\omega = 2\pi f. \tag{5-8b}$$

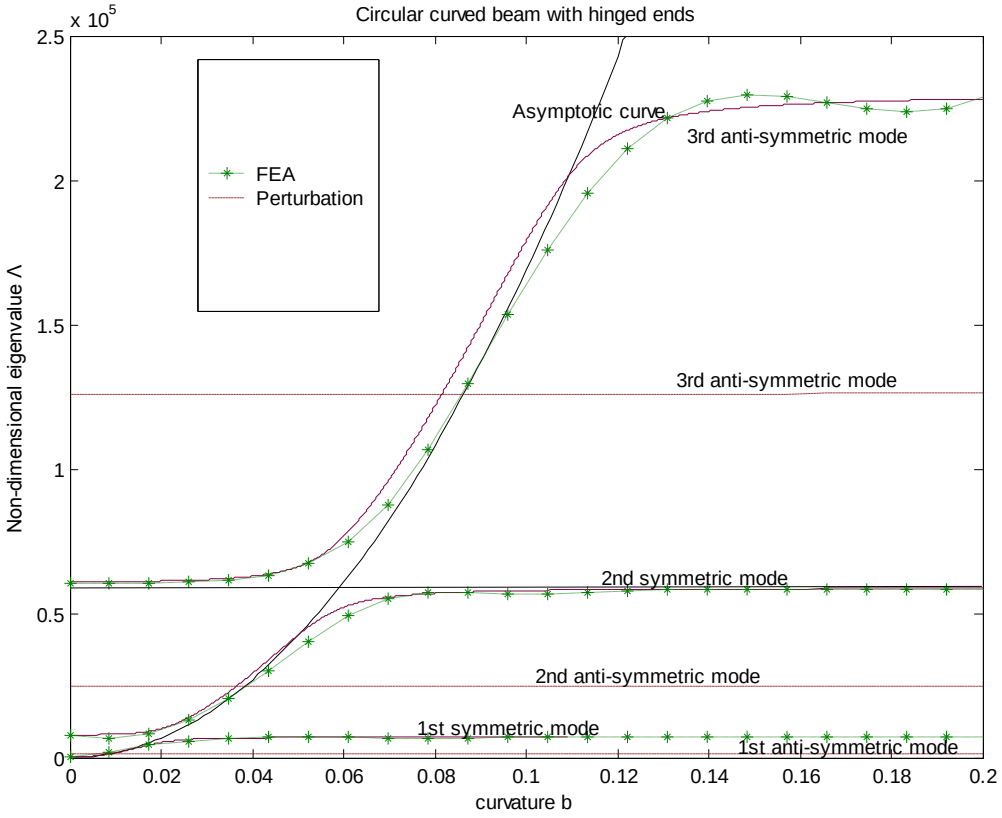

Figure 5.3 Comparisons of non-dimensional eigenvalue of circular curved beam with hinged boundary condition

Figure 5.3 combines results from both perturbation analysis and FEA. From Figure 5.3, it is observed that mode transitions occurred at several curvature values. For the first symmetric mode, it happens at about b=0.007. For the second symmetric mode, it happens at about b=0.038. For the third symmetric mode, it happens at about b=0.09. Another observation is the trend of the curves rises according to the increase in the curvature. Considering the second symmetric mode, there is a relatively rapid rise in frequency when the curvature amplitude b, attains a value of about 0.018. The rise continues till b attains a value of about 0.065, after which frequency is unaffected by the curvature. In a similar way at b=0.065, the third symmetric mode, which was invariant

with *b* till now, shows a rapid increase. The increase continues till *b* reaches about 0.14; after this the frequency is again unaffected. Thus, at a given range of *b* only one symmetric mode will experience a significant change in frequency; the others, lay and large, remain unaffected. Note that anti-symmetric modes are unaffected and generally invariant with changes in curvatures.

It has been demonstrated that the curvature bring the geometric coupling between the extensional mode and the flexural mode. In Figure 5.3, two sets of solid lines represent the asymptotic curves. The set of rising lines represents the membrane vibration. Another set of horizontal lines represents the pure flexural vibration. At the beginning, natural frequency curves rise to a higher value following the route of the membrane asymptotic line. The natural frequency stops increasing when it is close to the horizontal asymptotic line. The curve then moves following the flexural asymptotic line horizontally. It illustrates how the extensional stiffness and the flexural stiffness interact in the curved beams.

Figure 5.3 illustrate the effect of curvature on the natural frequency of curved circular beam. They also indicate that the symmetric and anti-symmetric modes sequence appears in a reverse order when a certain curvature is reached. The mode transition phenomena are illustrated using numerical results and shown in Figure 5.4. Three cases are given according to the value of radius of curvature. For the straight beam (case one), the mode shapes keep normal. As *b* increase (case two), the lowest natural frequency changes to respond the first even mode shape, which means the mode sequence changes. For case three, *b* is larger enough and then the first odd mode does not exist.

Case 1 b=0

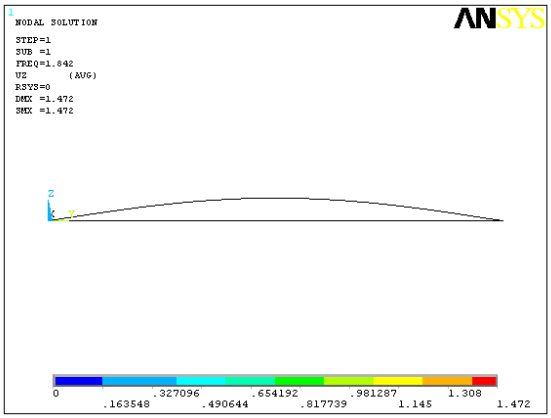

Mode l Symmetry, f =1.842 Hz

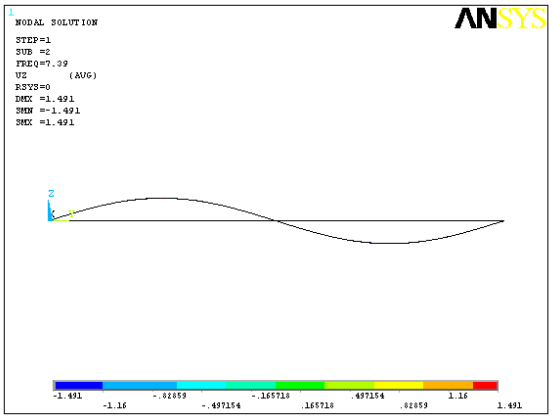

Mode 2 Anti-symmetry, f =7.39 Hz

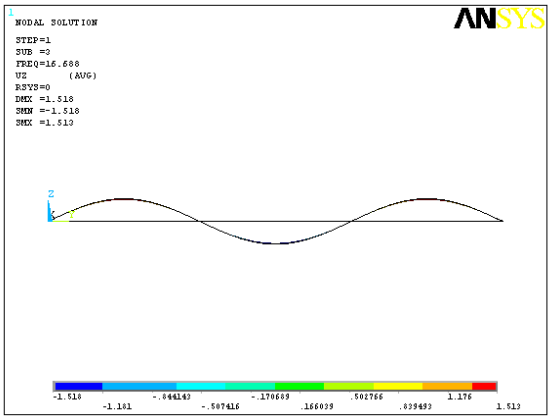

Mode 3 Symmetry, f =16.688 Hz

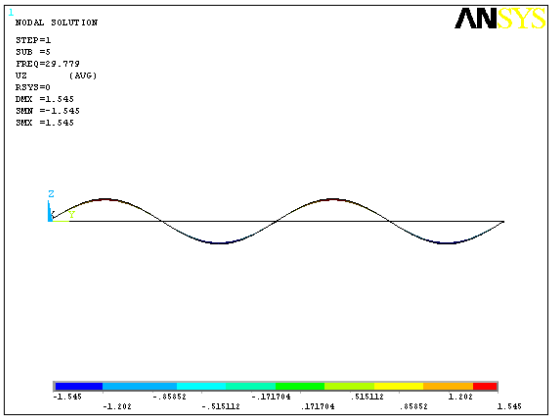

Mode 4 Anti-symmetry, f =29.779 Hz

Case 2 b=0.02

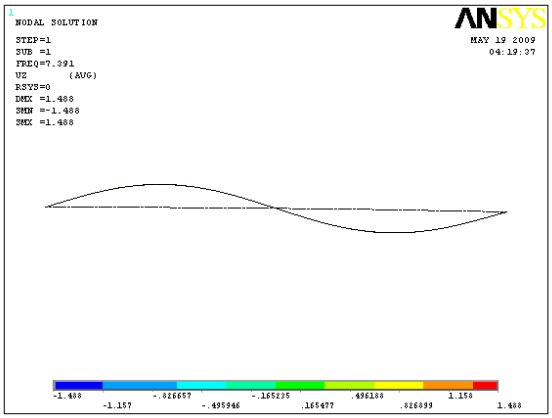

Mode l Anti-symmetry, f =7.391 Hz

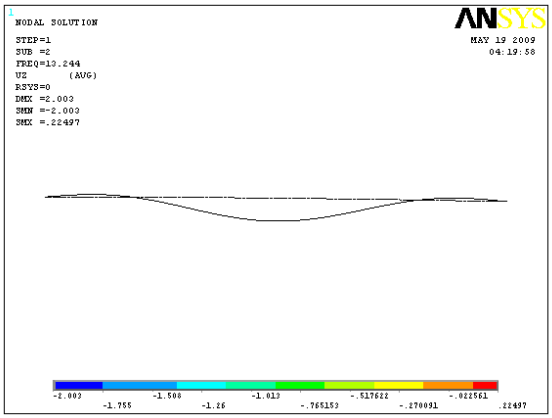

Mode 2 Symmetry, f =13.244 Hz

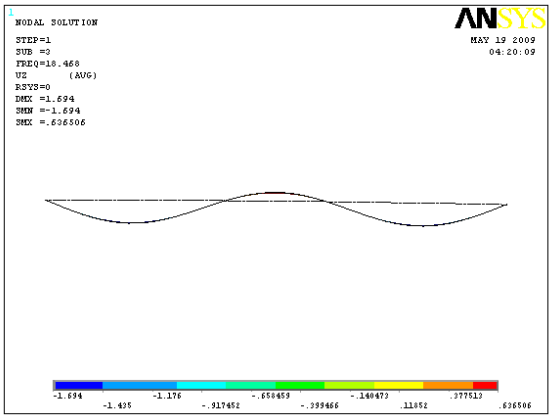

Mode 3 Symmetry, f =18.468 Hz

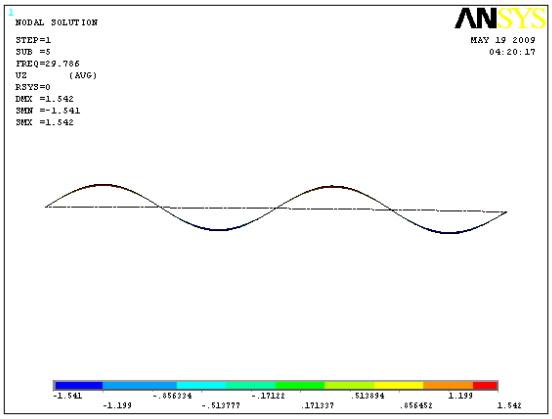

Mode 4 Anti-symmetry, f =29.786 Hz

Case 3 b=0.9

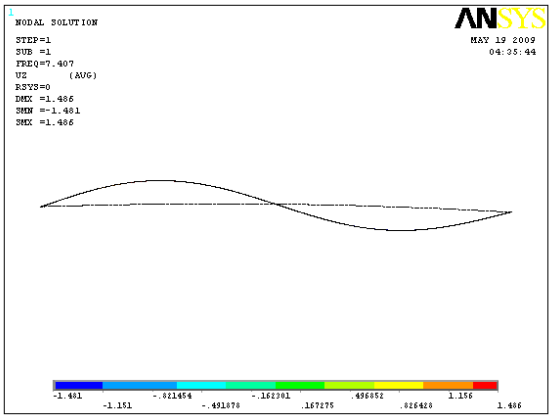

Mode l Anti-symmetry f =7.407 Hz

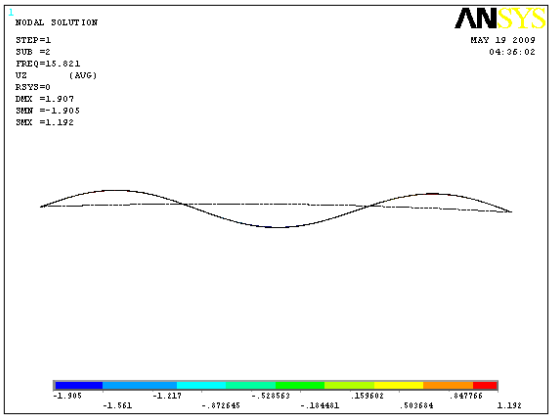

Mode 2 Symmetry f =15.821 Hz

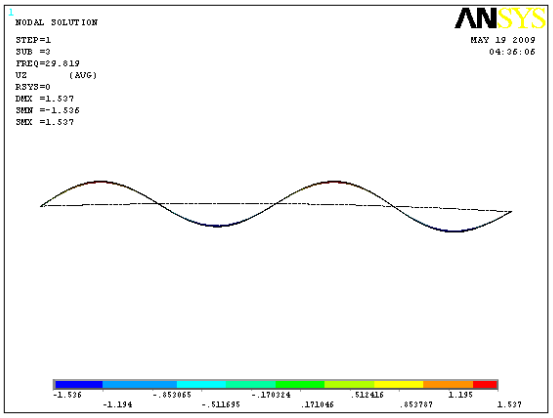

Mode 3 Anti-Symmetry f =29.819 Hz

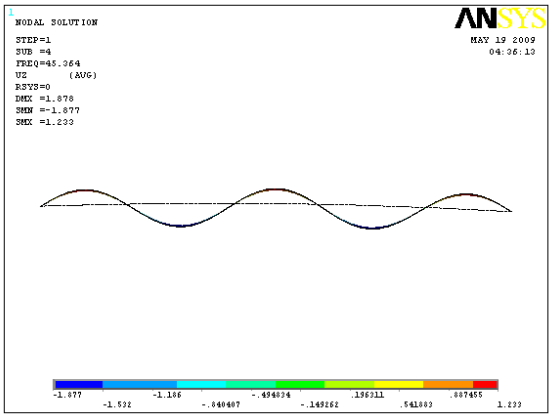

Mode 4 Symmetry f =45.364 Hz

Figure 5.4 Variation in mode sequence due to the rising in curvatures

5.1.2 Clamped boundary conditions

The clamped boundary conditions according to equation (2-38) can be treated as:

$$\overline{w}(0)=0\,,\ \overline{w}(1)=0\,,\ \frac{d\overline{w}(0)}{d\bar{s}}=0\,,\ \frac{d\overline{w}(1)}{d\bar{s}}=0\ . \tag{5-9}$$

Substituting boundary conditions shown in equation (5-9) into equation (5-2), it yields four equations. Three unknown constants C_1, C_2 and C_3 are obtained by solving these equations and shown as follows:

$$C_1=\frac{NH-MJ}{HI-GJ}\ , \tag{5-10}$$

$$C_2=\frac{MI-NG}{HI-GJ}\ , \tag{5-11}$$

$$C_3=-C_1\ . \tag{5-12}$$

where,

$$G=\sin\Lambda^{\frac{1}{4}}-\sinh\Lambda^{\frac{1}{4}}\ , \tag{5-13}$$

$$H=\cos\Lambda^{\frac{1}{4}}-1\ , \tag{5-14}$$

$$I=\Lambda^{\frac{1}{4}}\left(\cos\Lambda^{\frac{1}{4}}-\cosh\Lambda^{\frac{1}{4}}\right), \tag{5-15}$$

$$J=-\Lambda^{\frac{1}{4}}\sin\Lambda^{\frac{1}{4}}\ , \tag{5-16}$$

$$M=-\cosh\Lambda^{\frac{1}{4}}+1\ , \tag{5-17}$$

$$N=-\Lambda^{\frac{1}{4}}\sinh\Lambda^{\frac{1}{4}}\ . \tag{5-18}$$

Using the same procedure as shown in last section, substitute the first condition in equation (5-9) into equation (5-2) and it gives that:

$$b^2 = \frac{\Lambda(C_2+1)}{(C_2+1)-\Lambda^{-\frac{1}{4}}\left[C_1(1-\cos\Lambda^{\frac{1}{4}})+C_2\sin\Lambda^{\frac{1}{4}}+C_3(\cosh\Lambda^{\frac{1}{4}}-1)+\sinh\Lambda^{\frac{1}{4}}\right]}. \quad (5\text{-}19)$$

Equation (5-19) represents the relationship between eigenvalue and curvature, which is solved in MATLAB code and results are illustrated in Figure 5-5. The trends of mode transitions are similar the one with hinged boundary conditions.

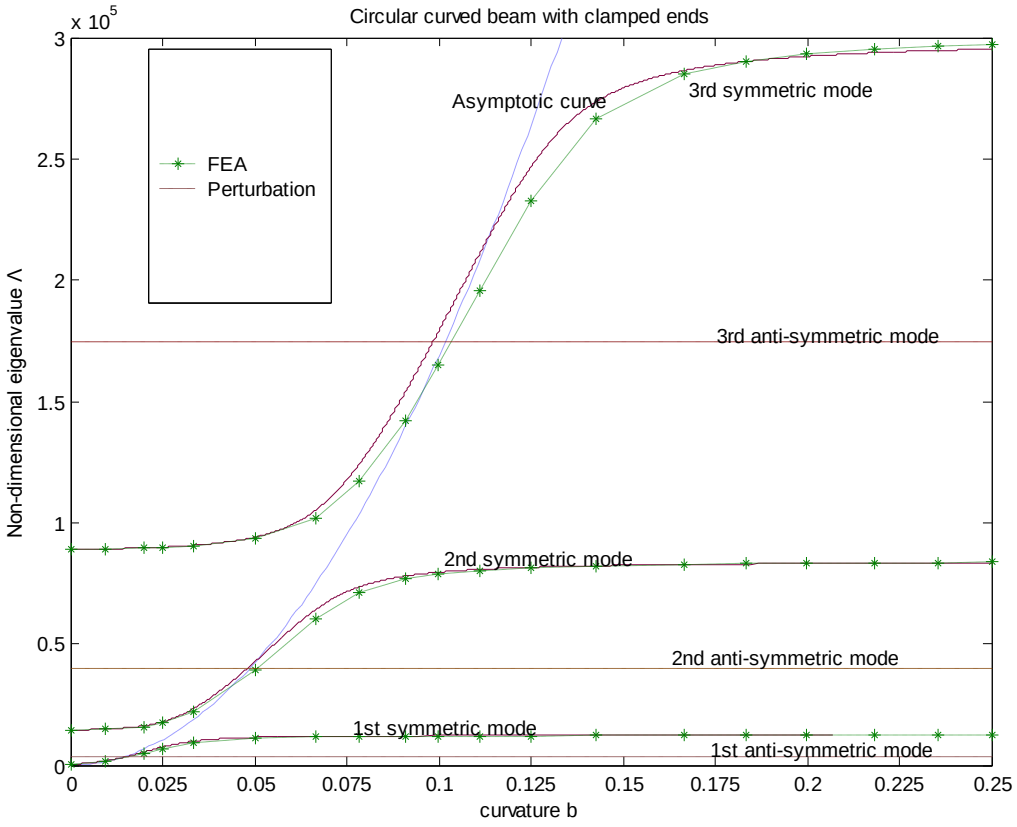

Figure 5.5 Non-dimensional eigenvalue of a circular beam with clamped boundary conditions

Substituting equation (5-19) into equation (5-2), the natural mode shape can be obtained, which is plotted in Figure 5.6. It clearly shows the natural modes changes from the anti-symmetric modes to the symmetric modes when the curvature increases.

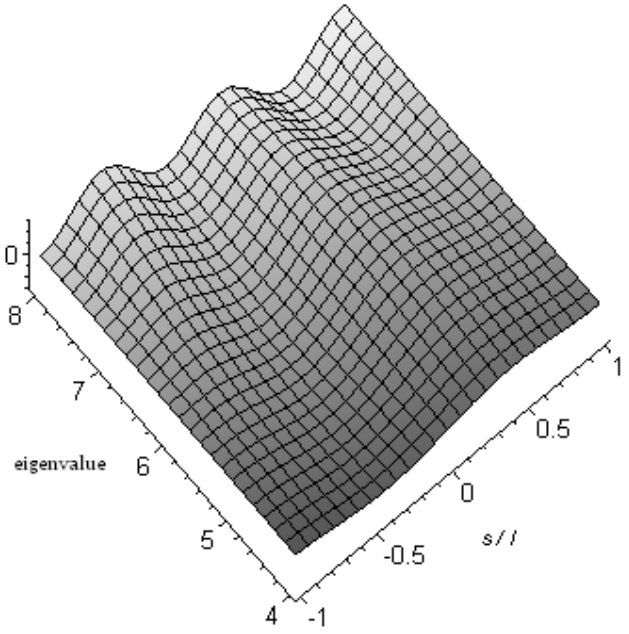

Figure 5.6 Mode shape for clamped circular curved beam with increasing curvatures

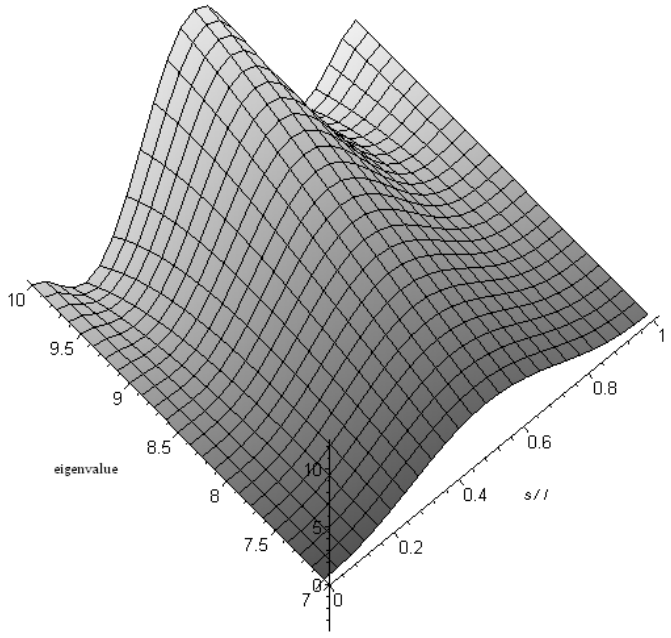

Figure 5.7 Symmetric mode shape transitions for a clamped circular curved beam

If the anti-symmetric mode is ignored, the transverse displacement is expressed as follows:

$$w_0 = C\left\{\sin\frac{\Lambda_0^{1/4}}{2}\cosh\left[\Lambda_0^{1/4}\left(\bar{s}-\frac{1}{2}\right)\right]+\sinh\frac{\Lambda_0^{1/4}}{2}\cos\left[\Lambda_0^{1/4}\left(\bar{s}-\frac{1}{2}\right)\right]-\sin\frac{\Lambda_0^{1/4}}{2}\cosh\frac{\Lambda_0^{1/4}}{2}-\sinh\frac{\Lambda_0^{1/4}}{2}\cos\frac{\Lambda_0^{1/4}}{2}\right\},$$

(5-20)

The mode shapes for only symmetrical modes and the extension vary during the transition stage are plotted in Figure 5.7 and Figure 5.8. It is found that the transition of mode shapes following the increase of the curvature is similar as the one with the hinged boundary condition.

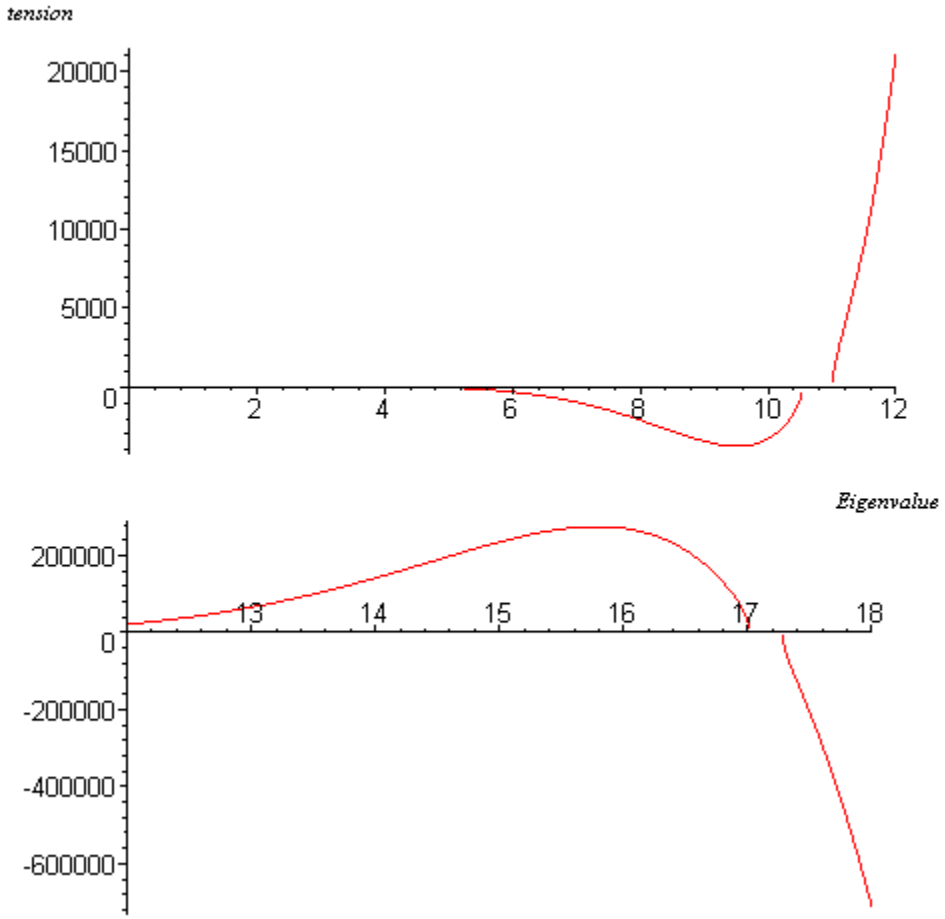

Figure 5.8 extension varies with the curvature

The tension are expressed by equation (3-16) as follows:

$$\frac{\partial \hat{u}_0}{\partial \bar{s}} + \hat{k}\hat{w}_0 = \tau,$$

Substituting the solution of eigenvalue and transverse displacement into above equation, the tension can be obtained as follows:

$$e = C\hat{b}\left[\sin\frac{\Lambda_0^{1/4}}{2}\cosh\frac{\Lambda_0^{1/4}}{2} + \sinh\frac{\Lambda_0^{1/4}}{2}\cos\frac{\Lambda_0^{1/4}}{2} - \frac{4}{\Lambda_0^{1/4}}\sin\frac{\Lambda_0^{1/4}}{2}\sinh\frac{\Lambda_0^{1/4}}{2}\right]. \quad (5\text{-}21)$$

Figure 5.8 also explains the mode transition phenomenon. When the eigenvalue increases, the tension also increases in one direction. At the brake point 10.2, the mode transition occurs. The extra tension released and the mode shape turns from the symmetrical to the anti-symmetrical. At the next brake point 10.5, mode shape turns to the symmetrical again but with higher half wave. The following transition happens at the brake point 17, similar as before.

5.1.3 Simply supported boundary conditions

For cases of those boundary conditions which have no tension constraint, all natural frequencies remain almost constant shown in Figure 5.9.

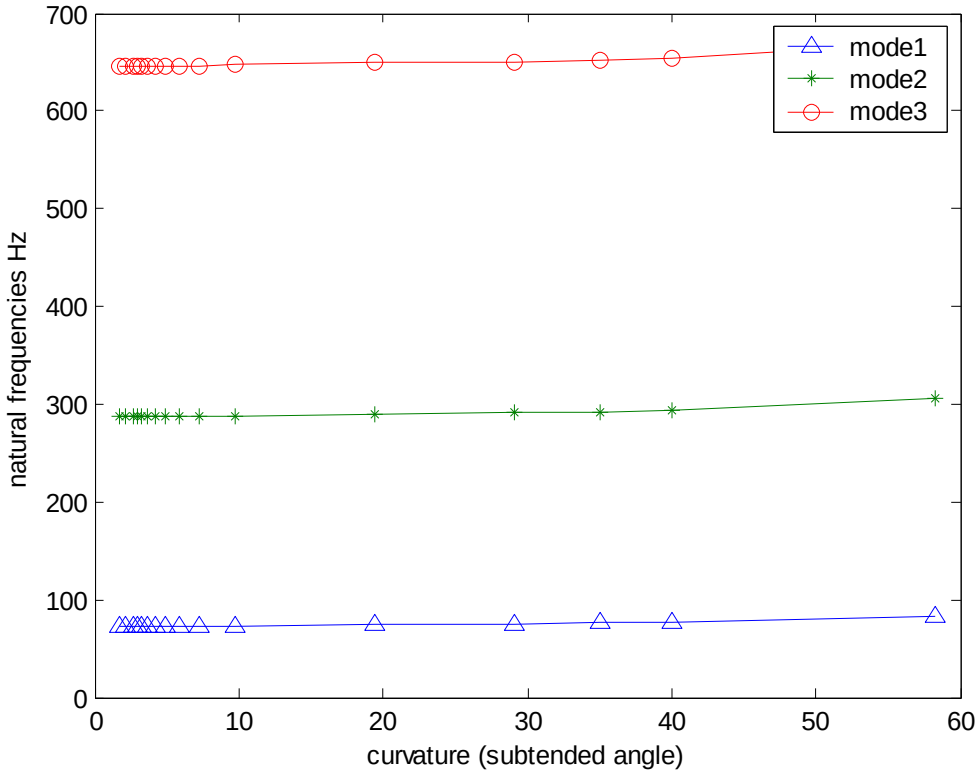

Figure 5.9 Simply support boundary condition

5.2 S-shape Strip

The analysis is not limited to the curved beam with constant curvature. The example S-shape strip has the following properties: length of the beam is 1000 mm, the width is 150 mm, the thickness is 0.8 mm, the density ρ is 7770 kg/m^3, Young's modulus E is 210 *GPa*, Poisson's ratio μ is 0.28. The curvature shape function in equation (3-21) allows curvature change to different forms. S-shape curved beam has different characteristics of natural behaviour, the curvature of which is taken as linear anti-symmetric. The shape function of s-shape strip can be simply expressed as follows:

$$\hat{K}(\bar{s}) = 2\bar{s} - 1,\ 0 \le \bar{s} \le 1 \tag{5-22}$$

Therefore equation (3-21) can be rewritten as follows:

$$\hat{k}(\bar{s}) = b(2\bar{s} - 1)\,. \tag{5-23}$$

where at both ends of the beam, the amplitude of curvature is maximum and it is equal to zero in the middle of the beam. Substituting equation (5-23) into equation (3-29), it results in:

$$\begin{aligned}
\overline{w} &= C_4\left[C_1 \sin(\Lambda^{\frac{1}{4}}\bar{s}) + C_2\cos(\Lambda^{\frac{1}{4}}\bar{s}) + C_3\sinh(\Lambda^{\frac{1}{4}}\bar{s}) + \cosh(\Lambda^{\frac{1}{4}}\bar{s})\right] \\
&\quad + \frac{\hat{k}\int_0^1 \hat{k}C_4\left[C_1 \sin(\Lambda^{\frac{1}{4}}\bar{s}) + C_2\cos(\Lambda^{\frac{1}{4}}\bar{s}) + C_3\sinh(\Lambda^{\frac{1}{4}}\bar{s}) + \cosh(\Lambda^{\frac{1}{4}}\bar{s})\right]d\bar{s}}{\Lambda - \int_0^1 \hat{k}^2\, d\bar{s}} \\
&= C\left[C_1 \sin(\Lambda^{\frac{1}{4}}\bar{s}) + C_2\cos(\Lambda^{\frac{1}{4}}\bar{s}) + C_3\sinh(\Lambda^{\frac{1}{4}}\bar{s}) + \cosh(\Lambda^{\frac{1}{4}}\bar{s})\right] \\
&\quad + \frac{Cb^2\left\{\begin{array}{l}\Lambda^{-\frac{1}{4}}\left[-C_1(\cos\Lambda^{\frac{1}{4}}+1) + C_2\sin\Lambda^{\frac{1}{4}} + C_3(\cosh\Lambda^{\frac{1}{4}}+1) + \sinh\Lambda^{\frac{1}{4}}\right] \\ +2\Lambda^{-\frac{1}{2}}\left[C_1\sin\Lambda^{\frac{1}{4}} + C_2(\cos\Lambda^{\frac{1}{4}}-1) - C_3\sinh\Lambda^{\frac{1}{4}} - (\cosh\Lambda^{\frac{1}{4}}-1)\right]\end{array}\right\}}{\Lambda - b^2/3}\,.
\end{aligned} \tag{5-24}$$

From the circular beam study, it is found that under both hinged and clamped boundary conditions, the transverse displacement at ends is equal to zero. Therefore substituting the condition ($\overline{w}(0)=0$) into equation (5-24), it gives the relationship between eigenvalue and amplitude of curvature, shown as follows:

$$b^2 = \frac{\Lambda(C_2+1)}{(C_2+1)\int_0^1 (2\bar{s}-1)^2 d\bar{s} + \int_0^1 (2\bar{s}-1)\left[C_1 \sin(\Lambda^{\frac{1}{4}}\bar{s}) + C_2 \cos(\Lambda^{\frac{1}{4}}\bar{s}) + C_3 \sinh(\Lambda^{\frac{1}{4}}\bar{s}) + \cosh(\Lambda^{\frac{1}{4}}\bar{s})\right] d\bar{s}}$$

$$= \frac{\Lambda(C_2+1)}{\left\{\begin{array}{l} 1/3(C_2+1) + \Lambda^{-\frac{1}{4}}\left[-C_1(\cos\Lambda^{\frac{1}{4}}+1) + C_2\sin\Lambda^{\frac{1}{4}} + C_3(\cosh\Lambda^{\frac{1}{4}}+1) + \sinh\Lambda^{\frac{1}{4}}\right] \\ + 2\Lambda^{-\frac{1}{2}}\left[C_1\sin\Lambda^{\frac{1}{4}} + C_2(\cos\Lambda^{\frac{1}{4}}-1) - C_3\sinh\Lambda^{\frac{1}{4}} - (\cosh\Lambda^{\frac{1}{4}}-1)\right] \end{array}\right\}} \tag{5-25}$$

where the constant C is eliminated by normalizing the transverse displacement and constants C_1, C_2 and C_3 need to be solved by using appropriate boundary conditions.

5.2.1 Hinged boundary conditions

Substituting equation (5-3) into equation (5-24), it yields four equations. Three unknown constants C_1, C_2 and C_3 are obtained by solving these equations and shown as follows:

$$C_1 = -\frac{1}{\sin\Lambda^{\frac{1}{4}}}\left(1+\cos\Lambda^{\frac{1}{4}}\right), \tag{5-26}$$

$$C_2 = 1, \tag{5-27}$$

$$C_3 = -\frac{1}{\sinh\Lambda^{\frac{1}{4}}}\left(1+\cosh\Lambda^{\frac{1}{4}}\right). \tag{5-28}$$

Therefore equation (5-25) can be solved by substituting equation (5-26) – (5-28). Results are illustrated in Figure 5.10. The horizontal coordinates is the amplitude of the curvature b. The vertical coordinates the non-dimensional eigenvalue Λ. The symmetric

modes are shown in dashed lines and the anti-symmetric modes are shown in solid lines. The trends of natural mode changes of the s-shape strip are different from that of the circular beam with constant curvatures. Unlike the circular beam, the symmetric modes of s-shape strip will not be significantly affected by changes in curvature. On the other hand, the anti-symmetric natural frequencies start increasing with the rising of curvature and will stop rising until reach a certain large curvature parameter. It can be concluded that the mode transitions of s-shape curved beam has a reverse order of the curved beam with constant curvature.

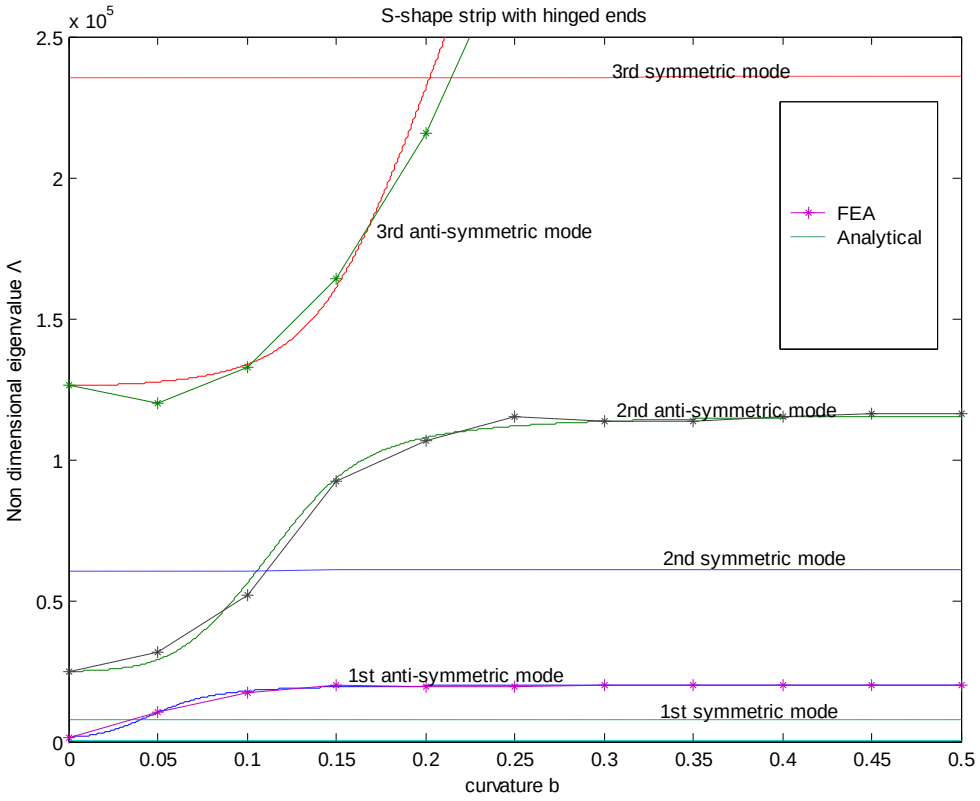

Figure 5.10 Non-dimensional eigenvalue of an s-shape strip with hinged end conditions

Mode transition behaviour is also illustrated in Figure 5.11. The first three natural modes for three different curvatures are plotted. Symmetric modes are noted by *s*, anti-symmetric modes are noted by *as*. The frequencies are given, which match with the non-dimensional eigenvalue after the convert by equation (5-8).

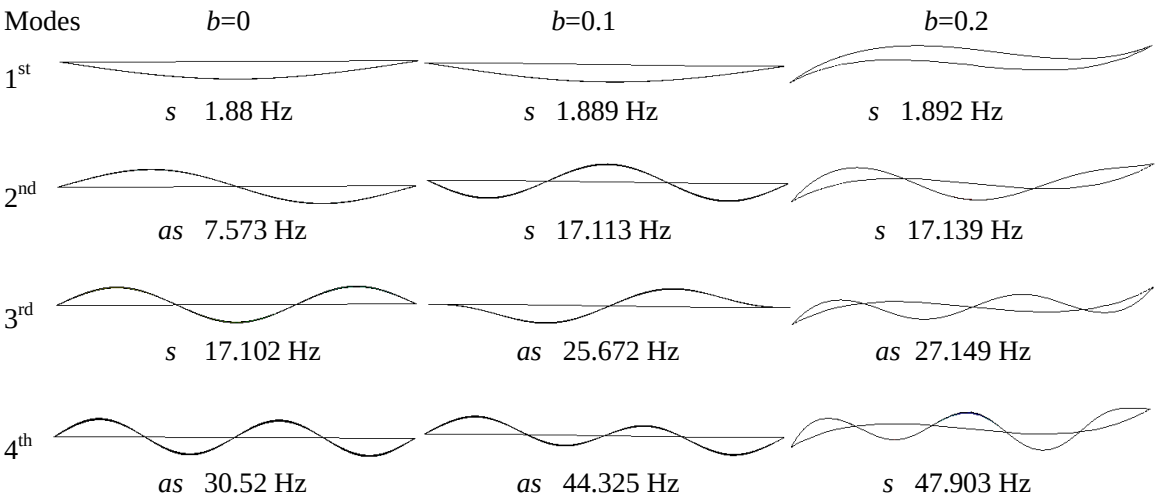

Figure 5.11 mode shape transition of S-shape with hinged boundaries

5.2.2 Clamped boundary conditions

Using the similar procedure with the hinged boundary condition case, the unknown constants here can be obtained as follows:

$$C_1 = \frac{NH - MJ}{HI - GJ} \quad , \tag{5-29}$$

$$C_2 = \frac{MI - NG}{HI - GJ} \quad , \tag{5-30}$$

$$C_3 = -2\Lambda^{-\frac{1}{4}}(C_2 + 1) - C_1 \ , \tag{5-31}$$

where,

$$G = -\left(\sin \Lambda^{\frac{1}{4}} - \sinh \Lambda^{\frac{1}{4}}\right), \tag{5-32}$$

$$H = -\cos \Lambda^{\frac{1}{4}} - 1 + 2\Lambda^{-\frac{1}{4}} \sinh \Lambda^{\frac{1}{4}} \ , \tag{5-33}$$

$$I = -\Lambda^{\frac{1}{4}}\left(\cos \Lambda^{\frac{1}{4}} - \cosh \Lambda^{\frac{1}{4}}\right) \ , \tag{5-34}$$

$$J = 2\cosh \Lambda^{\frac{1}{4}} + \Lambda^{\frac{1}{4}} \sin \Lambda^{\frac{1}{4}} - 2 \ , \tag{5-35}$$

$$M = \cosh \Lambda^{\frac{1}{4}} + 1 - 2\Lambda^{-\frac{1}{4}} \sinh \Lambda^{\frac{1}{4}} \ , \tag{5-36}$$

$$N = -2\cosh \Lambda^{\frac{1}{4}} + \Lambda^{\frac{1}{4}} \sinh \Lambda^{\frac{1}{4}} + 2 \ . \tag{5-37}$$

Substituting equation (5-29) – (5-31) into equation (5-25), eigenvalue can be obtained by giving a range of value of curvature. Results are illustrated in Figure 5.12. The trends of mode frequencies changing are similar with hinged boundary conditions.

It can be concluded that for a beam whose curvature is a symmetric or anti-symmetric function, only those modes possessing the same type of symmetry in the transverse displacement undergo a mode transition. It can be proven from equation (3-20) that if the curvature shape function is symmetric (or anti-symmetric) and the transverse displacement function is anti-symmetric (or symmetric), the integration will be equal to zero; thus no tension can be generated in the beam. Therefore, curvature does not affect the natural behaviour of curved beam.

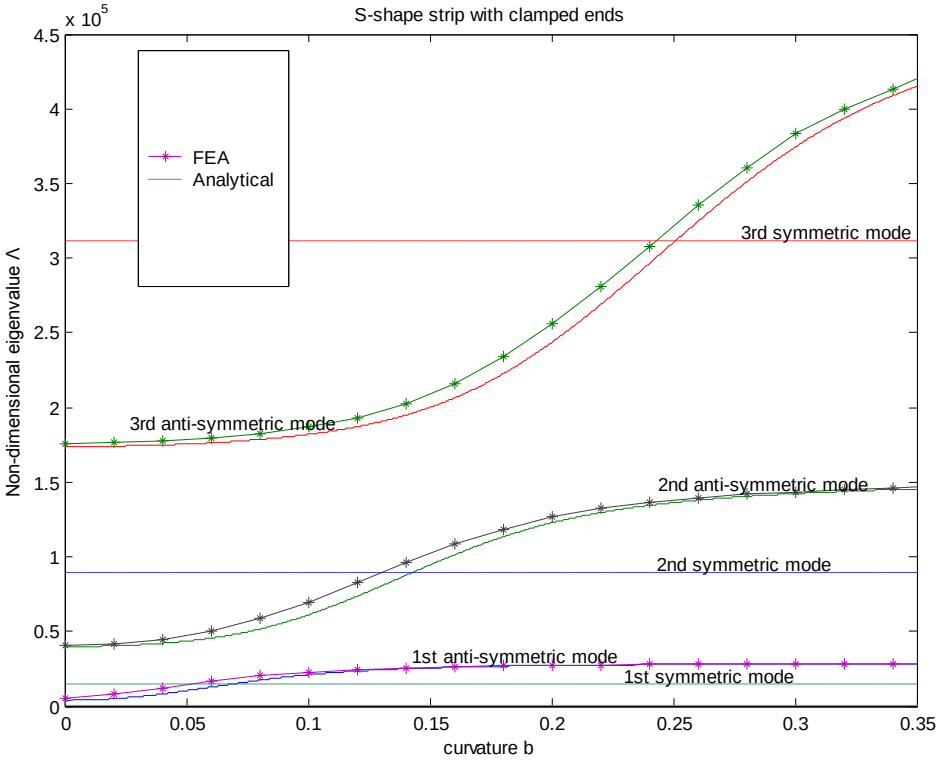

Figure 5.12 Non-dimensional eigenvalue of an s-shape strip with clamped end condition

5.3 Summary

5.3.1 Discussion on different order perturbations

The difference between different order perturbations results normally refer to the accuracy comparing with the closed form solution. As reviewed in the background, very limited closed form solution for curved beams with specific boundary conditions exists. Hence, in this section, the first natural frequency of a circular curved beam with clamped boundary condition is provided to demonstrate the accuracy of different order perturbation. FEA results are used for comparison.

From Figure 5.13, it is found that for a thin curved beam (thickness less than 1/20 of the length), the eigenvalue of different order perturbations are very similar. From equation (3-6), it is easy to see the parameter ξ is very small for small thickness, which explains all curves coincide together. When the thickness increased, in Figure 5.14, the curves of first order and second order perturbations are closer to the FEA results. Since the parameter ξ includes also the curvature parameter, it is noted that within the lower curvature range, all curves still coincide together until the curvature becomes large enough; parameter ξ starts to affect the trends of the eigenvalue.

5.3.2 Discussion on natural frequencies change for large curvatures

For example, in Figure 5.12, the curve for the first anti-symmetric mode rises rapidly before the value of curvature reach 0.1. After that, the trend of the curve remains steady. The first anti-symmetric mode gradually transits to the second anti-symmetric mode. If the curvature continues increasing, at a certain large curvature, say much larger than the value of 0.35, the second anti-symmetric mode will finish transition to the third second anti-symmetric. Therefore, at a certain large curvature, the first anti-symmetric mode will not exist and the curve for the first anti-symmetric mode will stop before that value. In such case, the first natural frequency of the curved beam with large curvature can be very high.

5.3.3 Summary

From the analysis in this Chapter, it is easy to conclude that for the curved beam whose curvature can be expressed as the function of the length of the arc, the perturbation solution can be derived. Different curved beams have different natural modes, but the changes in the curvature lead to the mode transition phenomena. These mode transition phenomena can be seen from plots of natural frequency, mode shape and tension of the curved beam. All analytical results are compared with FEA ones, showing very good agreement.

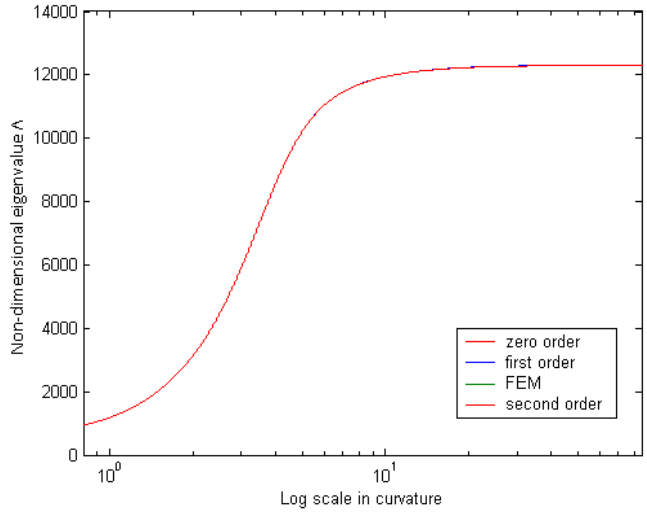

Figure 5.13 Non-dimensional eigenvalue comparisons of a thin (η=1e-6) circular curved beam with clamped ends

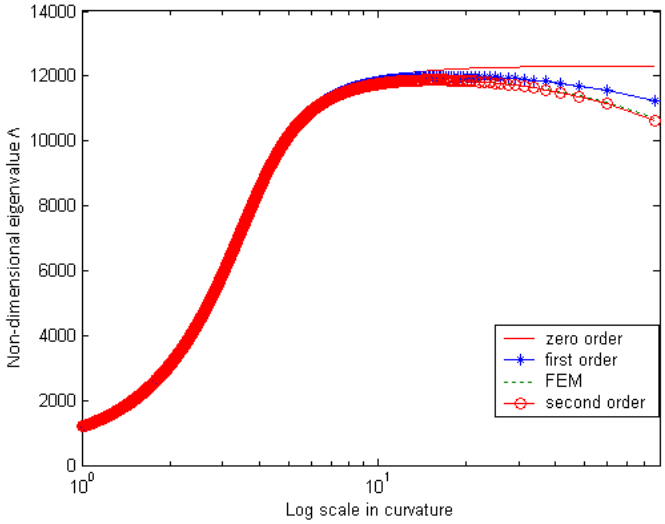

Figure 5.14 Non-dimensional eigenvalue comparisons of a thicker (η=1e-4) circular curved beam with clamped ends

Chapter 6 Curved Beam with Arbitrary Curvatures

Not all curvatures can be easily expressed as the function of the length of arc such as the curved beam with parabolic arc. Another example, in the construction industry, is that of curved beams requiring to be weld to straight beams at both ends. It is not straightforward to apply the perturbation method to those kinds of curved structures. In order to expand the present analysis suitable for arbitrary geometries, some transformations and assumptions are made in this Chapter.

6.1 Treatment of Arbitrary Curvature

It has been demonstrated that when the curvature can be expressed as the function of the length of arc, the natural behaviour can be investigated through the perturbation method. However, in real engineering applications, not all geometries can be ideally expressed by the curvature function. For a parabolic curved beam, shown in Figure 6.1, the arc length can be expressed as follows:

$$s(\theta) = \theta\sqrt{1+\theta^2} + \sinh^{-1}\theta \text{ , where } 0 \le \theta \le \pi \tag{6-1}$$

$$k = \frac{1}{2(1+\theta^2)^{\frac{3}{2}}}, \text{ where } 0 \le \theta \le \pi \tag{6-2}$$

According to equation (6-1) and (6-2), the curvature function can be derived as follows:

$$k(s) = \int \frac{dk}{ds} ds = \int \frac{dk}{d\theta}\frac{d\theta}{ds} ds, \tag{6-3}$$

where

$$\frac{d\theta}{ds} = \frac{1}{\sqrt{1+\theta^2}+\frac{\theta^2}{\sqrt{1+\theta^2}}-\frac{\cosh\theta}{\sinh^2\theta}}, \tag{6-4}$$

and $$\frac{dk}{d\theta} = \frac{\frac{3}{2}\theta}{(1+\theta^2)^{\frac{5}{2}}}. \tag{6-5}$$

By substituting equation (6-4) and (6-5) into equation (6-3), it is seen that if the curvature is assumed as the function of the arc length, the equation would be very complex. Therefore we try to seek another solution.

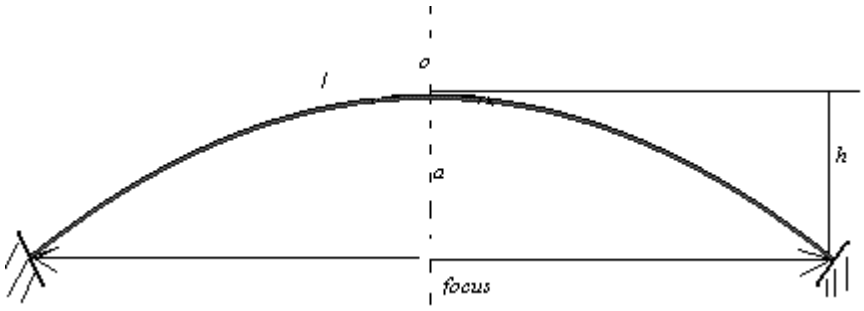

Figure 6.1 sketch of a parabolic curved beam

A parabola can also be obtained as the limit of a sequence of ellipses where one focus is kept fixed as the other is allowed to move arbitrarily far away in one direction. The equation of a parabola in rectangular coordinates is as follows:

$$y = ax^2. \tag{6-6}$$

Looking back to the curvature equation in Chapter 2, the curvature for the parabola arc is as follows:

$$k(x) = \frac{\frac{d^2y}{dx^2}}{\left[1+\left(\frac{dy}{dx}\right)^2\right]^{\frac{3}{2}}} = \frac{2a}{[1+(2ax)^2]^{\frac{3}{2}}}. \tag{6-7}$$

From the zero order perturbation equation, it is assumed that the solution of the curved beam is equal to the solution of the straight beam plus the particular solution. This assumption leads to $x \cong s$ for the curved beam with small amplitudes of curvature. Therefore, in rectangular coordinates, equation (3-12) transforms to the following equation:

$$\frac{\partial}{\partial \bar{x}}\left[\frac{1}{\hat{k}}\left(\frac{\partial^4 \hat{w}_0}{\partial \bar{x}} - \Lambda_0 \hat{w}_0\right)\right] = 0. \tag{6-8}$$

By substituting equation (6-7) into equation (6-8), the solution procedure is similar as previous analysis.

6.2 Natural Vibration of a Parabolic Arc

An example is given by Lee and Wilson (1989) for a parabolic arc with dimension of l=36.7cm and h=9.17cm, and with cross-section dimensions of 2.54cm and 0.635cm. The boundary condition is clamped at both ends. The natural frequencies are shown in Table 6.1.

Table 6.1 Natural frequency of parabolic arch (Hz)

Mode number	Lee and Wilson (1989)	Perturbation	FEM
1	363	356.4	358.6
2	818	770.8	810.6
3	1450	1360.3	1433.1

The zero and first order perturbation solutions are calculated. Because the thickness/length ratio is small < 1/50, results from both are similar. However, for second and third mode, the perturbation results are much lower than Lee and Wilson (1989), who used dynamic stiffness method. This is caused by that the transverse displacement and the curvature are the function of x other than s. Assume the length of the beam is fixed, due to the curved shape, the difference between x and s will generate the tolerance.

The mode shape transition of the parabolic arc behaves similar as the circular curved beam because they have the same symmetric configuration.

Chapter 7 Effect of Curvature on the Natural Vibration of Curved Plates

If the lateral direction of a curved beam cannot be ignored, it is called singly curved plate in this Chapter. Such curved structures are normally solved by the thin shell theory, which has been reviewed and derived in Chapter 1 and Chapter 2 respectively. For the curved plate with variable curvature, the governing equations become very complex, and researchers normally seek help from numerical approaches. In this Chapter, the perturbation method is shown to be applicable for the thin curved plate when combined with the Rayleigh-Ritz method. However, more features caused by changes in curvature are revealed by FEA results.

7.1 Application of Perturbation Solution

The most common analytical approach to deal with the natural behaviour of a flat plate is the Rayleigh-Ritz method. The natural frequency can be expressed as follows:

$$\omega^2 = \frac{V}{\rho A_{rea}/2 \int_0^a \int_0^b w^2 ds dx}, \tag{7-1}$$

where V is the strain energy

$$V = -\frac{1}{2}\int_0^s \mathbf{M}\kappa ds. \tag{7-2}$$

where $\mathbf{M}$ and κ can be found from equation (2-19) and (2-20).

and w is the transverse displacement,

$$w = \sum_{n=1}^{p} W_n \,, \tag{7-3}$$

where W_n is the displacement function for the curved beam and can be expressed as follows:

$$W_n = C_1 \sin(\frac{n\pi s}{l}) + C_2 \cos(\frac{n\pi s}{l}) + C_3 \sinh(\frac{n\pi s}{l}) + \cosh(\frac{n\pi s}{l}) + W_p \,. \tag{7-4}$$

W_p is the particular solution for curved beam and can be obtained following the same procedure shown in Chapter three, section 3.2. W_n can be obtained using the boundary conditions. Substituting w into equation (7-1), the natural frequency can be obtained for a circular curved beam with the property given in Chapter four, section 4.3.

Table 7.1 natural frequency of circular beam with hinged ends

Mode shape	Rayleigh-Ritz Hz	ANSYS Hz
1	318.4	325.2
2	659.1	668.4
3	1297.7	1308.3

For the singly curved plate, the transverse displacement functions for lateral and longitudinal directions are expressed as follows:

$$w = \sum_{m=1}^{p} \sum_{n=1}^{q} a_{mn} W_m W_n \,, \tag{7-5}$$

$$W_m = C_{m1} \sin(\frac{m\pi x}{a}) + C_{m2} \cos(\frac{m\pi x}{a}) + C_{m3} \sinh(\frac{m\pi x}{a}) + \cosh(\frac{m\pi x}{a}) \,, \tag{7-6}$$

$$W_n = C_{n1} \sin(\frac{n\pi s}{l}) + C_{n2} \cos(\frac{n\pi s}{l}) + C_{n3} \sinh(\frac{n\pi s}{l}) + \cosh(\frac{n\pi s}{l}) + W_p \,, \tag{7-7}$$

where the notation x represents the short straight edge with width a and s represents the curved edge with the length l. W_p is the particular solution for curved beam, see equation (3-25). Once the boundary conditions are known, W_m and W_n can be derived and then substituting to equation (7-1) to obtain the natural frequency. The natural frequency of a

circular curved plate with the same property given in Chapter four, section 4.3 is calculated as an example. Four edges are hinged. The result is shown in Table 7.2.

Table 7.2 Natural frequency of curved plate with hinged edges

Mode number	Rayleigh-Ritz Hz	ANSYS Hz
1,2	710.1	719.8
1,3	812.3	822.6
1,3	1087.3	1095
2,1	1128.6	1140

Although the energy method combining with the perturbation method is able to solve the curved plate problem, it needs large work on equation derivations for different boundary conditions. As comparisons, FEM is easier to solve the free vibration problem and more applicable to reveal most features related to the changes in curvatures.

7.2 Propagation Behaviour of the Curved Plate

7.2.1 Circular curved plate

Scott and Woodhouse (1992) calculated the wave propagation along an infinite strip of constant curvature. They used wave equations to demonstrate the impact of curvatures on wave propagation. The solution is not explicit until the present paper simulates the similar results by FEA. The transverse displacement in horizontal direction of a circular curved strip is calculated. The first three symmetric modes are shown in Figure 7.1. The transverse displacement varies along the strip. Using FEA result, Figure 7.2 simulates the wave propagation along a strip of constant curvature, comparing with results from Scott and Woodhouse (1992), it shows the similar trends of curves. The infinite strip is simulated by pinned boundary conditions. Three groups of curves represent three symmetric waveguide branches.

The first symmetric mode is represented by solid lines, called “bending-beam” mode. It can be found that four solid lines which represent curved beams with four different curvatures coincide together. This indicates curvature does not affect natural behaviour of infinite curved beams because there are no boundary conditions to provide tension to the beam. Dashed curves represent second symmetric modes. Four curves represent four strips with different curvatures (subtended). From bottom to top, the curvature increases from 0^o to 57.3^o. For the most curved strip, when the wave number increases, the natural frequency reduces initially and then increases. When the wave number exceeds 20, natural frequencies tend to be identical for all curved strips. In other words, the curvature can not affect the natural frequency when the mode number is large enough. For the third symmetric modes, dot curves indicate the trends appear to converge at large wave number. However, this involves very higher frequencies. Therefore no further works will be done in this case.

Other boundary condition corresponding to the second lateral symmetric modes are calculated and some is shown as follows, which illustrates how the natural frequencies change due to changes in curvature. Figure 7.3 is for the clamped circular curved strip, using the same property as in Chapter five, section 5.1, the lower natural frequency rises

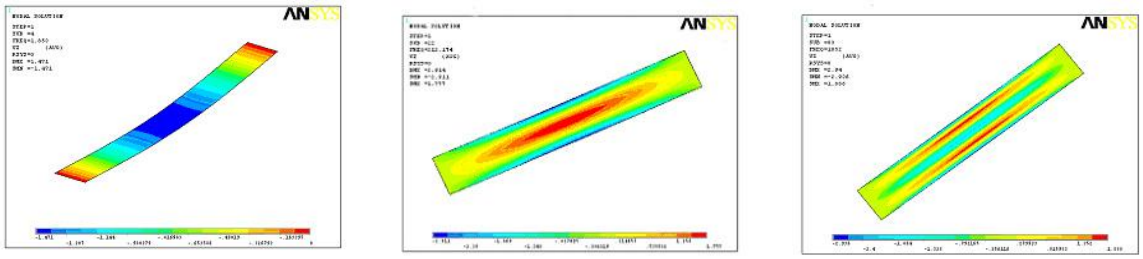

First symmetric mode
3.4 Hz

Second symmetric mode
263 Hz

Third symmetric mode
1190 Hz

Figure 7.1 transverse displacements for first three lateral symmetric modes of an elastic strip

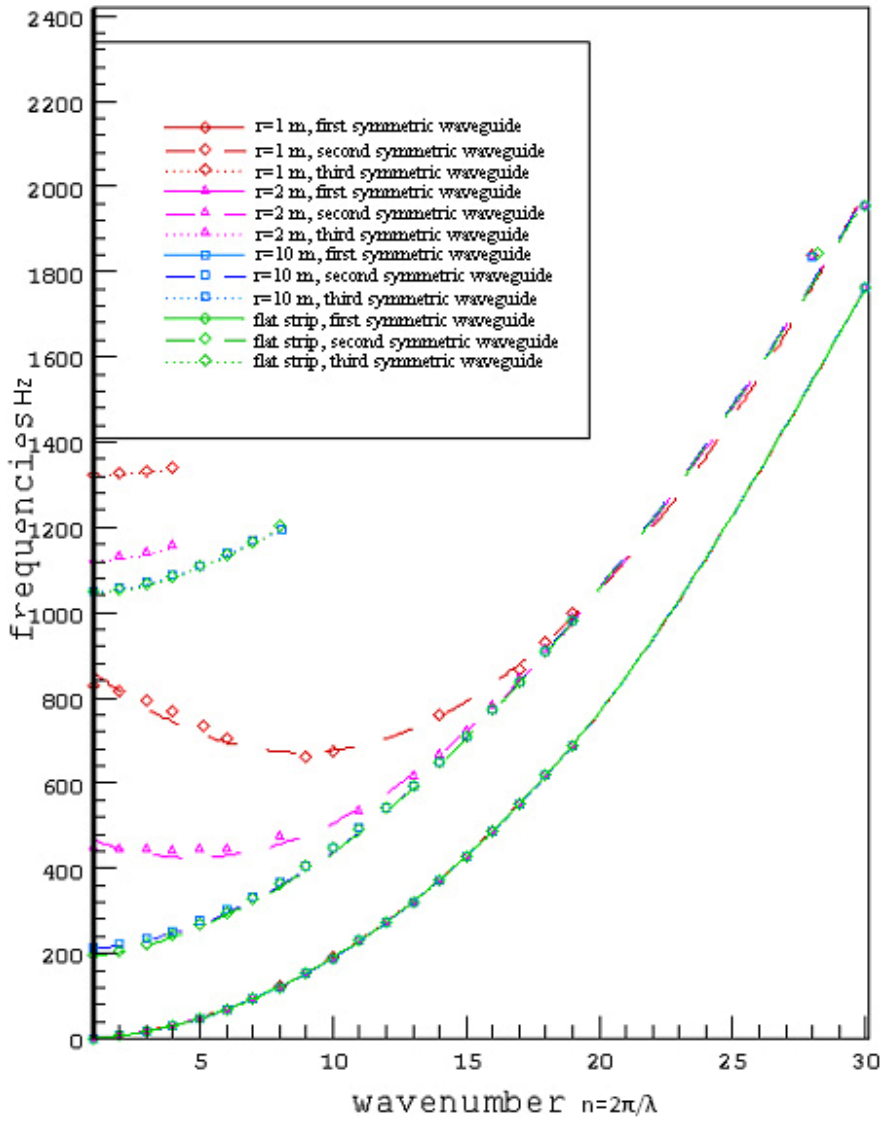

Figure 7.2 Dispersion curves for second symmetric lateral vibration mode of circular curved strip. Four curves represent four strips with different curvatures (subtended angles). The trends of curves is similar with one shown in Scott and Woodhouse (1992)

faster than the higher ones, which indicates the mode transition phenomenon occurring in large curvature strip. The fully clamped boundary condition in Figure 7.4 shows the similar result. It can be seen that the natural frequency of the circular curved beam has slight changes for different boundary conditions.

Figure 7.5 shows the curved plate with fully clamped boundaries. There is no first symmetric waveguide mode for the normal displacement function due to high stiffness in the longitudinal direction. The fully free boundary conditions show in Figure 7.6, that there is no mode transition occurring, but the lower modes increase more rapidly than higher modes. This indicates that the mode sequence will alter at a very large curvature.

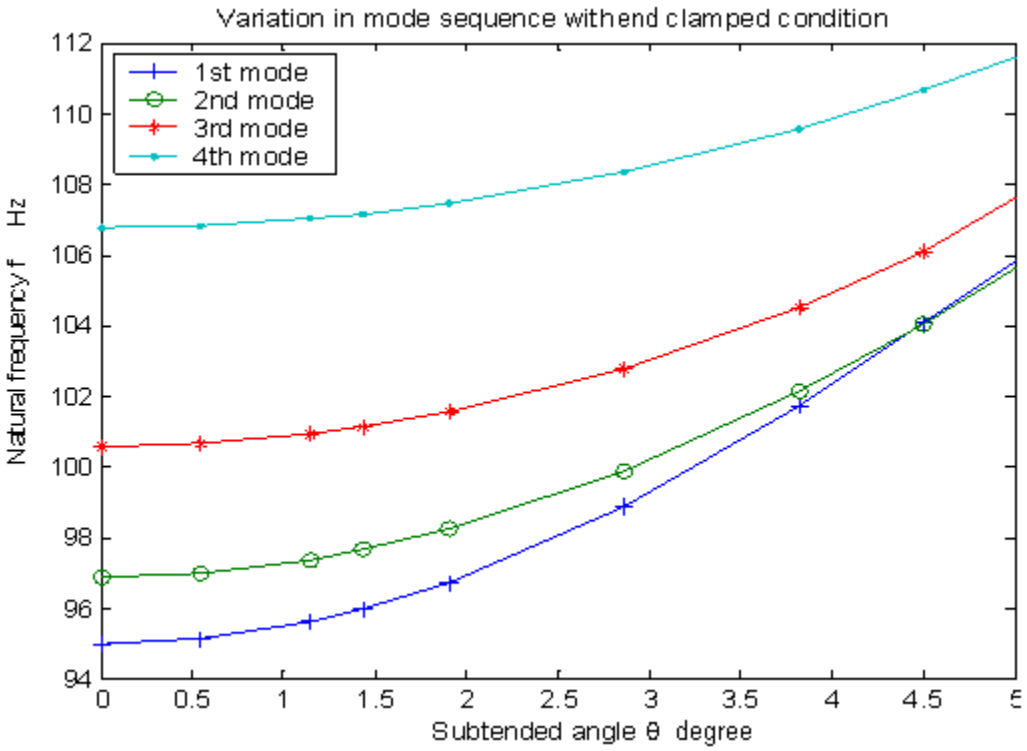

Figure 7.3 Natural frequencies of circular curved beam with two ends clamped for the second waveguide branch

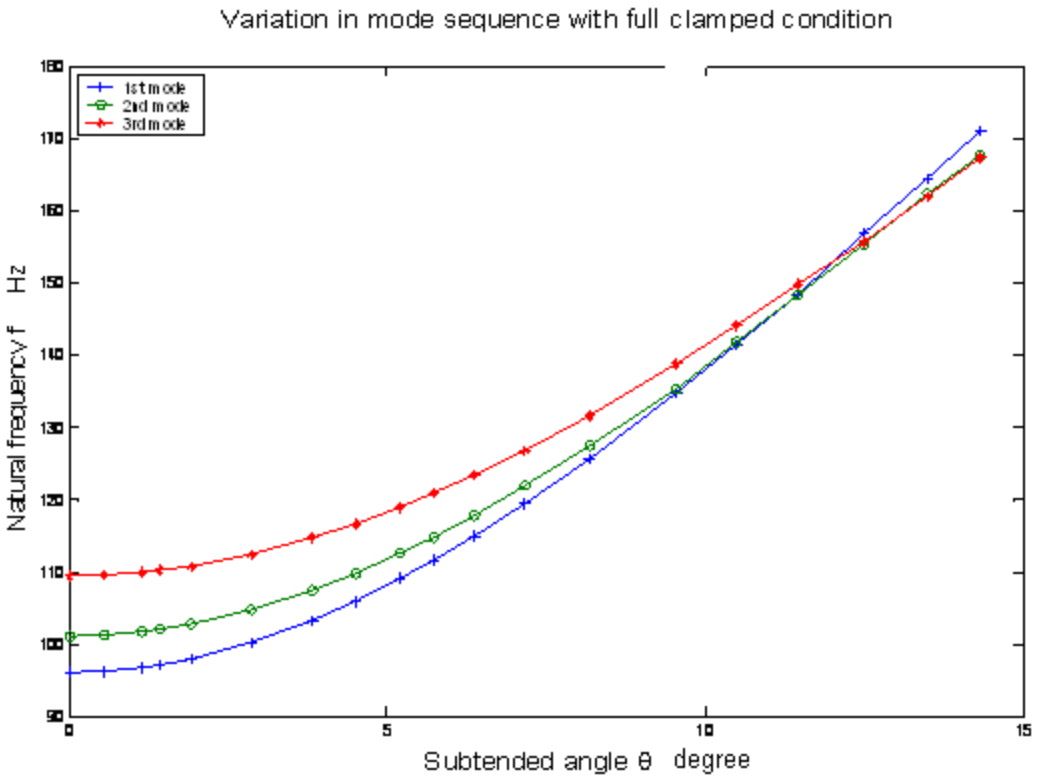

Figure 7.4 Natural frequencies of circular curved beam with full clamped boundaries for second waveguide branch

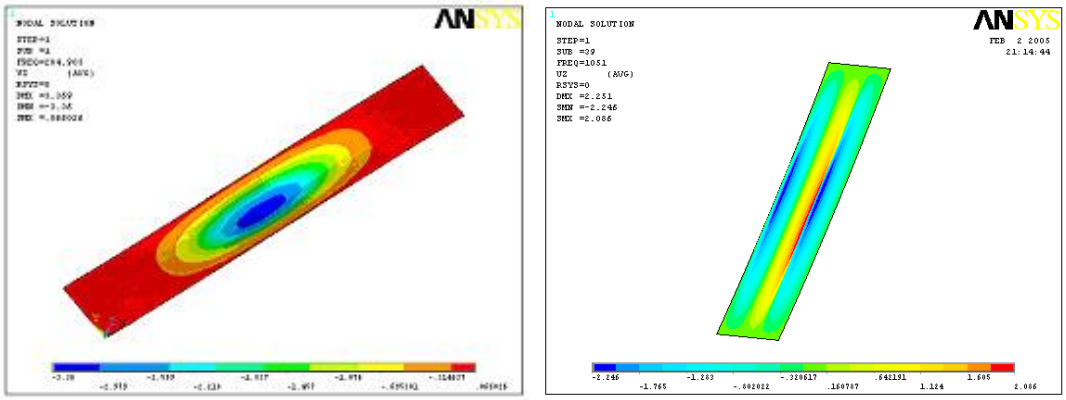

Figure 7.5 Curved plate with full clamped boundaries with second and third symmetric mode for second waveguide branch

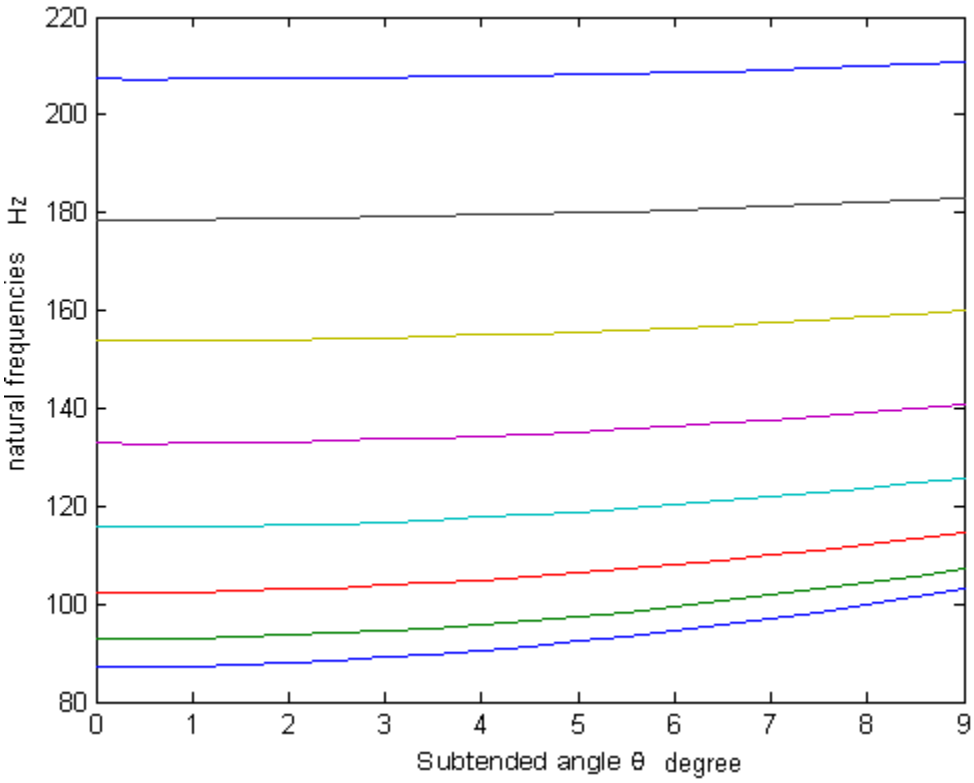

Figure 7.6 natural frequencies of curved plate with full free boundary condition

7.2.2 S-shape strip

The 'bending-beam' modes of the S-shape strip with different amplitude curvatures are shown in Figure 7.7, which shows the similar mode transition phenomena as the one-dimension curved strip shown in figure 5.11, but in this example, The strip is clamped at both ends and the property is same with the one shown in Chapter five, section 5.2.

In this chapter, more interest is focused on the lateral vibration modes. The first confined modes on first three second symmetric waveguide branch of the normal displacement function are shown in Figure 7.8. In Figure 7.8a, there is no transverse deflection in horizontal direction, which is called first symmetric waveguide mode. Figure 7.8b shows the transverse deflection in horizontal direction, which is called second symmetric waveguide mode. The mode shape shown in Figure 7.8c represents the third symmetric wave guide mode.

Case 1 *b=0*

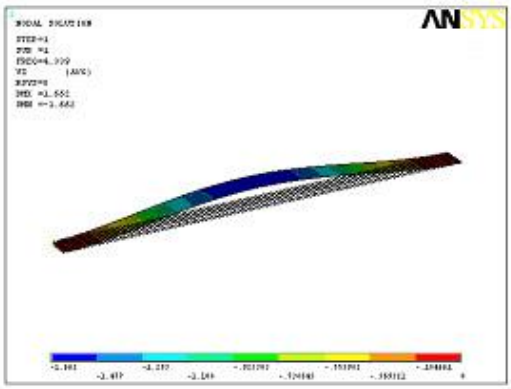

Mode 1 Symmetry *f*=4.4 Hz

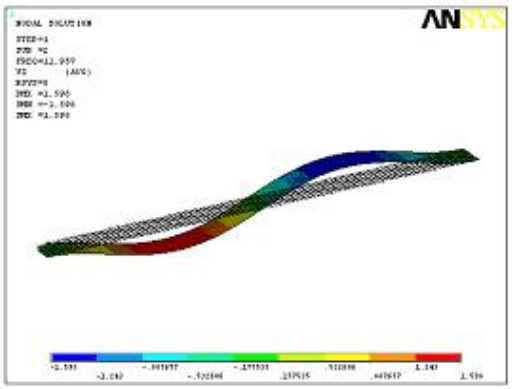

Mode 2 Anti-symmetry *f*=13.5 Hz

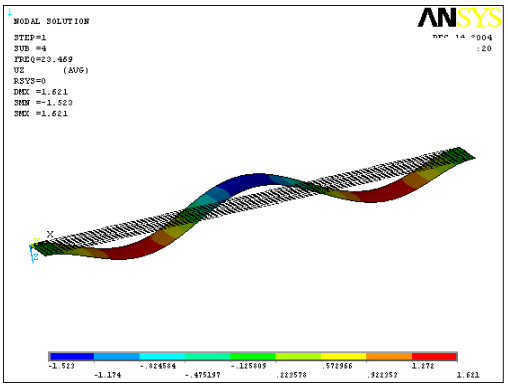

Mode 3 Symmetry *f*=23.9 Hz

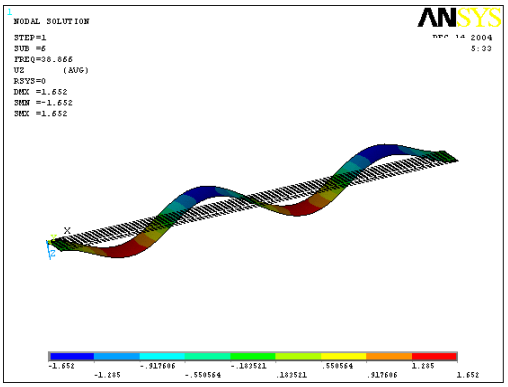

Mode 4 Anti-symmetry *f*=38.9 Hz

Case 2 *b=0.1*

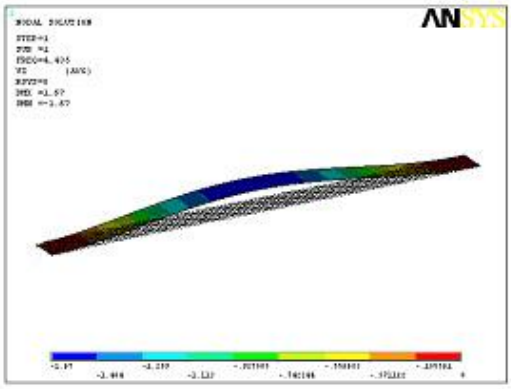

Mode 1 Symmetry *f*=4.4 Hz

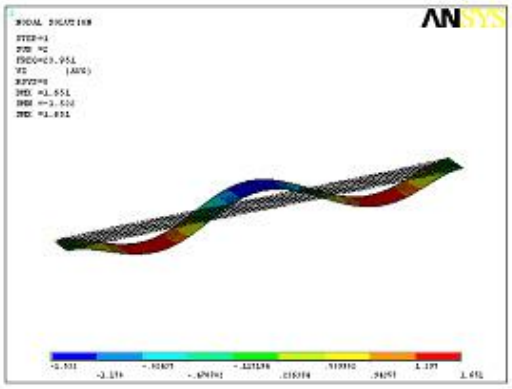

Mode 2 Symmetry *f*=24 Hz

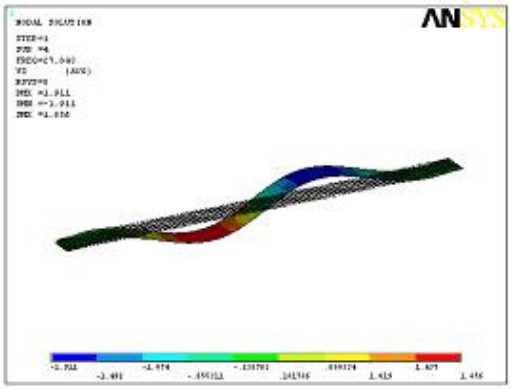

Mode 1 Anti-symmetry f=27.8 Hz

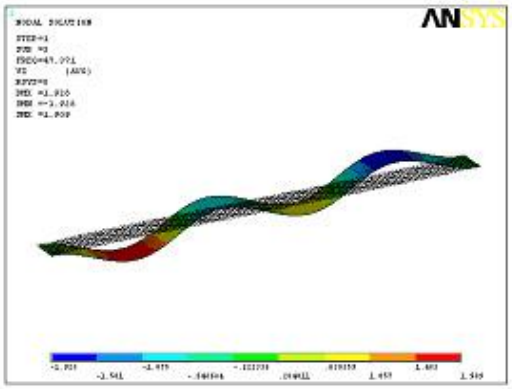

Mode 2 Anti-symmetry f=47.4 Hz

Case 3 *b=1.2*

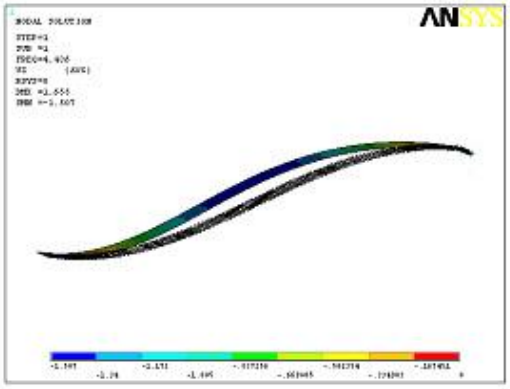

Mode 1 Symmetry f=4.5 Hz

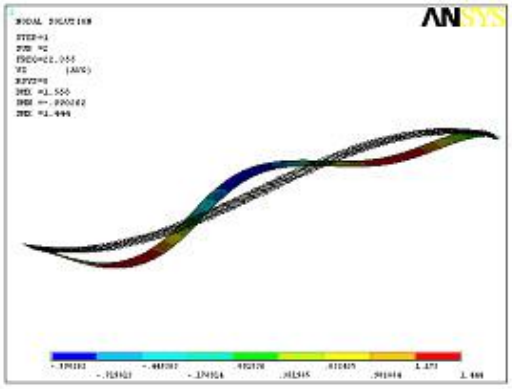

Mode 2 Symmetry f=23.9 Hz

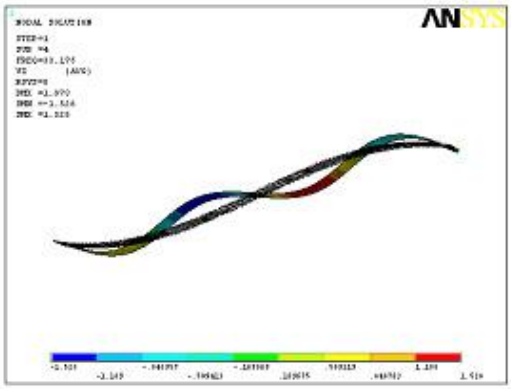

Mode 1 Anti-symmetry f=34 Hz

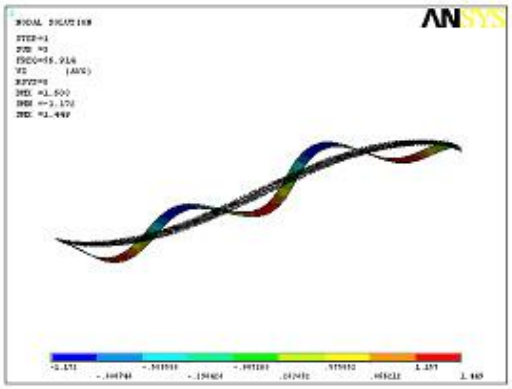

Mode 2 Symmetry f=59.4 Hz

Figure 7.7 Variation in mode sequence due to the rising of curvature parameter, the s-strip is clamped at both ends

For the second symmetric mode of wave propagation, the natural modes for the transverse displacement function are confined to the vicinity of the points of zero curvature and they are not affected by the boundary conditions at both ends of s-shape strip. This means the natural frequencies for each mode are same for any boundary conditions applied at ends of the beam.

The natural frequencies are illustrated in figure 7.9, which shows that the sequence of natural mode will not change following changes in curvatures. It can be seen that the curvature affects the natural frequency but no mode transition happens because the lower natural frequency increases also slower.

Considering fully clamped boundary conditions, the natural frequencies keep increasing with the rising in the curvature, shown in Figure 7.10, once again no mode transition happens.

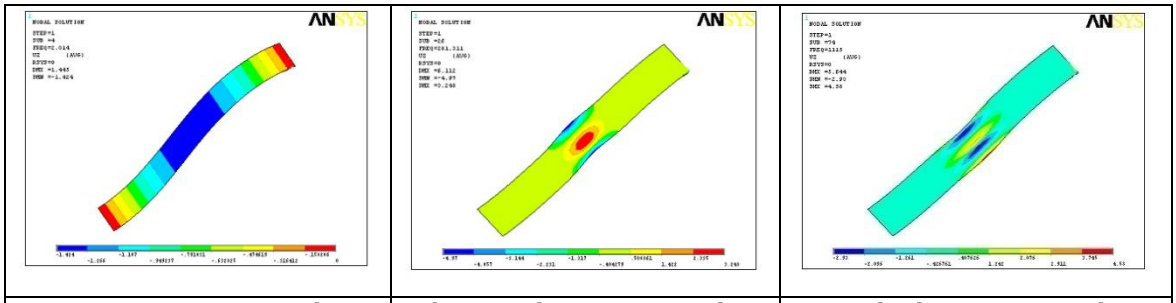

a. First symmetric mode 2.01 Hz	b. Second symmetric mode 281 Hz	c. Third symmetric mode 1115 Hz

Figure 7.8 the first three 2nd symmetric waveguide modes of an elastic strip of varying curvature

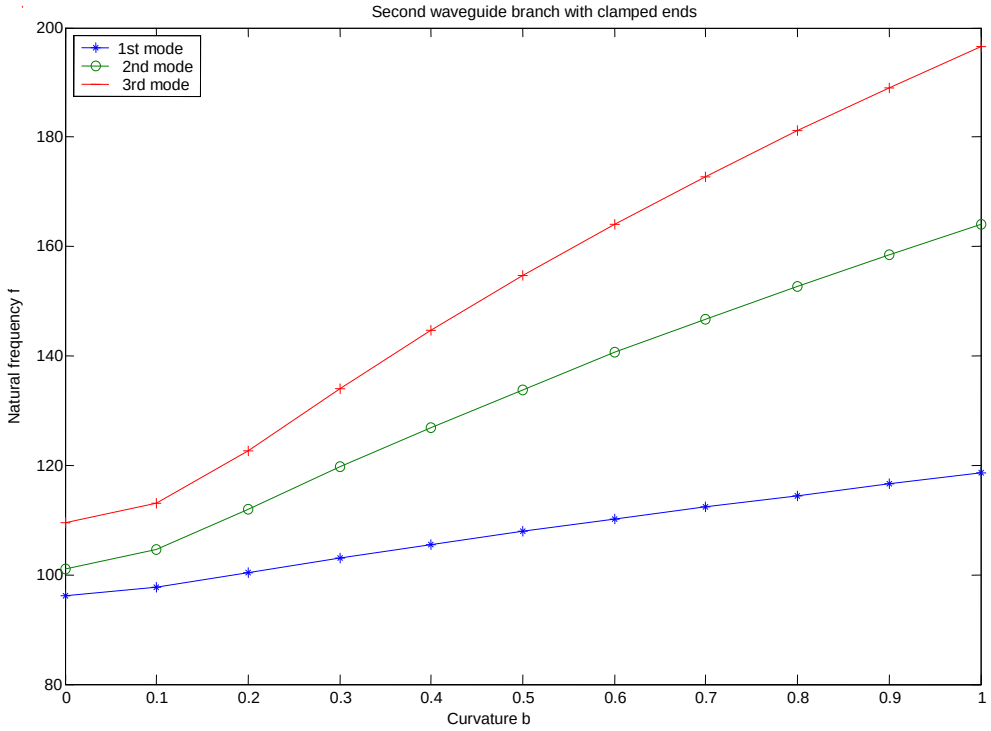

Figure 7.9 Natural frequencies (Hz) against curvatures for clamped boundary conditions at both ends (also for all kind boundary conditions at both ends)

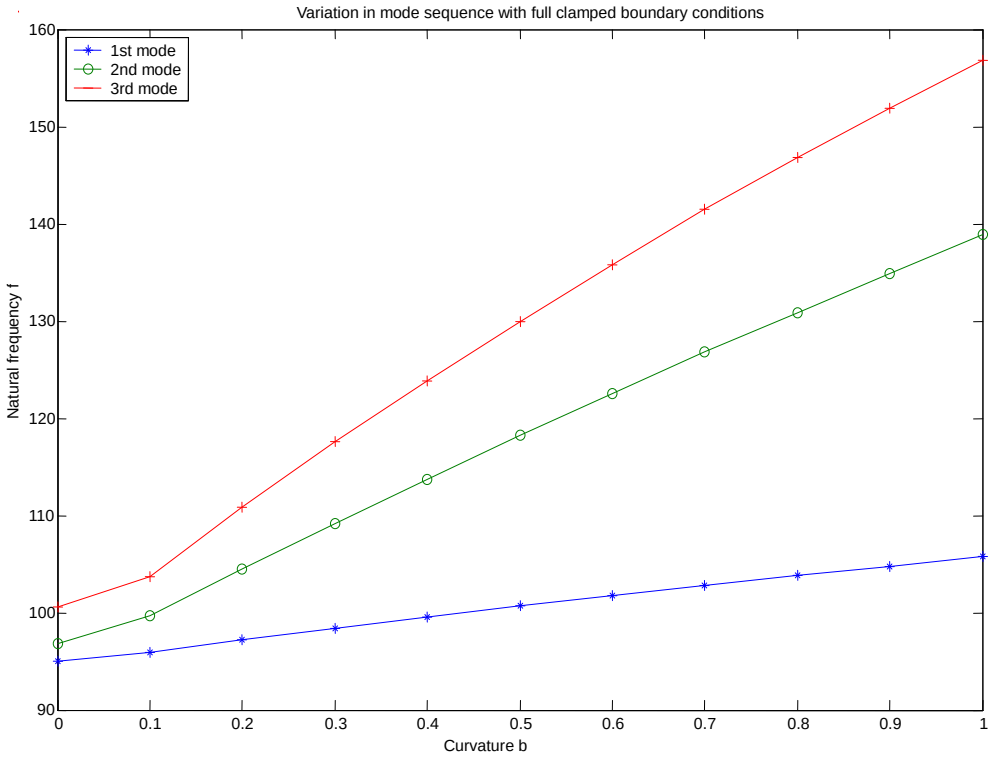

Figure 7.10 Natural frequencies (Hz) against curvature for full clamped boundary conditions

Chapter 8 Effect of Curvature on Natural Frequency of Composite Curved Beams

As discussed in Chapter three the parameter η represents the geometry and material properties. For the isotropic curved beam, the material property remains constant. For the composite material, the property will change due to different layered laminae. In this Chapter, the natural behaviour of curved beam will be discussed when both curvature and material property change.

8.1 Effect on Natural Frequency

Examples are given to show how the natural modes of laminated strips changes with the varying curvatures. The material properties of curved laminated beam are selected shown in Table 8-1:

Table 8.1 Material properties of curved laminated beam

	E_1(Gpa)	E_2(Gpa)	μ_{12}	G_{12}(Gpa)	ρ (kg/m^3)	ply
S-glass/eproxy	43	8.9	0.27	4.5	2000	[0/90/90/0]

The non-dimensional natural frequencies of an S-glass/proxy orthotropic laminated beam with constant curvature are calculated by both analytical and finite element methods. The circular curved beam has dimensions as the length of the beam is 1000 mm, the width is 150 mm, and the thickness is 0.8 mm. The beam is clamped at both ends. In the case of four layer symmetric ply [0/90/90/0], the results are shown in Figure 8.1. The analytical and numerical results are in agreement with each other, which prove that the zero order perturbation approximation can be used to solve the lower frequency eigenvalue problems. In figure 8.1, the two set of solid lines represent the asymptotic curves, which are given by (Tarnopolskaya 1996). The rising trends curve is called

membrane asymptotic curve and the horizontal line is the flexural asymptotic curve. It has been demonstrated that the rising of natural mode is caused by the extensional term in the governing equations. The extensional terms of the general eigenmode represent the eigenfunctions of the membrane. Hence, the natural modes rise to a higher value following the routine of membrane asymptotic curves. However, this membrane term will disappear in the vicinity of the point of the intersection of the two set of asymptotic curves and vibrations convert into only flexural ones. The natural frequencies will not pass over the flexural asymptotic curves.

Another example is illustrated in figure 8.2, which is the result comparison for s-shape strip (the length is 1000 mm, the width is 150 mm and the thickness is 0.8 mm) with clamped boundary conditions. The lower modes are in good agreement, but the error in third mode indicates the zero order approximation is not adequate for describing the higher eigenvalue problems.

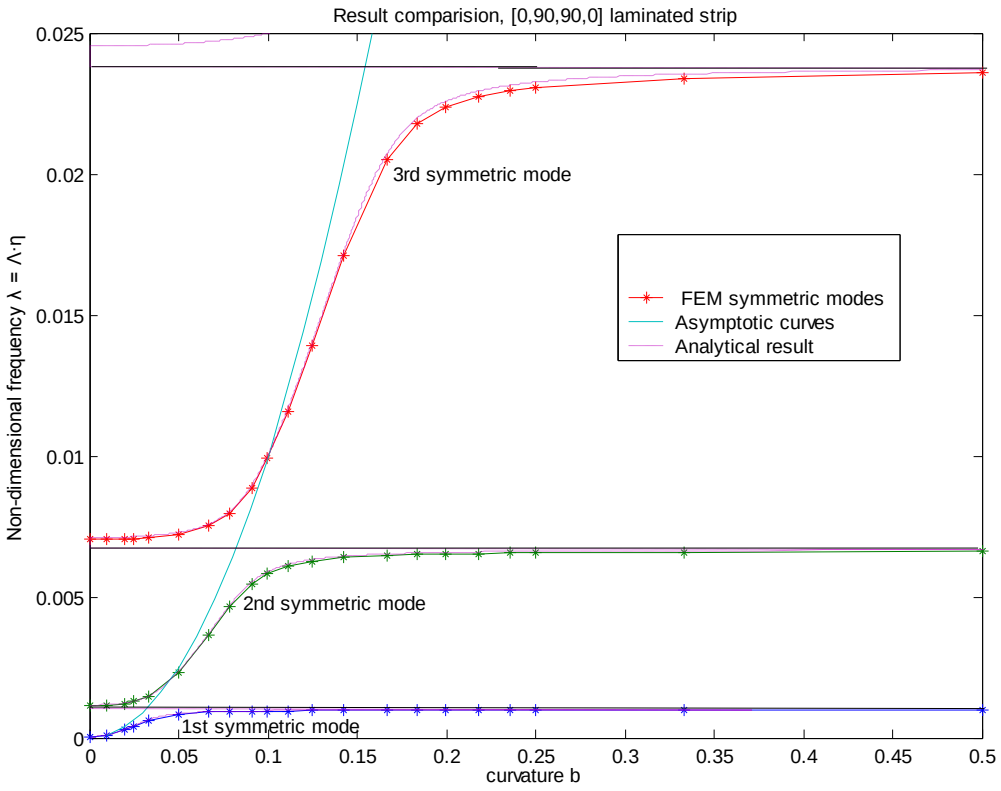

Figure 8.1 Clamped beam with constant curvature

Figure 8.3 represents how much the curvature can affect the natural frequencies for different modes. The frequency rising ratio is calculated by using natural frequency of curved beams divided by that of a flat beam. It is clear that the lower natural frequencies are affected much more than higher ones.

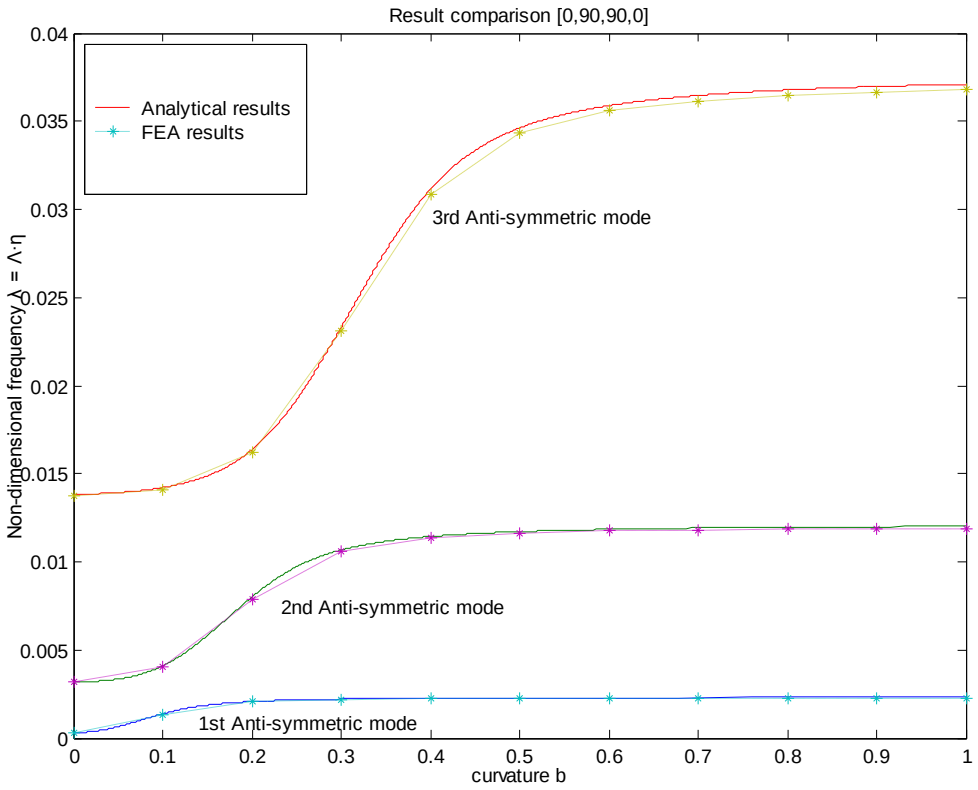

Figure 8.2 S-shape strip with clamped end conditions

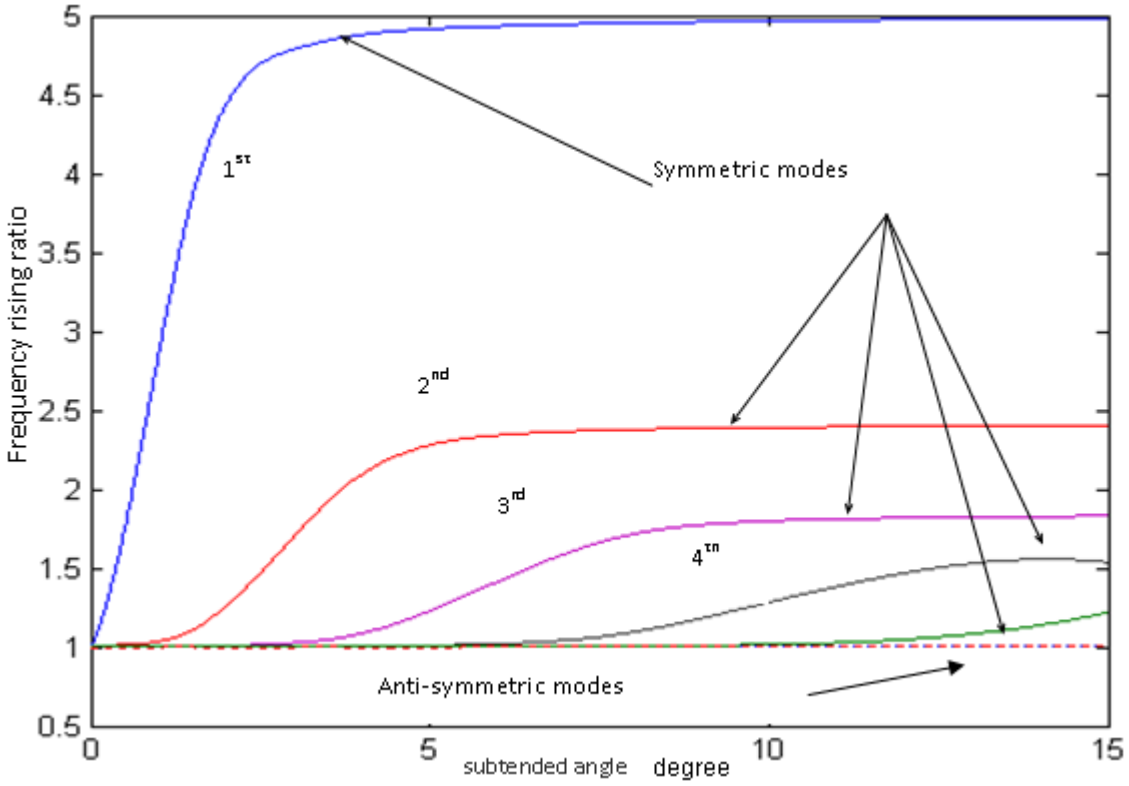

Figure 8.3 Natural frequency increasing ratio of circular curved beam

8.2 Result Comparisons

Three different laminates are selected to compare the effect of fibre orientation and stacking sequence on the non-dimensional natural frequency.

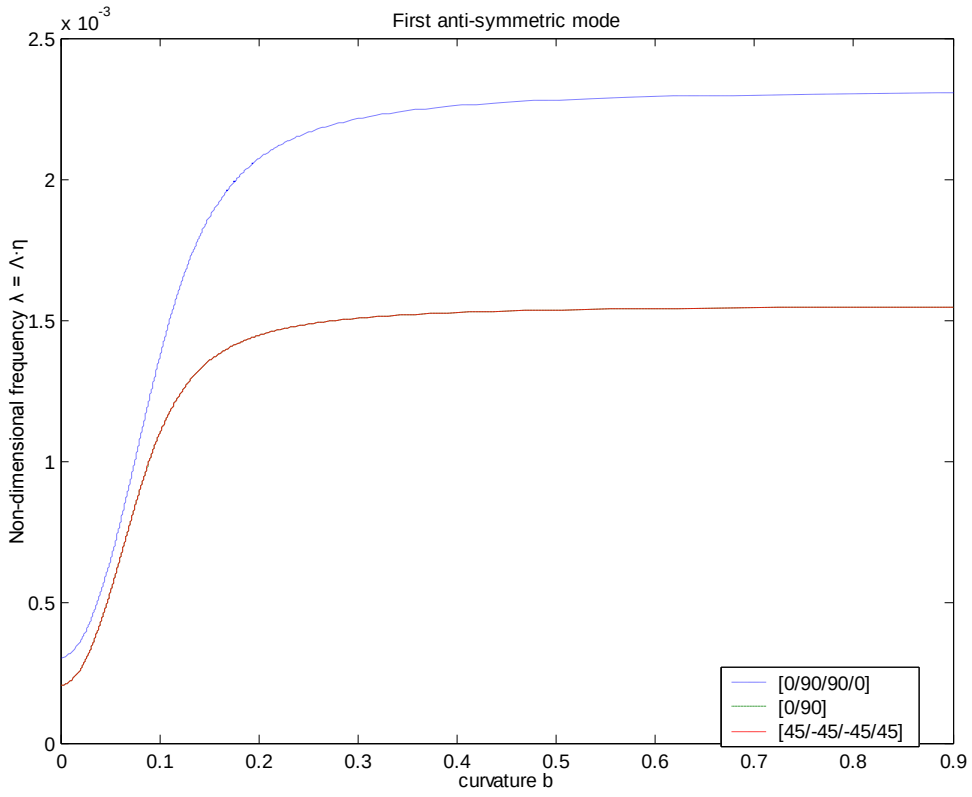

Figure 8.4 First anti-symmetric mode of clamped S-shape strip

These laminates are four ply laminate laid up in [0/90/90/0] stacking sequence, two ply laminate laid up in [0/90] stacking sequence and four ply laminate laid up in [45/-45/-45/45] stacking sequence. The first example is the clamped S-shape strip. The first anti-symmetric mode for three laminates is illustrated in Figure 8.4, from which it can be found that the laminate [0/90] and [45/-45/-45/45] coincide because they have the same ratio of D_{11} to A_{11}. The higher anti-symmetric modes of these three laminates have similar trends.

Another example is the hinged circular beam. The fundamental natural mode is plotted in Figure 8.5.

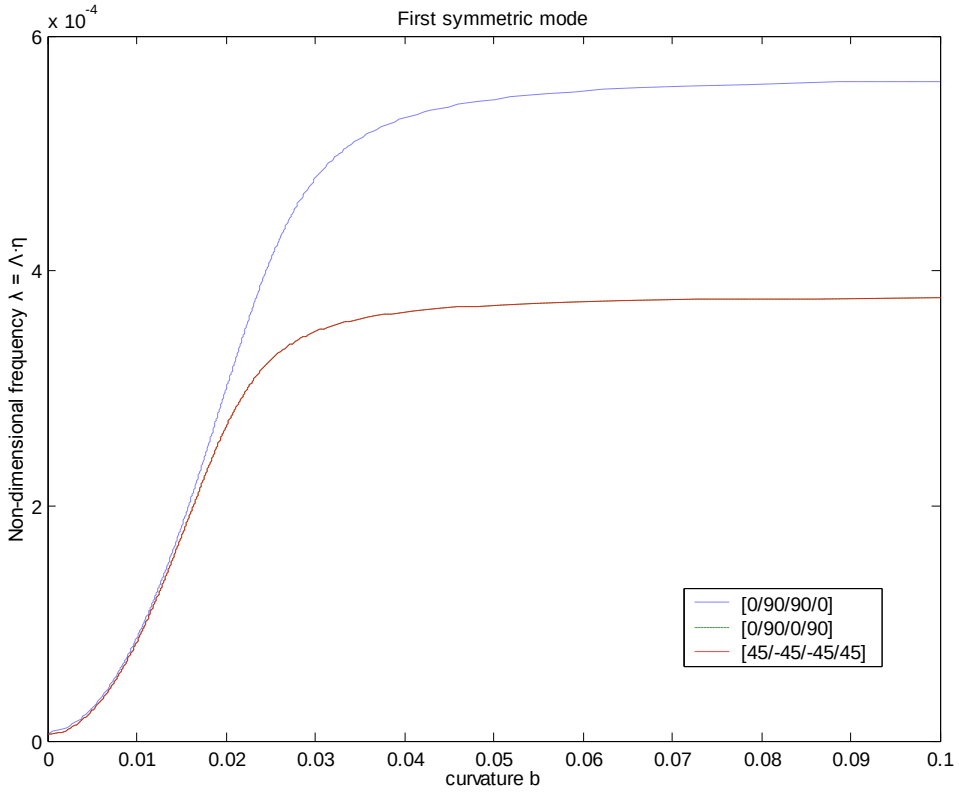

Figure 8.5 First symmetric mode of hinged circular beam

Both examples show that the laminate which has the higher D_{11} to A_{11} ratio will have a faster and higher rising of natural frequencies due to increasing curvature.

Chapter 9 Conclusions and Future Works

9.1 Achievements

The present thesis investigates the effect of curvature on the natural behaviour of curved beams and plates in many aspects.

1. The natural frequency changes in a regular way due to the variation in curvatures.
2. Mode shape transition phenomena happen due to the changes in curvatures
3. Effects from different kinds of curvatures.
4. Effects of curvature on the lateral vibration of curved plates
5. Impacts from various boundary condition
6. Natural behaviour of composite curved beams

All aspects are investigated based on both analytical and numerical approaches. The present research further develops the work by Tarnopolskaya and Hoog (1999) to the second order perturbation approximations which gives more accurate results and reveals more characteristics mathematically due to changes of curvatures. The characteristics caused by the changing in curvature have been physically interpreted, which are detailed in following sections.

9.1.1 Mode sequence changes

The present studies reveal that a very slight change in curvature of curved beams could cause significant variation in the natural characteristics. Under the boundary conditions with extensional constraints, the natural frequency of the first symmetric (or anti-symmetric depending on symmetry characteristics of curvature) mode increases

rapidly with a small increase in the subtended angle, but this small change in the curvature will not affect other natural modes. During the rapid increase in frequency there is a change in mode shape and the mode ends up as a second symmetric (or anti-symmetric) mode. In turn, the frequency of the original second symmetric (or anti-symmetric) mode begins to increase rapidly with a further small increase in the subtended angle, and ends up as a third symmetric (or anti-symmetric) mode. All the symmetric (or anti-symmetric) modes are seen to behave in this manner. The anti-symmetric (or symmetric) modes remain almost constant. Hence, as the symmetric (or anti-symmetric) mode increases and crosses the anti-symmetric (or symmetric) mode, the two modes exist with the same frequency for a particular value of curvature.

Such mode transitions can only happen if the curvature function and the transverse displacement function have the same symmetric or anti-symmetric state.

9.1.2 Boundary conditions

The natural characteristics of curved beam and plate with various boundary conditions have been analyzed. It has been shown that the natural characteristics of the curved structure with external constraints at both ends are influenced significantly by the variation in curvature; however, for the curved structure with no external constraints at both ends, the varying curvatures do not cause significant change in the natural characteristics.

9.1.3 Wave propagation behaviour

The wave propagation behaviour of a singly curved plate is demonstrated using numerical results, which was shown to agree with analytical results (perturbation methods) for one case only. For the second symmetric waveguide modes, the natural behaviour of the curved structure with any boundary conditions has the same trends, shown in Chapter five. For the S-shaped strip, the second symmetric waveguide modes are not influenced at all by the boundary conditions at two ends.

FEA is proved adequate to simulate the wave propagation behaviour of curved plates.

9.1.4 Effects from characteristics of composite materials

Results show that the higher ratio of flexural stiffness to extensional stiffness causes faster and higher value rising of natural frequencies with increasing curvature. The composite characteristics of curved beams will significantly affect the characteristics due to the changes in curvatures according to Figure 8.4 and Figure 8.5.

9.2 Conclusions

Many features of natural behaviour of curved beams and plates are revealed; however, the perturbation approximation method has some limits to demonstrate effect on natural behaviours of curved beams due to the changing in curvatures. Firstly, the approximation can obtain accurate results for very thin beams. If the height-length ratio increases, the accuracy decreases. The reason is that the governing equations are derived based on the classical thin beam theory. Next, the governing equations are derived to deal with curved beam problems. In order to be applicable to singly curved plate, it needs to be combined with the Rayleigh-Ritz method. However, even for the zero order perturbation it is time consuming to derive equations. Neither first nor second order perturbation solutions have been carried out on it. Only one boundary condition is examined. Thirdly, lower order perturbation approximation only obtains accurate results for the lower frequency mode transition.

To overcome the above shortcomings of analytical approach, the finite element method is also used to analyze the curved beams with continuous varying curvatures for the first time. Results are compared with analytical ones. It shows that FEA has the advantage in modelling and results are more accurate in higher frequency vibrations. It is found that FEA could perform the lateral vibration of curved structures without difficulty, results from which can demonstrate the wave propagation behaviour of continuously varying curvature.

On the other hand, finite element method also has limitations. For example, in order to calculate beams with different curvatures, all these beams need to be modelled, which is time consuming and not convenient to analyze a series of problems. If using analytical solution, only changes the curvature parameter, one can obtain the expected results.

Overall, the present thesis gives comprehensive review on the natural behaviour of curved structures; investigates many features related to the variable curvature, which provides the reference to engineers when curved beams and plates need to be considered in the design.

9.3 Future works

Although the perturbation method is applicable to the curved beams, from the complex second order equations, we can see that it is not convenient for the thicker beams analysis. Therefore a more applicable way needs to be found which could combine the advantages of the present analytical solutions.

Another interesting research may be the damage and buckling of curved beams and plates. Using the present analytical solution for the curved structures could be more straightforward than numerical methods.

References

D.R. Ambur and N. Jaunky, Optimal design of grid-stiffened panels and shells with variable curvature, Composite Structures, vol. 52, n^{o}2, 173-180, (2001)

A. E., Armenkas, and E. S., Reitz, Propagation of harmonic waves in orthotropic, circular cylindrical shell, ASME Journal of Applied Mechanics,168-174, (1973)

N. M. Auciello and M. A. De Rosa, Free vibrations of circular arches: A review, Journal of Sound and Vibration, 176 (4), 433-458, (1994)

J. Awrejcewicz, V. A. Krysko and A. N. Kutsemako, Free vibration of doubly curved in-plane non-homogeneous shell, Journal of Sound and Vibration, vol. 225, I4, 701-722, (1999)

N. S. Bardell, J. M. Dunsdon and R. S. Langley, On the free vibration of completely free, open, cylindrically curved isotropic shell panels, Journal of Sound and Vibration, 207(5), 647-669, (1997)

E W. Boyce, Goodwin B. E Random transverse variation of elastic beams. SIAM Journal, vol. 12, 613-629, (1964)

D E. Boyd, Analysis of open non-circular cylindrical shells, AIAA Journal, vol. 7, I3, 563-565, (1969)

E. Bozhevolnaya and Y. Frostig, Free vibration of Curved Sandwich beams with a

transversely flexible core, Journal of Sandwich Structures and Materials, vol.3, (2001)

E. Bozhevolnaya and J. Q. Sun, Free Vibration Analysis of Curved Sandwich Beams**,** Journal of Sandwich Structures and Materials, vol. 6, n^{o}1, 47-73**,** (2004)

T. E. Carmichael, The vibration of a rectangular plate with edges elastically restrained against rotation, The Quarterly Journal of Mechanics and Applied Mathematics, 12(1):29-42, (1959)

D. Chakravorty, J.N. Bandyopadhyay and Sinha, Finite element free vibration analysis of doubly curved laminated composite shells, Journal of Sound and Vibration, 191, 491-504, (1996)

J. P. Charpie and C. B. Burroughs, An analytic model for the free in-plane vibration of beams of variable curvature and depth, Journal of the Acoustical Society of America, 94, 866-879, (1993)

D. S. Chehil and R. Jategaonkar, Determination of natural frequencies of a curved beam with varying cross section properties, Journal of Sound and Vibration 115, 423-436, (1987)

C.-N. Chen, DQEM analysis of in-plane vibration of curved beam structures, Advances in Engineering Software, vol.36 n.6, 412-424, (2005)

P. Chidamparam and A W. Leissa, Vibrations of planar curved beams, rings, and arches, Applied Mechanic Reviews, 46, 467-483, (1993)

J. D. Cole, Perturbation Methods in Applied Mathematics, Blaisdell Publishing Company, (1968)

P. Cunningham, R.G. White and G.S. Aglietti, The effects of various design parameters on the free vibration of doubly curved composite sandwich structures, Journal of Sound and Vibration, 230(3), 617-648, (2000)

J.P. Den Hartog, The lowest frequency of circular arcs, Philosophical Magazine 5, 400–408, (1928)

M. Eisenberer and E. Efraim, In-plane vibrations of shear deformable curved beams, International Journal for Numerical Methods in Engineering, 52:1221-1234, (2001)

D A. Evensen, Nonlinear vibration of beams with various boundary conditions. AIAA Journal, vol.6, 370-372, (1968)

M. E. Fares, Y. G. Youssif and A. E. Alamir, Minimization of the dynamic response of composite laminated doubly curved shells using design and control optimization, Composite structures, vol. 59, n°3, pp. 369-383, (2003)

C. C. Fleischer, Dynamic Analysis of Curved Structures, PhD Thesis, University of Southampton, (1974)

K. Försberg, Influence of boundary conditions on the modal characteristics of thin cylindrical shells, American Institute of Aeronautics and Astronautics Journal, 2(12), 1520-1527, (1964)

C. Förster, T. Weidl, Trapped modes for an elastic strip with perturbation of the material properties, Quarterly Journal of Mechanics and Applied Mathematics, vol. 59 (3), 399-418, (2006)

Z. Friedman and J. B. Kosmatka, An accurate two-node finite element for shear deformable curved beams, International Journal for Numerical Methods In Engineering, vol.41, 473-498, (1998)

B. Geist, Eigenvalue formulas for the uniform Timoshenko beam: The free-free problem, Electronic Research Ann., AMS, vol. 4, (1998)

J. K. S. Goh, Analysis of pressurized arch-shells, Master of Science Thesis, Virginia Polytechnic Institute and State University, (1998)

D. Gridin, A.T. I. Adamou' and R.V. Craster, Trapped modes in bent elastic rods, Wave Motion, Vol 42, Issue 4, Pages 352-366, (2005)

R. H. Gutierrez, P. A. A. Laura, R. E. Rossi, R. Bertero and A. Villiggi, In-plane vibrations of non-circular arcs of non-uniform cross-section, Journal of Sound and Vibration, 129, 181-200, (1989)

R. H. Gutierrez, P. A. A. Laura and R. E. Rossi, Fundamental frequency of vibration of a Timoshenko beam of non-uniform thickness, Journal of Sound and Vibration, 145, 341-344, (1991)

E. Hinton, M. Özakca, N. Rao, Free vibration analysis and shape optimization of variable thickness plates, prismatic folded plates and curved shells. I: Finite strip formulation, Journal of sound and vibration, vol. 181, n^{o}4, 553-566, (1995)

K. Z. Huang, M. W. Lu and M. D. Xue, Theory of thin shells, Engineering Mechanics Series, Xin Hua Publication, 2nd edition, (1988)

C. S. Huang, Y. P. Tseng, A. W. Leissa and K. Y. Nieh, An exact solution for in-plane vibrations of an arch having variable curvature and cross section, International Journal of Mechanic Science, vol.40, n^{o}11, 1159-1173, (1998)

C. S. Huang, M. C. Yang, and K. Y. Nieh, In-plane free vibration and stability of loaded and shear deformable circular arches", International Journal of Solids and Structures, 40(22), 5865-5886, (2003)

T. Irie, G. Yamada and I. Takahashi, In-plane vibration of a free-clamped slender arc of varying cross-section, Bulletin of the Japan Society of Mechanical Engineers, 23, 567-573, (1980)

N. Jaunky, N. F. Knight Jr. and D. R. Ambur, Buckling analysis of anisotropic variable-curvature panels and shells, Composite Structures, 43, 321-329, (1999)

I. A. Jones, A curved laminated orthotropic axisymmetric element based upon Flügge

thin shell theory, Computers and Structures, vol.60, n°3, 487-503, (1996)

B. Kang, C.H. Riedel, C.A. Tan, Free vibration analysis of planar curved beams by wave propagation, Journal of Sound and Vibration, 260, 19-44T, (2003)

M. Y. Kim, N. I. Kim, Y. Hee-Taekb, Exact dynamic and static stiffness matrices of shear deformable thin-walled beam-columns, Journal of Sound and Vibration, 267 29–55, (2003)

M. Y. Kim, N. I. Kim and B. C. Min, Analytical and numerical study on spatial free vibration of non-symmetric thin-walled curved beams, Journal of Sound and Vibration v258 595-618, (2002)

V. K. Koumousis and A. E. Armenakas, Free vibration of non-circular panels with simply supported curved edges. ASCE Journal of Engineering Mechanics, 110 (5), 810-827, (1984)

H. Krauss, Thin Elastic Shells, New York: Wiley, (1967)

K.Y. Lam, C.T. Loy, Influence of boundary conditions and fiber orientation on the frequencies of thin orthotropic laminated cylindrical shells, Composite Structures, 31 21–30, (1995)

P. A. A. Laura and P. L. Verniere de Irassar, A note on in-plane vibration of arch-type structures of non-uniform cross-section: the case of linear varying thickness, Journal of Sound and Vibration, 124, 1-12, (1988)

Y. S. Lee, M. H. Choi, and J. H. Kim, Free vibration of laminated composite cylindrical shells with an interior rectangular plate, Journal of Sound and Vibration, 265 795-817, (2003)

S. Y. Lee and J. Y. Hsiao**,** Free in-plane vibrations of curved non-uniform beams**,** Acta Mechanica, 155, 173-189 (2002)

B. K. Lee and J. F. Wilson, Free vibration of arches with variable curvature, Journal of Sound and Vibration, 136, 75-89, (1989)

A.W. Leissa, Vibration of Shells, Nasa SP-288,US Government Printing Office, Washington, DC, (1973) (reprinted by the Acoustical Society of America, (1993)

A. Y. T. Leung and W. E. Zhou, Dynamic stiffness analysis of non-uniform Timoshenko beams, Journal of Sound and Vibration, 181, 447-456, (1995)

K.M. Liew and Z.C. Feng, Vibration characteristics of conical shell panels with three-dimensional flexibility, J. Appl. Mech. vol. 67, I2, 314-320, (2000)

K.M. Liew, C.W. Lim, S. Kitipornchai, Vibration of shallow shells: a review with bibliography, Transactions of the American Society of Mechanical Engineers, Applied Mechanics Review, 50, 431–444, (1997)

S. M. Lin, Exact solutions for extensible circular curved Timoshenko beams with nonhomogeneous elastic boundary conditions, Acta Mechanica, vol. 130, n^{o}1-2, 67-79, (1998)

P. Litewka, J. Rakowski, An efficient 3D curved beam finite element, CAMES, vol.7, 707-716, (2000)

K. H. Lo, R. M. Christensen and E. M. Wu, A high-order theory of plate deformation, Part II: laminated plates, Journal of Applied Mechanics, 44, 669 -676, (1978), (a)

K. H. Lo, R. M. Christensen and E. M. Wu, Stress solution determination for higher order plate theory, Int. J. Solids Struct, 14, 655-662, (1978), (b)

A. E. H. Love, On the Small Free Vibrations and Deformations of Elastic Shells, Philosophical Transaction of the Royal Society (London), Series A, **17**, 491-549, (1888)

A.E.H. Love, A Treatise on the Mathematical Theory of Elasticity, New York: Dover Publication, fourth edition, (1944)

P. Malatkar, Nonlinear vibrations of cantilever beams and plates, PhD Thesis, Virginia Polytechnic Institute and State University, (2003)

R D. Mindlin, Inuence of rotatory inertia and shear on exural motions of isotropic, elastic plates, Journal of Applied Mechanics, 38:31-38, (1951)

F. Moser, L. J. Jacobs and J. Qu, Modeling elastic wave propagation in waveguides with the finite element method, NDT&E International 32, 225-234, (1999)

Deb Nath, J. M Dynamics of Curved Plates, PhD Thesis, University of Southampton, (1969)

A. H. Nayfeh and H. N. Arafat, An overview of nonlinear system dynamics, in Structural Dynamics in 2000: Current status and future directions, Ewins, D. J. and Inman, D. J., eds., Research Studies Press, 225-256, (2001)

A.K. Nayak, S.S.J. Moy, R.A. Shenoi, Free vibration analysis of composite sandwich plates based on Reddy's higher-order theory, Composites: Part B 33 505–519, (2002)

A. T. Nettles, Basic mechanics of laminated composite plates, NASA Reference Publication 1351, (1994)

A K. Noor, WS Burton, Computational models for sandwich panels and shells, Applied Mechanics Review, vol. 49, no 3, (1996)

A. Nosier and J.N. Reddy, Vibration and stability analyses of cross-ply laminated circular cylindrical shells, Journal of Sound and Vibration, 157,139–159, (1992)

S. J. Oh, B.K. Lee and I. W Lee, Natural frequencies of non-circular arches with rotator inertia and shear deformation, Journal of Sound and Vibration, 219 (1), 23-33, (1999)

R. Pedro, A p-version, first order shear deformation, finite element for geometrically non-linear vibration of curved beams, International Journal for Numerical Methods in Engineering, Vol.61, 2696-2715, (2004)

M. Pramod, Nonlinear Vibrations of Cantilever Beams and Plates, PhD thesis, Virginia Polytechnic Institute and State University, (2003)

N. M. Price, M. Liu, R. E. Taylor and A. J. Keane, Vibrations of cylindrical pipes and open shells, Journal of Sound and Vibration, 218 (3), 361-387, (1998)

M.S. Qatu, Vibration of doubly cantilevered laminated-composite thin shallow shells, Thin-Walled Structures, 15 (3) 235–248, (1993)

J. Qu, Y. Berthelot and Z. Li, Dispersion of guided circumferential waves in a circular annulus, Review of Progress in Quantitative Nondestructive Evaluation, D. O. Thompson and D. E. Chimenti, eds, Plenum, New York,15, 169-176, (1996)

W. Qu and H. Tang, Handbook of Mechanical Vibration, Industry of Mechanics Publication, PR China, (2000)

P. Raveendranath, G. Singh and B. Pradhan, Free vibration of arches using a curved beam element based on a coupled polynomial displacement field, Computers and Structures, 78, 583-590, (2000)

J. N. Reddy, A simple higher-order theory for laminated composite plates, Journal of Applied Mechanics, 51, 745-752, (1984)

J. N. Reddy, An evaluation of equivalent single-layer and layerwise theories of composite laminates, Composite Structures, 25, 31-35, (1993)

J. N. Reddy, C. M. Wang and K. H. Lee, Relationships between bending solutions of classical and shear deformation beam theories, International Journal of Solids Structures, Vol. 34, 26, 3373-3384, (1997)

J. N. Reddy, Mechanics of Laminated Composite Plates - Theory and Applications, CRC Press, (1997)

E. Reissner, The effect of transverse shear deformation on the bending of elastic plates,

Journal of Applied Mechanics, 12: 69-77, (1945)

P. Ribeiro, A p-version, first order shear deformation, finite element for geometrically non-linear vibration of curved beams, International Journal for Numerical Methods in Engineering, vol.6, n.15, 2696-2715, (2004)

E. Romanelli, P. Laura, Fundamental frequencies of non-circular, elastic, hinged arcs, Journal of Sound and Vibration, vol. 24, Issue 1, 17-22, (1972)

T. Sakiyama, Free vibrations of arches with variable cross-section and non-symmetrical axis, Journal of Sound and vibration, 102, 448-452, (1985)

Scott and J. Woodhouse, Vibration of an elastic strip with varying curvature, Phil Trans. R. Soc. Loud A., 339, 887-625, (1992)

K. Suzuki and S. Takahashi, In-plane vibrations of curved bars, Bulletin of the Japan Society of Mechanical Engineers, 20 (148), 1236-1243, (1977)

T. Tarnopolskaya and F. De. Hoog, Asymptotic analysis of the free in-plane vibration of beams with arbitrarily varying curvature and cross-section, Journal of Sound and Vibration, 196, 659-680, (1996)

T. Tarnopolskaya, F.R. De Hoog, and N. H. Fletcher, Lower-frequency mode transition in the free in-plane vibration of curved beams, Journal of Sound and Vibration, 228(1), 69-90, (1999)

T. Tarnopolskaya and F. R. de Hoog, Asymptotic approximations for vibrational modes of helices, ANZIAM J. 42, 1398-1419, (2000)

S. Towfighi and T. Kundu, Elastic wave propagation in anisotropic spherical curved plates, International Journal of Solids and Structures, 40, 5495-5510, (2003)

Y. P. Tseng, C. S. Huang and C. J. Lin, Dynamic stiffness analysis for in-plane vibration of arches with variable curvature, Journal of Sound and Vibration, 207 (1), 15-31, (1997)

Y. P. Tseng, C. S. Huang and M. S. Kao, In-plane vibration of laminated curved beams with variable curvature by dynamic stiffness analysis. Composite Structures, 50, 103-114, (2000)

E. Tufekci, O. Y. Dogruer, Exact solution of out-of-plane problems of an arch with varying curvature and cross section, Journal of engineering mechanics, vol. 132, n°6, 600-609, (2006)

J. R. Vinson, The behaviour of Thin Walled Structures: Beams, Plates, and Shells, Mechanics of Surface Structures, Kluwer Academic Publishers, (1989)

S. J. Walsh, R.G. White, Vibrational power transmission in curved beams, Journal of Sound and Vibration, 233 (3), 455-488, (2000)

T.M. Wang, Effect of variable curvature on fundamental frequency of clamped parabolic arcs. Journal of Sound and Vibration 41, 247-251, (1975)

C. M. Wang, Timoshenko beam-bending solutions in terms of Euler-Bernoulli solutions, Journal of Enigneering Mechanics ASCE 121, 763-765, (1995)

T. M. Wang and J. A. Moore, Lowest natural extensional frequency of clamped elliptic arcs, Journal of Sound and Vibration, 30 (1), 1-7, (1973)

W. Wang, Analytical approaches to predict flexural behaviour of curved composite beams, Ph.D Thesis, University of Southampton, (2001)

W. Wang and R. A. Shenoi, Local free vibration analysis of initially stressed curved sandwich beam, Proceedings of the 7th International Conference on Sandwich Structures, Aalborg University, Aalborg, Denmark, 29–31 (2005)

X. Q. Wang and R. M. C. So, Various standing waves in a Timoshenko beam, Journal of Sound and Vibration, 280 311-328, (2005)

E.A. Witmer, Elementary Bernoulli-Euler beam theory, MIT Unified Engineering Course

Notes, pp 5-114 to 5-164, (1991-1992)

J. S. Wu, L. K. Chiang, Free vibration analysis of arches using curved beam elements, International Journal for Numerical Methods in Engineering, 58, 1907-1936, (2003)

J. S. Wu and L. K. Chiang, Dynamic analysis of an arch due to a moving load, Journal of Sound and Vibration, 269, 511-534, (2004)

N. Yahnioglu and S. Selim, Bending of a Composite Material Strip with Curved Structure in the Geometrically Nonlinear Statement, Mechanics of Composite Materials, vol.36, n.6, 459-464, (2000)

S. Y. Yang and H. C. Sin, Curvature based beam elements for the analysis of Timoshenko and shear deformable curved beams, Journal of Sound and Vibration, Vol. 187, n. 4, 569-584, (1995)

V. Yildirm, A computer program for the free vibration analysis of elastic arcs, Computers & Structures Volume 62, Issue 3, Pages 475-485, (1997)

S. D. Yu, W. L. Cleghorn and R. G. Fenton, On the accurate analysis of free vibration of open circular cylindrical shells, Journal of Sound and Vibration, 188 (3), 315-336, (1995)

Y. Zhao, H. Kang, R. Feng and W. Lao, Advances of research on curved beams, Advances in Mechanic, Vol 36 No.2 (2006)

ANSYS Help System. Elements Manual. ANSYS, Inc, (2002)

Appendix I

The strain-displacement equations of the three-dimensional theory of elasticity in orthogonal curvilinear coordinates can be derived as follows:

$$\overrightarrow{PQ_1} = A\overrightarrow{e_1}d\alpha, \quad \overrightarrow{PQ_1}' = A'\overrightarrow{e_1}'d\beta, \tag{I-1}$$

$$\overrightarrow{PQ_2} = B\overrightarrow{e_2}d\alpha, \quad \overrightarrow{PQ_2}' = B'\overrightarrow{e_2}'d\beta, \tag{I-2}$$

From equation (2-12), we can obtain

$$\frac{\partial \vec{R}}{\partial \alpha} = \frac{\partial \vec{r}}{\partial \alpha} + \frac{\partial \vec{\Delta}}{\partial \alpha}$$

$$= A\left(1 + \frac{1}{A}\frac{\partial U}{\partial \alpha} + \frac{1}{AB}\frac{\partial A}{\partial \alpha}V + \frac{W}{R_1}\right)\overrightarrow{e_1} + \left(\frac{\partial V}{\partial \alpha} - \frac{1}{B}\frac{\partial A}{\partial \beta}U\right)\overrightarrow{e_2} + \left(\frac{\partial W}{\partial \alpha} - \frac{A}{R_1}U\right)\overrightarrow{e_n}, \tag{I-3}$$

By ignore the second order items, we can obtain

$$A' = \sqrt{\frac{\partial \vec{R}}{\partial \alpha} \cdot \frac{\partial \vec{R}}{\partial \alpha}} = A\left(1 + \frac{1}{A}\frac{\partial U}{\partial \alpha} + \frac{1}{AB}\frac{\partial A}{\partial \beta}V + \frac{W}{R_1}\right), \tag{I-4}$$

and also

$$B' = \sqrt{\frac{\partial \vec{R}}{\partial \beta} \cdot \frac{\partial \vec{R}}{\partial \beta}} = B\left(1 + \frac{1}{B}\frac{\partial V}{\partial \beta} + \frac{1}{AB}\frac{\partial B}{\partial \alpha}U + \frac{W}{R_2}\right), \tag{I-5}$$

we also two tangent vectors of curves

$$\overrightarrow{e_1}' = \frac{1}{A'}\frac{\partial \vec{R}}{\partial \alpha} = \overrightarrow{e_1} + \omega_1\overrightarrow{e_2} + \vartheta\overrightarrow{e_n}, \tag{I-6}$$

$$\overrightarrow{e_2}' = \frac{1}{B'}\frac{\partial \vec{R}}{\partial \beta} = \overrightarrow{e_2} + \omega_2 \overrightarrow{e_1} + \varphi \overrightarrow{e_n}, \tag{I-7}$$

From equation (I-5) and equation (I-6), we can obtain

$$\omega_1 = \frac{1}{A}\frac{\partial V}{\partial \alpha} - \frac{1}{AB}\frac{\partial A}{\partial \beta}U, \ \vartheta = \frac{1}{A}\frac{\partial W}{\partial \alpha} - \frac{U}{R_1} \tag{I-8}$$

$$\omega_2 = \frac{1}{B}\frac{\partial U}{\partial \beta} - \frac{1}{AB}\frac{\partial B}{\partial \alpha}V, \ \varphi = \frac{1}{B}\frac{\partial W}{\partial \beta} - \frac{V}{R_2} \tag{I-9}$$

Finally, the strain can be expressed as follows:

$$\epsilon_\alpha = \frac{P'Q'_\alpha - PQ_\alpha}{PQ_\alpha} = \frac{A' - A}{A} = \frac{1}{A}\frac{\partial U}{\partial \alpha} + \frac{V}{AB}\frac{\partial A}{\partial \beta} + \frac{W}{R_\alpha} \tag{I-10a}$$

$$\epsilon_\beta = \frac{P'Q'_\beta - PQ_\beta}{PQ_\beta} = \frac{B' - B}{B} = \frac{1}{AB}\frac{\partial B}{\partial \alpha} + \frac{U}{B}\frac{\partial V}{\partial \beta} + \frac{W}{R_\beta} \tag{I-10b}$$

$$\epsilon_{\alpha\beta} = \frac{A}{B}\frac{\partial}{\partial \beta}\left(\frac{U}{A}\right) + \frac{B}{A}\frac{\partial}{\partial \alpha}\left(\frac{V}{B}\right) \tag{I-10c}$$

where e_α, $e_\beta$and $e_{\alpha\beta}$ are strains at an arbitrary point of the curved body.

Appendix II

In this section, we consider plate analysis for layered orthotropic materials. Recall from plate theory (Shenoi and Wellicome, 1993), the following relationships:

Kinematics:

$$\{\varepsilon\} = \begin{Bmatrix} \frac{\partial u}{\partial x} \\ \frac{\partial v}{\partial y} \\ \frac{\partial u}{\partial y} + \frac{\partial v}{\partial x} \end{Bmatrix} = \begin{Bmatrix} \frac{\partial u}{\partial x} \\ \frac{\partial v}{\partial y} \\ \frac{\partial u}{\partial y} + \frac{\partial v}{\partial x} \end{Bmatrix} + z \begin{Bmatrix} -\frac{\partial^2 w}{\partial x^2} \\ -\frac{\partial^2 w}{\partial y^2} \\ -2\frac{\partial^2 w}{\partial x \partial y} \end{Bmatrix} \equiv \begin{Bmatrix} \varepsilon_{x0} \\ \varepsilon_{y0} \\ \varepsilon_{xy0} \end{Bmatrix} + z \begin{Bmatrix} \kappa_x \\ \kappa_y \\ \kappa_{xy} \end{Bmatrix} \tag{AII-1}$$

The terms $\{\varepsilon_{x0}, \varepsilon_{y0}, \varepsilon_{xy0}\}$ are the mid-surface extensional and shear strains for plate; while $\{\kappa_x, \kappa_y, \kappa_{xy}\}$ are the *curvatures* about the x and y axes, respectively, plus the twisting curvature (xy).

Constitutive (orthotropic laminae) :

$$\begin{Bmatrix} \sigma_{xx} \\ \sigma_{yy} \\ \tau_{xy} \end{Bmatrix} = [\bar{Q}] \begin{Bmatrix} \varepsilon_{xx} \\ \varepsilon_{yy} \\ \varepsilon_{xy} = \gamma_{xy}/2 \end{Bmatrix} = \begin{bmatrix} \bar{Q}_{11} & \bar{Q}_{12} & \bar{Q}_{16} \\ \bar{Q}_{21} & \bar{Q}_{22} & \bar{Q}_{26} \\ \bar{Q}_{61} & \bar{Q}_{62} & \bar{Q}_{66} \end{bmatrix} \begin{Bmatrix} \varepsilon_{xx} \\ \varepsilon_{yy} \\ \varepsilon_{xy} = \gamma_{xy}/2 \end{Bmatrix} \tag{AII-2}$$

Force and Moment Resultants:

$$N_x = \int_t \sigma_{xx} dz, \quad N_y = \int_t \sigma_{yy} dz, \quad N_{xy} = N_{yx} = \int_t \sigma_{xy} dz$$
$$M_x = -\int_t z\ \sigma_{xx} dz, \quad M_y = -\int_t z\ \sigma_{yy} dz, \quad M_{xy} = M_{yx} = -\int_t z\ \sigma_{xy} dz \qquad \text{(AII-3)}$$
$$Q_x = -\int_t \sigma_{xz} dz, \quad Q_y = -\int_t \sigma_{yz} dz$$

Consider now a plate made of "N" layers (lamina) arranged as shown below.

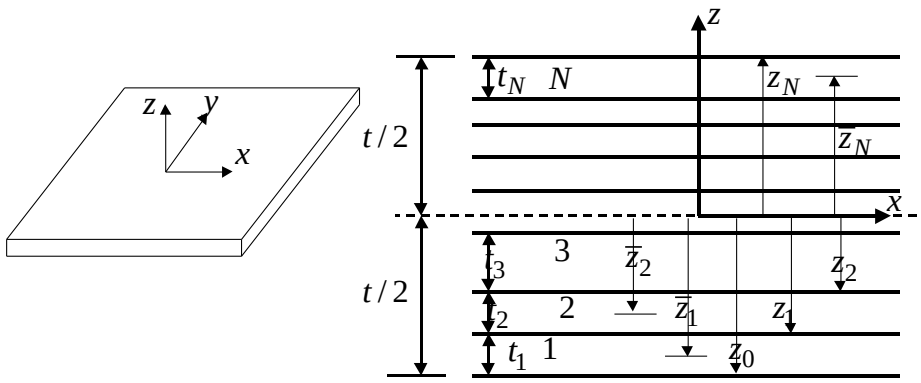

Figure II.1 Sketch of lamina

t_i = thickness of layer i = $z_i - z_{i-1}$

$\bar{z}_i$ = z centroid of layer i = $z_{i-1} + t_i / 2$

Now, substitute (AII-1) and (AII-2) into (AII-3), and integrate over the thickness. The integral can be replaced by a summation over all N layers.

$$\begin{Bmatrix} N_x \\ N_y \\ N_{xy} \end{Bmatrix} = \int_{-t/2}^{t/2} \begin{Bmatrix} \sigma_{xx} \\ \sigma_{yy} \\ \sigma_{xy} \end{Bmatrix} dz = \int_{-t/2}^{t/2} [\bar{Q}] \begin{Bmatrix} \varepsilon_{xx} \\ \varepsilon_{yy} \\ \varepsilon_{xy} \end{Bmatrix} dz \qquad \text{(AII-4)}$$
$$= \int_{-t/2}^{t/2} [\bar{Q}] \left(\begin{Bmatrix} \varepsilon_{x0} \\ \varepsilon_{y0} \\ \varepsilon_{xy0} \end{Bmatrix} + z \begin{Bmatrix} \kappa_x \\ \kappa_y \\ \kappa_{xy} \end{Bmatrix} \right) dz$$

or, summing over all N layers:

$$\begin{Bmatrix} N_x \\ N_y \\ N_{xy} \end{Bmatrix} = \sum_{k=1}^{N} [\bar{Q}]_k \left\{ \int_{z_{k-1}}^{z_k} \begin{Bmatrix} \varepsilon_{x0} \\ \varepsilon_{y0} \\ \varepsilon_{xy0} \end{Bmatrix} dz + \int_{z_{k-1}}^{z_k} \begin{Bmatrix} \kappa_x \\ \kappa_y \\ \kappa_{xy} \end{Bmatrix} z dz \right\} \tag{AII-5}$$

Both the mid-surface strains $\{\varepsilon_{x0}, \varepsilon_{y0}, \varepsilon_{xy0}\}$ and curvatures $\{\kappa)$ are independent of z for the laminated plate, i.e., the mid-surface strains are at the laminated plate mid-surface (z=0) and the curvature of each lamina is the same. Hence, the last equation can be written as:

$$\begin{Bmatrix} N_x \\ N_y \\ N_{xy} \end{Bmatrix} = \sum_{k=1}^{N} [\bar{Q}]_k \left\{ \begin{Bmatrix} \varepsilon_{x0} \\ \varepsilon_{y0} \\ \varepsilon_{xy0} \end{Bmatrix} \int_{z_{k-1}}^{z_k} dz + \begin{Bmatrix} \kappa_x \\ \kappa_y \\ \kappa_{xy} \end{Bmatrix} \int_{z_{k-1}}^{z_k} z dz \right\} \tag{AII-6}$$

The moment resultants can be similarly written.

$$\begin{Bmatrix} M_x \\ M_y \\ M_{xy} \end{Bmatrix} = -\int_{-t/2}^{t/2} \begin{Bmatrix} \sigma_{xx} \\ \sigma_{yy} \\ \sigma_{xy} \end{Bmatrix} z dz = -\int_{-t/2}^{t/2} [\bar{Q}] \begin{Bmatrix} \varepsilon_{xx} \\ \varepsilon_{yy} \\ \varepsilon_{xy} \end{Bmatrix} z dz$$

$$= -\int_{-t/2}^{t/2} [\bar{Q}] \left(\begin{Bmatrix} \varepsilon_{x0} \\ \varepsilon_{y0} \\ \varepsilon_{xy0} \end{Bmatrix} + z \begin{Bmatrix} \kappa_x \\ \kappa_y \\ \kappa_{xy} \end{Bmatrix} \right) z dz \tag{AII-7}$$

$$\begin{Bmatrix} M_x \\ M_y \\ M_{xy} \end{Bmatrix} = -\sum_{k=1}^{N} [\bar{Q}]_k \left\{ \int_{z_{k-1}}^{z_k} \begin{Bmatrix} \varepsilon_{x0} \\ \varepsilon_{y0} \\ \varepsilon_{xy0} \end{Bmatrix} z dz + \int_{z_{k-1}}^{z_k} \begin{Bmatrix} \kappa_x \\ \kappa_y \\ \kappa_{xy} \end{Bmatrix} z^2 dz \right\} \tag{AII-8}$$

$$\begin{Bmatrix} M_x \\ M_y \\ M_{xy} \end{Bmatrix} = -\sum_{k=1}^{N} [\bar{Q}]_k \left\{ \begin{Bmatrix} \varepsilon_{x0} \\ \varepsilon_{y0} \\ \varepsilon_{xy0} \end{Bmatrix} \int_{z_{k-1}}^{z_k} z\,dz + \begin{Bmatrix} \kappa_x \\ \kappa_y \\ \kappa_{xy} \end{Bmatrix} \int_{z_{k-1}}^{z_k} z^2\,dz \right\} \quad \text{(AII-9)}$$

Now do the following:

- integrate with respect to z for layer k,
- multiply $[\bar{Q}]_k$ times the integral result for layer k, and
- sum over all N layers.

The result can be written as follows:

$$\begin{Bmatrix} N_x \\ N_y \\ N_{xy} \end{Bmatrix} = \begin{bmatrix} A_{11} & A_{12} & A_{16} \\ A_{21} & A_{22} & A_{26} \\ A_{61} & A_{62} & A_{66} \end{bmatrix} \begin{Bmatrix} \varepsilon_{x0} \\ \varepsilon_{y0} \\ \varepsilon_{xy0} \end{Bmatrix} + \begin{bmatrix} B_{11} & B_{12} & B_{16} \\ B_{21} & B_{22} & B_{26} \\ B_{61} & B_{62} & B_{66} \end{bmatrix} \begin{Bmatrix} \kappa_x \\ \kappa_y \\ \kappa_{xy} \end{Bmatrix} \quad \text{(AII-10)}$$

and

$$\begin{Bmatrix} M_x \\ M_y \\ M_{xy} \end{Bmatrix} = \begin{bmatrix} B_{11} & B_{12} & B_{16} \\ B_{21} & B_{22} & B_{26} \\ B_{61} & B_{62} & B_{66} \end{bmatrix} \begin{Bmatrix} \varepsilon_{x0} \\ \varepsilon_{y0} \\ \varepsilon_{xy0} \end{Bmatrix} + \begin{bmatrix} D_{11} & D_{12} & D_{16} \\ D_{21} & D_{22} & D_{26} \\ D_{61} & D_{62} & D_{66} \end{bmatrix} \begin{Bmatrix} \kappa_x \\ \kappa_y \\ \kappa_{xy} \end{Bmatrix} \quad \text{(AII-11)}$$

where the A, B and D coefficients are given by

(AII-12)

$$A_{ij} = \sum_{k=1}^{N} (\bar{Q}_{ij})_k (z_k - z_{k-1})$$

$$B_{ij} = \tfrac{1}{2} \sum_{k=1}^{N} (\bar{Q}_{ij})_k (z_k^2 - z_{k-1}^2)$$

$$D_{ij} = \tfrac{1}{3} \sum_{k=1}^{N} (\bar{Q}_{ij})_k (z_k^3 - z_{k-1}^3)$$

Using $t_k = z_k - z_{k-1}$ and $\overline{z}_k = z_{k-1} + t_k / 2$, then above becomes:

(AII-13)

$$A_{ij} = \sum_{k=1}^{N} (\bar{Q}_{ij})_k \; t_k$$

$$B_{ij} = \sum_{k=1}^{N} (\bar{Q}_{ij})_k \; t_k \overline{z}_k$$

$$D_{ij} = \sum_{k=1}^{N} (\bar{Q}_{ij})_k \left(t_k \overline{z}_k^2 + \frac{t_k^3}{12} \right)$$

Note that equations (AII-10) and (AII-11) could be combined and written as follows:

(AII-14)

$$\begin{Bmatrix} N \\ M \end{Bmatrix} = \begin{bmatrix} A & B \\ B & D \end{bmatrix} \begin{Bmatrix} \varepsilon_0 \\ \kappa \end{Bmatrix} = [E] \begin{Bmatrix} \varepsilon_0 \\ \kappa \end{Bmatrix}$$

References for Appendix II:

R. A. Shenoi and J. F. Wellicome, Composite Materials in Maritime Structure, Britain: Cambridge University Press, (1993).